Master Thesis, Department of Geosciences

Formation of thortveitite and garnet chemistry in the Evje-Iveland pegmatite field

Kjetil Stokkeland

UNIVERSITY OF OSLO

FACULTY OF MATHEMATICS AND NATURAL SCIENCES

Formation of thortveitite and garnet chemistry in the Evje-Iveland pegmatite field

Kjetil Stokkeland

Master Thesis in Geosciences
Discipline: Mineral Resources
Natural History Museum
Faculty of Mathematics and Natural Sciences

University of Oslo
1. February 2016

© Kjetil Stokkeland
Supervisors: Associate prof. Rune Snæring Selbekk, Henrik Friis and prof. Tom Andersen

Cover-image: Stamp with a thortveitite crystal in feldspar from Evje-Iveland, issued by the Norwegian Postal Service for the 100th anniversary of NGF (Norwegian Geological Society) (Image retrieved from Selbekk, 2012)

Acknowledgements

Abstract

Chemical analyzes and observations gives new information on the formation of the Sc-silicate thortveitite in the Evje-Iveland pegmatite field. A correlation between a muscovite- or biotite dominated pegmatite and the occurrence of thortveitite may indicate that temperature explain why thortveitite is only found in biotite-rich pegmatites in Evje-Iveland. Biotite start to form at higher temperatures than muscovite, the partitioning of Sc between muscovite and biotite (Yang and Rivers, 2000) and the crystallization temperature of pegmatite quartz in Evje-Iveland (Müller et al., 2015). Chemical analysis on garnets from pegmatites in Evje-Iveland indicate fractionation-trends in the pegmatites. These trends covers the pegmatites from the least fractionated Steli, with a Mn/(Fe+Mn)-ratio of 0.38, to the fractionated Røykkvartsbruddet pegmatite with a Mn/(Fe+Mn)-ratio of 0.97. Pegmatites usually become more fractionated as one moves away from the magmatic or thermal surce (Cerny, 1991a). This is not the case for the pegmatites in Evje-Iveland, which show no regional zoning when it comes to fractionation. Some of the pegmatites are primitive members of the niobium-yttrium-fluorine (NYF)-family, while others are characterized as mixed NYF and litium-cesium-tanatlaum (LCT)-pegmatites in which of they contain a replacement zone with a LCT-component (Müller et al., 2015). The Mn/(Fe+Mn)-ratio, along with the Y and REE content, in the core and rim of a garnet and comparison of averages of the mentioned chemistry between several garnets from different zones in a pegmatite, helps in identifying the presence of a LCT-replacement zone. A good example of the latter is the Solås pegmatite, in which garnets from the wall zone have a Mn/(Fe+Mn)-ratio of 0.6 and 0.9 and Y content of 0.031 and 0.07 apfu, while a garnet from the replacement zone has a Mn/(Fe+Mn)-ratio of 0.98 and Y content of 0.0028 apfu. While the garnets from the wall zone show a normal enrichment of the HREEs, the garnet from the replacement zone show a drop in the HREE-enrichment. Garnets from other pegmatites that have similar results as those from Solås, can indicate the presence of a replacement zone that is not yet excavated, such as the Hovåsen pegmatite at Eptevann.

Table of contents

Introduction

Thortveitite, the first scandium-mineral ever known, was first discovered in the Evje-Iveland pegmatite field (Schetelig, 1911). As the reported occurrences of thortveitite in the pegmatites are showing a scattered distribution, one would investigate the reason for this case. The term "scattered" refers to the fact that thortveitite-bearing pegmatites are observed lying next to non-thortveitite-bearing pegmatites and scattered throughout the pegmatite field. As of this, it is of interest to investigate what the factors could be for the formation of thortveitite in Evje-Iveland. Thortveitite crystals were sampled from different pegmatites, along with garnets and micas. By collecting and investigate the chemistry in garnets from different zones in the pegmatites, a better understanding of the evolution of the pegmatites in Evje-Iveland can be obtained. Methods involve major- and trace-element analyses with Electron Microprobe (EMP) and Laser Ablation-Inductive Coupled Plasma-Mass Spectrometry (LA-ICP-MS), respectively. The results from the thortveitite and garnets analyzes are compared with other analysis from both Evje-Iveland and other locations.

What defines a pegmatite is its texture, like the very coarse size (>2 cm) of crystals which is a general attribute of many pegmatites and that they are derived from a melt. Pegmatites can either form from an aqueous melt solution that has been differentiated from a parental magma or from partial melting of crustal material (Roedder, 1984; London, 2008).Other textures or mineral fabrics e.g. the graphic granite, increase of crystal size towards the center or a spatial zonation of mineral assemblages that are sharply bounded, can alone or in a combination be evidence enough to identify a pegmatite. As pegmatites reflect the composition of their derived source rock, they can have granitic (most common), mafic, syenitic or carbonatitic composition (London, 2008; Rainer et al., 2012).

The fourth chapter of this thesis describes the general regional geology in Southern Norway, followed by a more detailed geological description of the Evje-Iveland area. This chapter is important to help the reader understand the geological history, which have contributed to the observed features of today.

Methods of study, including fieldwork, sampling and geochemical analyses, will be presented in chapter five. The new observations and data are presented in chapter six.

In chapter seven, the new results will be discussed, compared with published results and interpreted.

The conclusion will be presented in chapter eight.

Regional geology

A major part of Southern Norway and South-Western Sweden represents the Sveconorwegian orogeny (**Error! Reference source not found.**). Various authors have dated this event to have lasted from about 1140 Ma to about 900 Ma (Bingen et al., 2008) or 1250-900 (Bingen et al., 2008; Pedersen et al., 2009 and Nijland et al., 2014). Bingen et al. (2008) divides the event into four phases containing both magmatic and metamorphic events; the **Arendal phase** (1140-1080 Ma), the **Agder phase** (1050-980 Ma), the **Falkenberg phase** (980-970 Ma) and the **Dalane phase** (970-900 Ma). Several authors have divided the area into different tectonometamorphic domains. Pedersen et al. (2009) uses the term block, introduced by Andersen (2005).

Two more recent events influencing the Sveconorwegian area are the Caledonian orogeny (500-405 Ma) and the younger Late Carboniferous to Early Triassic Oslo paleorift (310-241 Ma) (Ramberg et al., 2007). However, these events did not affect the lithologies of the studied area of this thesis and are therefore not described in this study. The study area is situated in the Telemark domain, which is described in the following part. The geological Telemark domain is not confined to Telemark County. The study area, Evje-Iveland, is situated in Aust-Agder County.
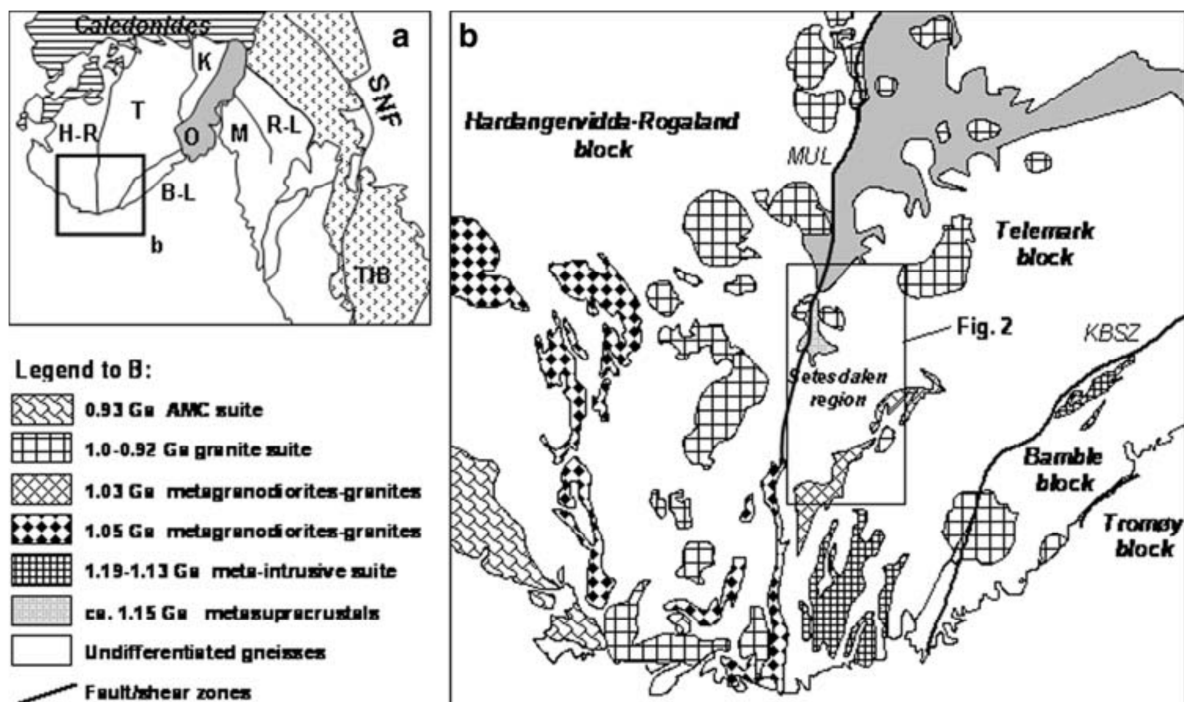
Figure 1: Geologic sketch over Southern Norway and South-Western Sweden with the blocks; Hardangervidda-Rogaland (H-R), Telemark (T), Bamble-Lillesand (B-L), Tromøy, Kongsberg-Marstrand (K-M) and Randsfjord-Lygneren (R-L). SNF= Sveconorwegian front, TIB= Transcandinavian Igneous Belt, O= Oslo paleorift,MUL= Mandal-Ustaoset lineament, KBSZ =Kristiansand-Bagn Shear Zone (Pedersen et al. 2009)

Area of the Telemark Domain

Several authors have described the area of Southern Norway. In the publication by Pedersen et al. (2009), the Hardangervidda-Rogaland block and the Telemark block are separated by the Mandal-Ustaoset lineament. (MUL in **Error! Reference source not found.**)Despite its name, recent studies by Bingen et al. (2005) shows that the lineament only stretches from Ustaoset in the north to about southwest of southern Setesdal. Pedersen et al. (2009) suggests that the lineament is a brittle reactivation of an older shear zone. The border between the Bamble and Telemark block is defined by the Kristiansand-Porsgrunn Shear-Zone. This zone show first a thrusting of Bamble in NW-direction, on top of Telemark. Bamble was later downthrown, as a result of normal faulting and shearing in the same zone (Henderson and Ihlen, 2004; Mulch et al., 2005)   Dating of muscovite (Ar/Ar) suggest that this last movement in the shear zone occurred between 891 and 880 Ma (Mulch et al., 2005). The Rogaland anorthosite-mangerite-charnockite complex (AMC) was emplaced between 930 and 920 Ma in the Hardangervidda-Rogaland block, during the **Dalane phase** (Bingen et al., 2008).

Telemark sector

The study area is situated in the Telemark sector, more specific in the Setesdalen area. The area outside of Setesdalen hosts a large number of geological units and history, but will not be further described.

Geology in the Setesdalen area
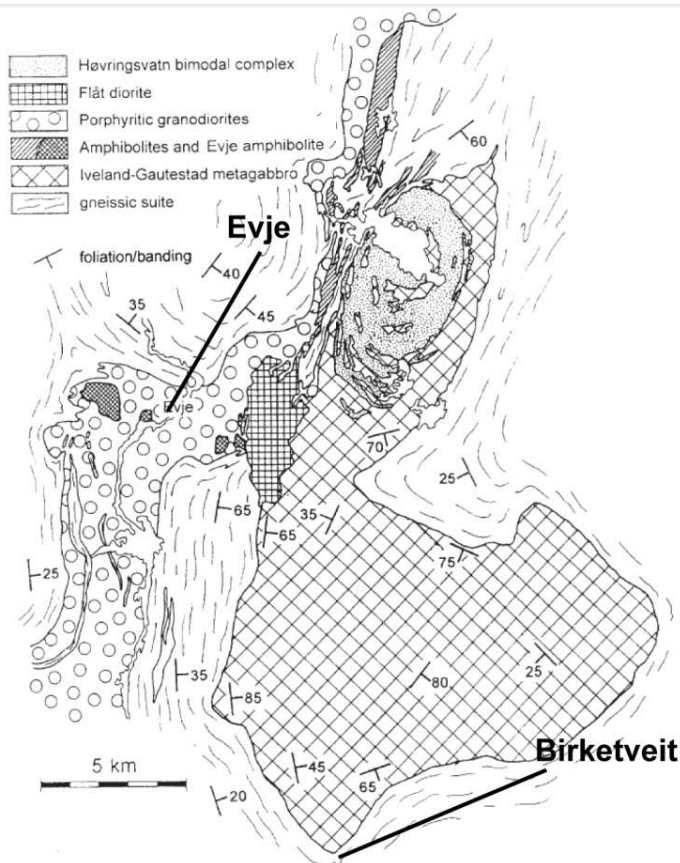
Figure 2: Geological map of the main lithological units in the Evje-Iveland area (modified after Pedersen and Konnerup-Madsen, 2000)

A large part of Setesdalen area is covered by the Iveland-Gautestad complex, which consists of amphibole gneisses of originally ultramafic to intermediary composition and is generally considered as the Iveland-Gautestad metagabbro (Barth, 1947; Pedersen and Konnerup-Madsen, 2000; Pedersen et al., 2009). Dating of zircons (U/Pb) from the complex gave an intrusion age of 1279±3 Ma (Pedersen and Konnerup-Madsen, 2000) and 1285±8 Ma and 1271±11 Ma (Pedersen et al., 2009).

In the time right before the Sveconorwegian orogeny, the Setesdalen area underwent both deposition of different sediments and volcanism (Pedersen and Konnerup-Madsen, 2000).

Syn- to late-Sveconorwegian magmatism

During the Sveconorwegian orogeny, the Setesdalen area underwent two larger magmatic events. The Fennefoss and Grimsvatn augen gneisses, which today are deformed granodiorite and granite respectively, were emplaced in the earliest magmatic event occurring at ca. 1040-1020 Ma (Pedersen and Konnerup-Madsen, 2000). These ages are corresponding with the Sirdal magmatism described by Coint et al. (2015), which also covers granitic magmatism west of the Mandal-Ustaoset zone

(Coint et al., 2015). Apart from the Fennefoss and Grimsvatn gneisses, the Flåt metadiorites were emplaced at the end or shortly after emplacement of Fennefoss. Zircon dating (U/Pb) gave an age of 1031±2 Ma for Fennefoss and 1034±2 Ma for one of the Flåt metadiorites, the Mykleås metadiorite (Pedersen and Konnerup-Madsen, 2000; Snook, 2014). The Flåt metadiorite complex is located E of Evje and hosts the former Flåt nickel mine (Bjørlykke 1947)

Sveconorwegian post-tectonic intrusions

The younger igneous event in Setesdalen is represented by plutons of monzonitic and granitic composition with an approximate emplacement age of 980 to 950 Ma. The Høvringsvatn complex, situated immediately NE of the Evje-Iveland pegmatite field, consists of multiple ring-like intrusions of granitic to monzodioritic composition. Different facies of the granites have been recently dated by Snook (2014) and given emplacement ages of 983±4 Ma and 980±4 Ma. Pedersen and Konnerup-Madsen (2000) proposed the possible presence of similar plutons in depth based on the observation of dykes and plugs, with similar composition as the complexes, other places in the Setesdalen area. A Bouguer anomaly map, however, show no signs of underlying rocks that have same density as the rocks under the Høvringsvatn granites (Snook, 2014).

Methods

Fieldwork and sampling

Fieldwork

The Granatgruva-pegmatite, at Ljoslandknipan and the main pegmatite in this study, was mapped in more detail than the other visited pegmatites. The other pegmatites that were visited and where garnet samples were obtained are the Heliodor- and Thortveitittbruddet-pegmatite at Ljoslandknipan, the Solås pegmatite, the Hovåsen-pegmatite at Eptevann, the Slobrekka- and Tuftane-pegmatite at Frikstad and the Brattekleiv-pegmatite.

Sampling

Garnets from several zones of the main pegmatite were obtained, although they all were brittle and fell apart into small pieces. This is the result of the shock generated by explosives used during mining-activity. Some of the garnets from other pegmatites were sampled from the collection of the Natural History Museum. A white rim, between quartz and microcline, was observed in the intermediate zone at Granatgruva and a sample of this was obtained (KG2-7). Muscovite and biotite were collected from the different zones in the pegmatite. The quartz-core of the pegmatite had been removed and no analyses of this are available. No thortveitites were found during the field work. The thortveitite samples for analyzes are from the Natural History Museum, UiO.
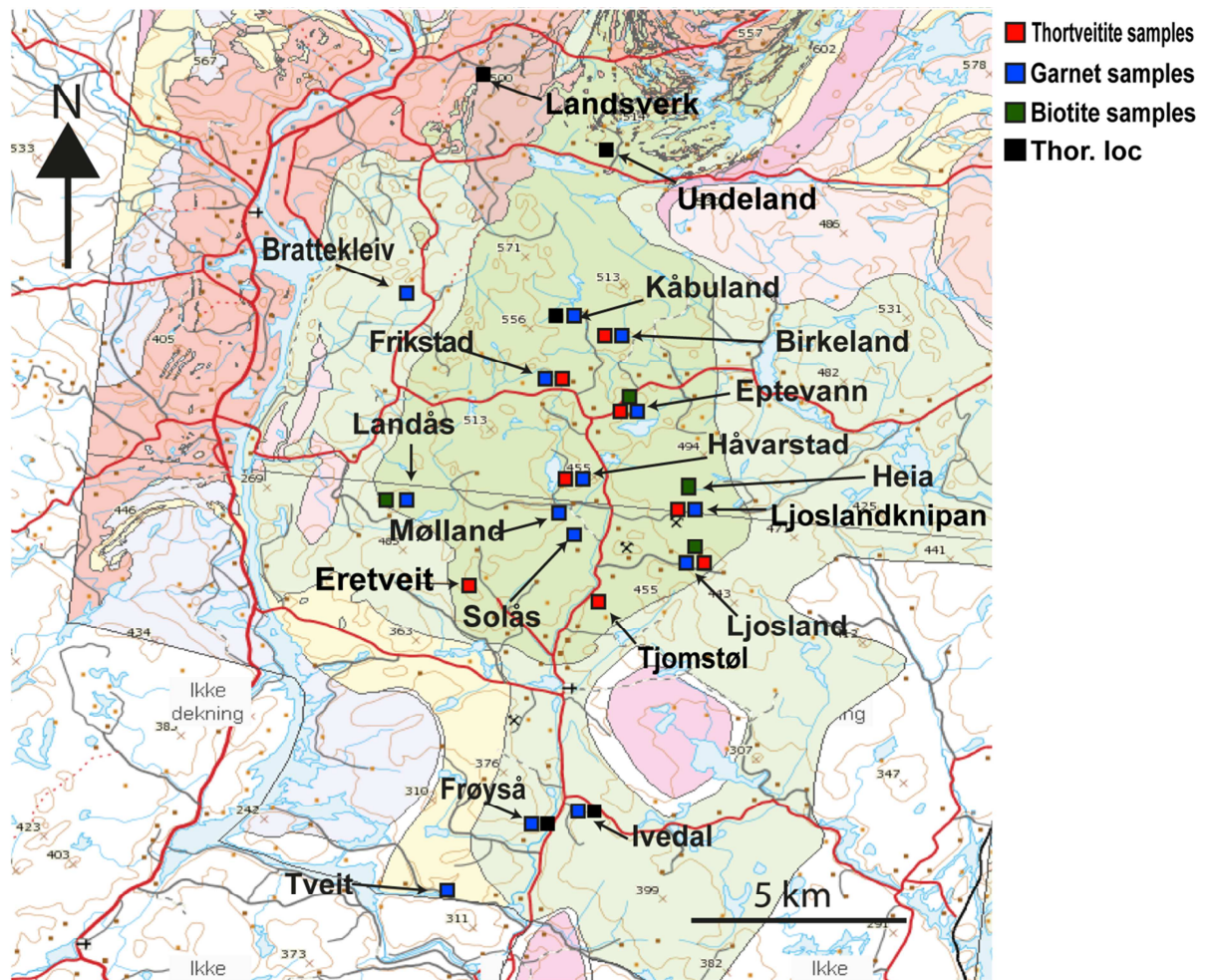
Figure 3:Map showing the location of the collected garnet, thortveitite and biotite samples. "Thor. loc." refers to pegmatites where thortveitite has been found but are not included in the analyzes (Map modified after NGU; data after www.mindat.org (2015))

Sample preparation

Samples for SEM, EMP and LA-ICP-MS were mounted in epoxy and polished. The mounting were done at NHM by the students using Epofix resin. Polishing of the samples containing the garnets and thortveitites was undertaken by the Department of Geosciences at UiO. The epoxies with the micas were polished at the Natural History Museum with a Bueler MiniMet1000 Grinder-Polisher, with the minimum size of 3µ of the polishing material. The remaining polishing was done by hand at the Department of Geosciences.

Thin-sections were prepared at the Department of Geosciences at UiO.

Major-element analysis of minerals

Scanning electron microscope (SEM)

The micas, thortveitites and garnets were first analyzed in a Scanning Electron Microscope (SEM). This was done in the SEM-model Hitachi S-3600N equipped with an EDS detector at NHM. The working pressure in the chamber was usually at 20Pa, enabling semi-quantitative analyses of uncoated samples with the EDS-detector, and the voltage of 15-20 kV. The program used in this analysis was Bruker Esprit 1.9. The SEM was used to identify other minerals observed in the thortveitite samples.

Electron microprobe (EMP)

The Cameca SX 100 electron microprobe at the Department of Geosciences, fitted with five wavelength-dispersive spectrometers, was used to analyze the thortveitites, garnets and micas. While the microprobe already had a standard program for analysis of the garnets and micas, a new program was designed for the thortveitite analyzes.

Thortveitite

The "thortveitite-program" was made by first acquiring the full wavelength dispersive spectrum (WDS) on three thortveitite crystals. X-ray lines in the WDS-spectrum were used to identify major and minor elements (Kα, Lβ etc.). Background positions were established with the help of partial WDS. Interference-free areas were searched for around each peak in the spectrum, to put the background positions. The matrix correction procedure used was PAP (Pouchou and Pichoir, 1985) which is implemented in the Cameca software. The data retrieved from the analyses were within a standard deviation of 3σ, but the results presented here are within 2σ.

Calibration standards, along with respective X-ray lines and crystals that were used are: wollastonite (Si Kα TAP, Ca Kα PET), synthetic MgO (Mg Kα TAP), Fe metal (Fe Kα LLIF), pyrophanite (Mn Kα LLIF), synthetic orthophosphates of REE (Dy Lβ, Er Lβ, Yb Lα and Lu Lβ LLIF), Y (Y Lα LTAP) and metallic Sc (Sc Kα PET) (from the Smithsonian Institute (Jarosewich and Boatner, 1980)), Monastery Mine Zircon (Zr Lα LTAP) and metal Hf (Hf Lα LLIF). Accelerating voltage and beam current used on the thortveitite samples were 20kV and 20nA respectively, with a beam size of 5µm. Total counting time were 40s (2x10 for the background) for the elements Sc, Y, Mn, Fe and Si, while 30s (2x15 for background) on other elements.

Points for analysis were chosen on the basis of zoning in the crystal. The zoning was observed in the BSE-images provided by the microprobe and three points per different zone were usually set.

Biotite

WDS-analysis was used on four biotite samples, three from thortveitite-bearing pegmatites and one from non-thortveitite-bearing pegmatites, to check if any Sc was present at all. The first analyzes acquired the major elements of the biotites. If Sc was identified in a biotite during the second analysis, the major elements for that biotite from the first analysis were used as matrix correction.

All data presented are corrected for a limit of detection of 60ppm. Total counting time was 2 min. (2x30 for background) The X-ray line and crystal used to identify Sc was Sc Kα and LPET. Accelerating voltage was set to 15kV, beam current was 50nA and the beam size was 5µm.

Calibration standards used were: Wollastonite(Ca Kα, Si Kα), pyrophanite(Mn Kα, Ti Kα) metallic iron (Fe Kα) synthetic MgO(Mg Kα) synthetic Al2O3 (Al Kα) albite (Na Kα), orthoclase (K Kα), Sc orthophosphate ScPO4 (Sc Kα) (Jarosewich and Boatner, 1991)

Garnet

Calibration standards, along with respective X-ray lines and crystals used were: Wollastonite(Ca Kα, Si Kα), pyrophanite(Mn Kα, Ti Kα) metallic iron (Fe Kα) synthetic MgO(Mg Kα) synthetic Al2O3 (Al Kα) albite (Na Kα), orthoclase (K Kα).

To analyze the garnets, a standard major element program for silicates was used.

Accelerating voltage was set to15kV, with a beam current of 20nA. The peak-count time was 10s, with a focused electron beam. All data presented are corrected for limit of detection and the PAP procedure of Pouchou and Pichoir (1985) was used for matrix correction.

Calculating end-members were done using a spread-sheet made by Locock (2008)

Trace-element analysis

Trace-element analyses were performed on the thortveitite- and garnet-samples using a Bruker Auroroa Elite quadropole ICPMS with a CTAC LXS213G2+ laser microprobe, at the Department of Geosciences at UiO. The wavelength of the laser was 213nm. Helium was used as carrier gas. All ICPMS data are corrected for limit of detection and dead-time overload. Si measurements from the microprobe were used as internal standard while a NIST600-glass, with certified reference initial for range of elements at given concentrations, was used as an external standard. The data obtained from the ICPMS have been processed for data reduction in the Glitter 4.4.2 program (Griffin et al., 2008). Error margins vary between 5 to 10 percent.

Thortveitite

For the thortveitite-analysis, the energy of the laser was usually at 30%, with a frequency of 10Hz, energy of 0.65mJ and an energy fluence of 32 J/cm^2. In some cases with too little ablation in the beginning, the energy was set to 40% and then reduced to 30% after 1-2 seconds. The ablation width was set to 50µm

Usually, three analyze-points were set per each zone, following the same points used on the microprobe. Since the LA-ICP-MS, unlike the microprobe, is not equipped with a BSE-detector, the author had to navigate to the right spots/zones with the help of printed BSE-images and regular images of the crystals.

Garnets

The Laser ablation width was set to 50µm. The energy of the laser was on 40% when used on the garnets and increased to 60% on the standard. The number of analyzing spots was usually 10 (5 on core and rim) on the large crystals and 3-5 on the smaller crystals. Average measurements were obtained on the smaller crystals. NIST SR 610 was the standard glass used to correct for instrumental drift after ca. 10 spots on the crystals.

Results

Granatgruva

Located at Ljoslandknipan, approximately 5km north-east of Birketveit (58°29´57´´ N 7°57´10´´ E), the municipally-center of Iveland. This pegmatite is called Aril Omestads gruve by Corneliussen (2015).

General features

The pegmatite is hosted by the Iveland-Gautestad amphibolite. Extensive mining activity of the pegmatite has helped in giving information about the field relationship of the pegmatite. Based on the small patches of exposure of the border zone between megacrystic K-feldspar and the amphibolite under the tailing just up the small hill from the road (circle A in Figure 4), the approximate length of the pegmatite is ca. 20-30m. The height measured from the standing ground and to the top of the pegmatite is about 6m. From west to east, with a width of about 10m, the pegmatite appears to lack symmetry as it is thinned out in the eastern part. The pegmatite has a shallow dip towards the north-east. When it comes to grain size, the Granatgruva pegmatite has a regular concentric zoning of texture as the grain size increases from the outer parts of the pegmatite and in towards the core. The border zone, a zone with a thickness of a few centimeters and is fine-grained (ca. 2-5 mm) (London, 2008; Snook, 2014), was observed at two places in the outermost region of the wall zone. Because of the small size of the border zone, compared to the wall zone, and the limited exposure, this zone was incorporated into the wall zone in **Error! Reference source not found.**. The wall zone was identified by its coarser grain-size (1-2 cm) and graphic granite (London, 2008; Snook, 2014).

The zoning pattern, when it comes to composition, is asymmetric. This can be observed in the intermediate zone, which is dominated almost completely by plagioclase in the eastern part of the pegmatite while microcline dominates in the same zone-level in the western part (Figure 5). While the overall crystal size in the plagioclase intermediate zone is less than 1m, but large enough to be distinguished from the wall zone, the microcline intermediate zone contains crystals that exceeds 1m in size. The wall in the innermost part of the mine has a mix of megacrystic plagioclase, microcline and quartz crystals, adding a third intermediate zone. Along the floor of the innermost wall, a zone which is attributed to the plagioclase intermediate zone can be observed. The core of the pegmatite was not observed in its sequential position, although, based on the observation of large crystals of quartz it is assumed that it was quartz-dominated.

Field observations in the surrounding area, which is extensively covered with vegetation, show no trace of further exposure of the pegmatite than in the excavated area. Also, a few meters behind the

studied pegmatite, is a new mine which was based in a different pegmatite. This is based on the report of Corneliussen (2015) on the Granatgruva-pegmatite being a muscovite-dominated mine, while the other is biotite-dominated.
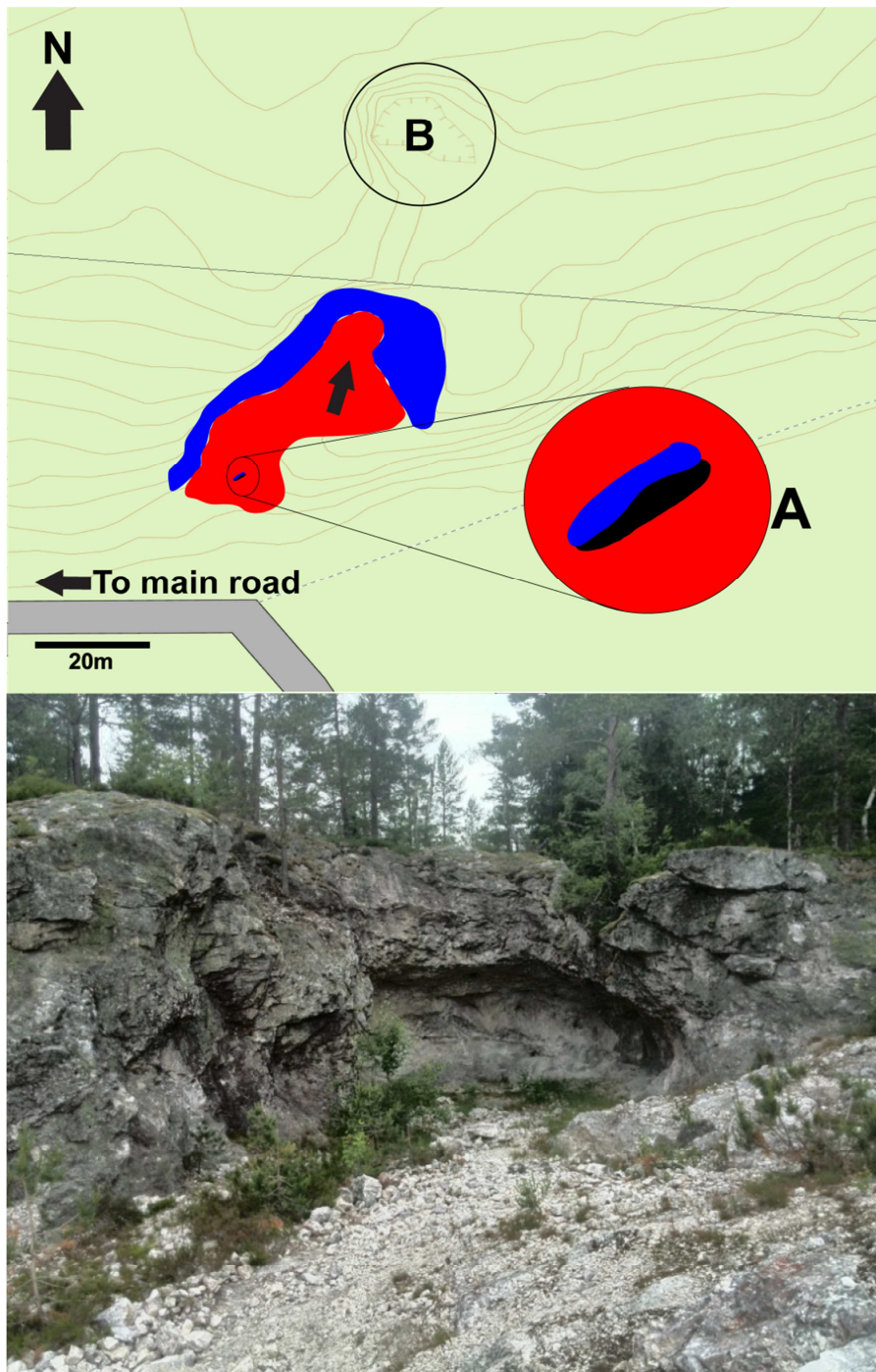
Figure 4: Map and picture of the Granatgruva pegmatite. Red-colored area is tailing from mining activity while blue covered area show where the pegmatite is exposed. Circle A indicate the small patch of megacrystic feldspar in contact with the amphibolite host rock (black). B is a second mine located a few meters to the north. Arrow in the top picture indicates the viewing direction of the bottom picture.
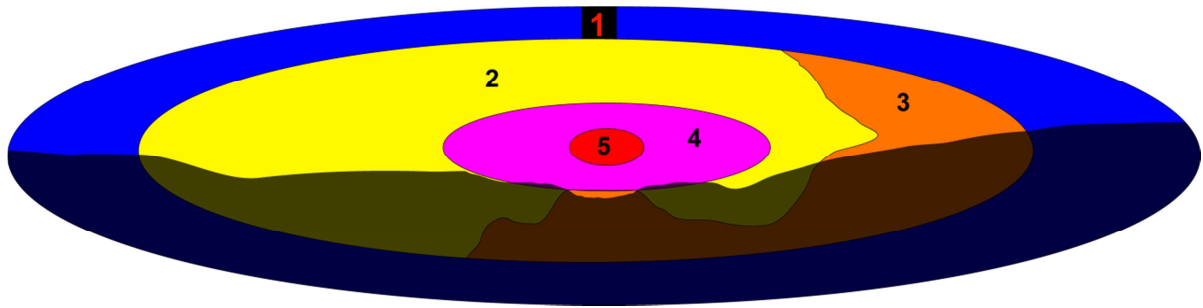
Figure 5:: Schematic sketch of the interpreted zoning of the Granatgruva pegmatite. 1: Wall zone, 2: K-feldspar intermediate zone, 3: Albite intermediate zone, 4: Feldspar intermediate zone, 5: Core. Note that the dark area is what is covered by tailings.

Pegmatite petrography

Quartz (SiO₂)

The quartz is either of a milky/transparent or smoky variety.

The milky/transparent quartz is accompanied by the white plagioclase. This quartz varies from less than 1cm to more than 1m towards the former core of the pegmatite. The crystals are anhedral throughout the pegmatite.

The smoky variety is usually observed in contact with both albite and microcline. The size of the quartz crystals varies from a few centimeters to meter-sized crystals in the pegmatite. The smoky quartz is observed to be anhedral throughout the pegmatite.

A white rim between microcline and smoky quartz was observed in the innermost part of the mine and sampled for thin-section (KG2-7). The thin-section reveals that the white rim consists of a matrix dominated by (an- and subhedral) plagioclase and quarts, with a few K-feldspar crystals (**Error! Reference source not found.**).
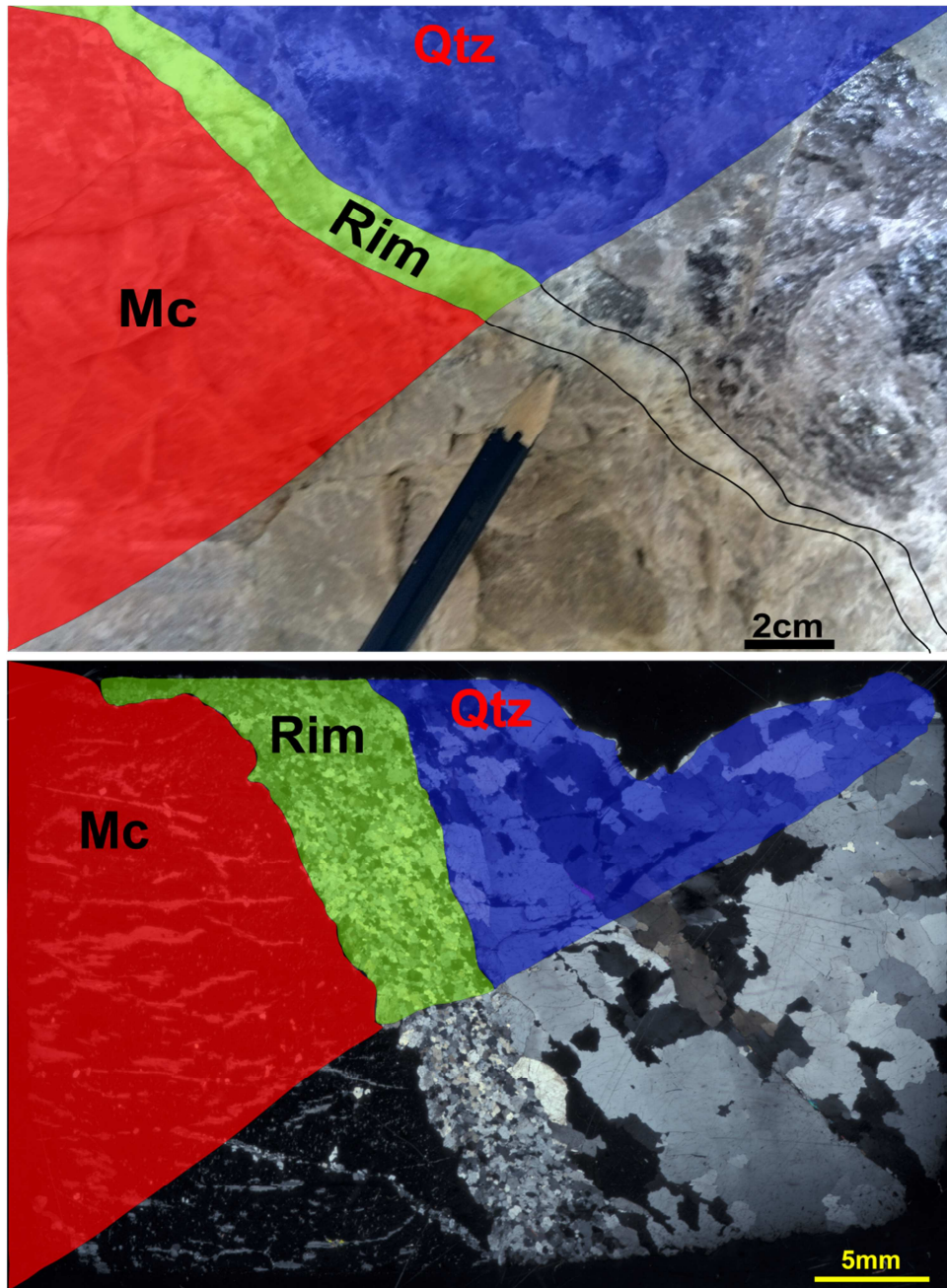
Figure 6:Picture and thin section(under cross-polarized light) of the white rim (green) between quartz (blue) and microcline (red) in innermost part of the Granatgruva pegmatite. (Mc =Microcline, Qtz= quartz)

Feldspars: K-feldspar, KAlSi3O8; Plagioclase, (Na,Ca)AlSi3O8

K-feldspar dominates over plagioclase in the graphic granite and in the wall zone in the western side of the Mine.

Plagioclase occurs as anhedral in contact with quartz, while it is an- to subhedral when in contact with other feldspars in thin-section. Twinning in the plagioclase is polysynthetic and no zoning is observed in cross-polarized light.

There are large crystals of both K-feldspar and plagioclase in the intermediate zones. K-feldspar tends (0.5-1 m) to be larger than plagioclase (< 0.5 m).

Mica: Muscovite, $KAl_2(AlSi_3O_{10})(OH)_2$; Biotite, $K(Mg,Fe)_3(AlSi_3O_{10})(OH)_2$

Some biotite is observed throughout the pegmatite but it is dominated by muscovite. Muscovite occurs in the intermediate zone of the pegmatite. The clusters of muscovite are found in both K-feldspar and plagioclase. Orientation of crystals varies between clusters, but an orientation with the (001) plane at right angles to the contact of the wall is dominant. Observation of fully evolved crystals in the feldspars, indicate that the micas crystallized prior to the feldspars. Muscovite is also found between plagioclase or microcline crystals.

Garnet: Spessartine-Almandine mix $((Mn_3Al_2)-(Fe_3Al_2)Si_3O_{12}$ (Spessartine rich)

Garnet occurs throughout the intermediate and zones in the pegmatite. A larger number of garnet crystals are observed in the plagioclase, usually accompanied by muscovite, in the eastern part of the mine. Clusters of sub- to euhedral garnets, less than 1 cm in size are observed in the plagioclase-intermediate zone. The color of these crystals is deep dark red. Larger sub- to euhedral garnet crystals, more than 1 cm in size, are observed in the K-feldspar intermediate zone. These crystals have a lighter red color compared to the ones in the plagioclase-intermediate zone. There is a larger distance between the single crystals (0.5->1m), compared to the ones in the plagioclase-intermediate zone (<1 m).

Oxides

Magnetite, $Fe^{2+}Fe^{3+}_2O_4$

Magnetite is found in the wall zone. The crystals vary from less than 5mm to about 1cm in size and are anhedral.

Euxenite-(Y) / Polycrase-(Y), $(Y, Ca, Ce, U, Th)(Ti, Ta, Nb)_2O_6$

Small euxenite-(Y) or polycrase-(Y) crystals, up to 1cm in size, occur mainly in the wall zone and almost absent in the intermediate zones. The crystals are observed to be in the vicinity of magnetite crystals. The form observed on the crystals is tabular and euhedral. Despite the chemical difference between the minerals it was not possible to fully confirm which of the two occurs in the mine. The reason for this is that both are partly to fully metamict, which makes EDS analyzes challenging and even more so XRD.

Zone	Wall zone	Intermediate zone(s)	Core
Milky qtz		—————————	
Smoky qtz	———————————————————		– – – – –
Albite	——————————————		
Microcline	————————————————————		
Muscovite		———————————————	
Biotite		—	
Magnetite	——		
Eux-(Y)/Poly-(Y)	—— – – – –	—— – – – –	
Garnet		———————	

Figure 7: Paragenetic sequence for the Granatgruva pegmatite

Chemical analysis

Biotites

Table 1: EMP-analysis of the collected biotites..

	2190Landås 7	Thor.for. Eptevann	26762Heia	22300Torvelona
n	1	1	1	1
SiO2	34.54	35.41	35.16	35.55
Sc2O3	0.060(2)*	0.135(4)*	0.1162(9)*	0.159(3)*
Fe2O3**	23.34	22.15	23.36	22.78
FeO	3.93	-	-	1.52
K2O	9.47	9.63	9.61	9.71
Al2O	16.11	16.49	15	15.77
TiO2	2.77	3.2	3.2	3.07
Na2O	0.04	0.12	0.11	0.14
MnO	1.00	1.07	0.67	1.77
MgO	5.45	8.64	8.89	6.54
CaO	-	-	-	-
Total	96.71	96.84	96.11	97.00
	Molecular proportions based on 12 oxygen			
Si apfu	2.82	2.82	2.83	2.87
Sc	0.004	0.009	0.008	0.011
Fe3+**	1.43	1.32	1.41	1.38
Fe2+	0.269	0.00	0.00	0.103
K	0.99	0.97	0.98	1.00
Al	1.55	1.54	1.42	1.50
Ti	0.17	0.19	0.19	0.18
Na	0.006	0.019	0.018	0.022
Mn	0.069	0.072	0.045	0.121
Mg	0.665	1.02	1.06	0.78
Ca	0.00	0.00	0.00	0.00
Total	7.973	7.96	7.961	7.967

*The Sc_2O_3 content is the average of 3 analysis, while the matrix correction is based on one analysis from each sample. **Calculating Fe^{3+} is based on Droop (1987)

The biotite samples *22300Torvelona* (0.159 wt.% Sc_2O_3), *22386Thor.for., Eptevann* (0.135 wt.% Sc_2O_3) and *26762Heia* (0.1162 wt.% Sc_2O_3) have the highest Sc content, while *2190Landås 7*(0.060 wt.% Sc_2O_3)) has the lowest Sc content.

Garnets

The garnets collected in field occurred either as clusters, intergrowths with quartz and muscovite, or as single and euhedral crystals.

The majority of the collected garnets have no visually observable compositional zoning. The few garnets in which compositional zoning is observed have an oscillating zoning pattern, e.g. *KG-4Granatgruva* and *MS-6Solås*, or patchy zoning , e.g. *KT-1Thortveitittgruva* and *25370Kåbuland* (Figure 8). The darker spots in *25370Kåbuland* contain small inclusions of ilmenite.
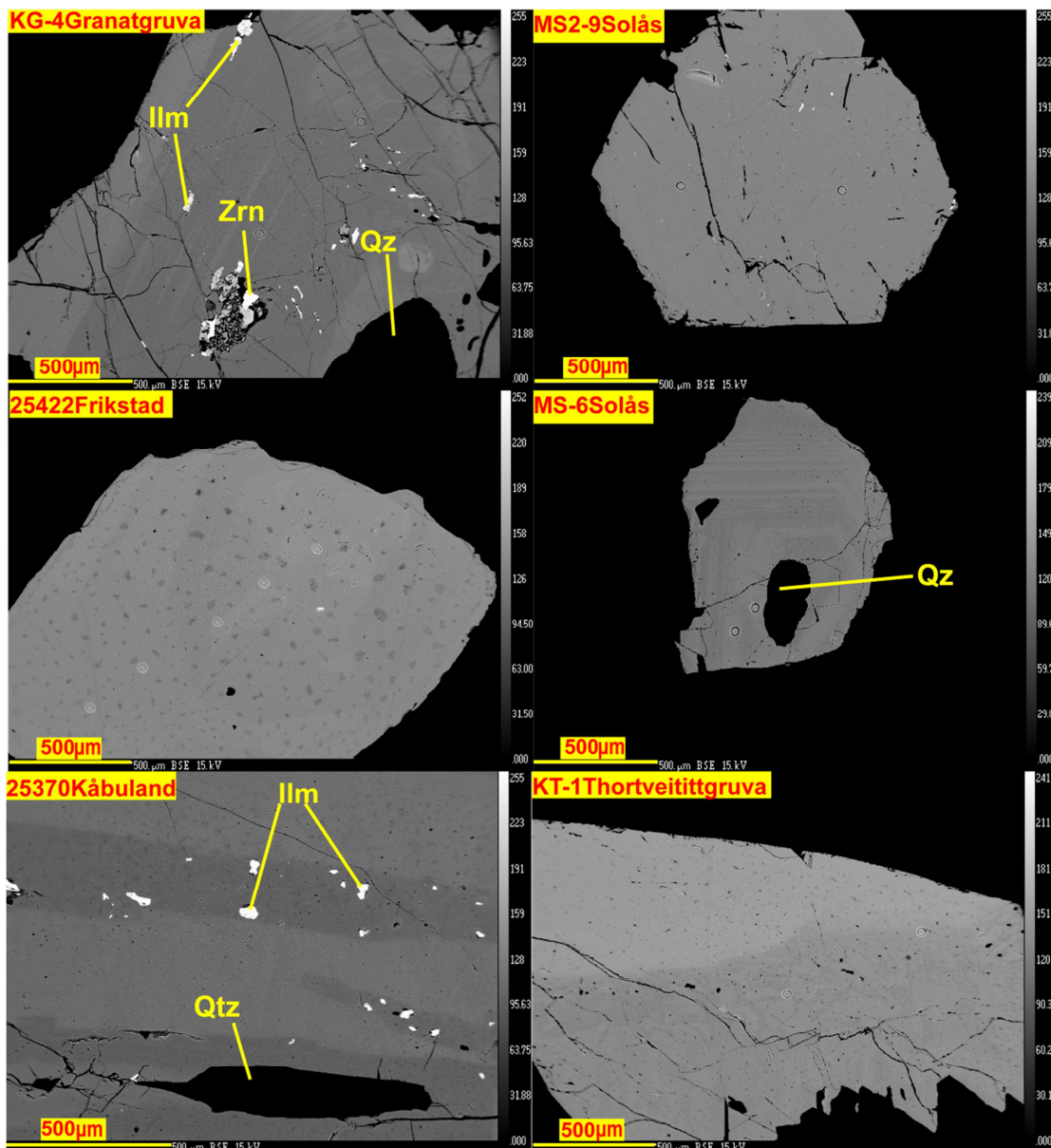
Figure 8: BSE-images of samples KG-4Granatgruva (top left), MS2-9Solås (top right), 25422Frikstad (middle left),MS-6Solås (middle right), 25370Kåbuland (bottom left) and KT-1Thortveitittgruva (bottom right). Qz= quartz. Zrn = zircon. Ilm= Ilmenite

Major and minor element chemistry

The average wt.% oxide, apfu and end-member components in the garnets are presented in Table 2. For all the analyzis spots, see Table 9, Appendix 3.

Table 2: Average wt.% oxide and apfu of elements in the collected garnets.

	KB-1 Heiliodorgruva	25432 Heia	KTU-7 Tuftane	MS-9 Solås	25427 Steli	25370 Kåbuland	25409 Landås
n	6	6	4	4	6	7	6
SiO_2 wt%	36.3(6)	36.2(3)	36.1(3)	35.1(2)	36.1(3)	36.0(4)	35.4(7)
Al_2O_3	19.9(1)	20.1(2)	20.2(3)	20.3(2)	20.2(1)	20.2(5)	20.34(7)
FeO	15 (2)	17(2)	17(2)	0.6(4)	25(1)	19(2)	15(1)
Fe_2O_3	1.3(8)	1(1)	1.4(7)	3.6(5)	1.1(5)	1.3(6)	1.4(7)
MnO	25.5(9)	24(2)	22(1)	40.0(3)	15(1)	20(2)	24.6(9)
TiO_2	-	-	0.08(2)	0.04(1)	0.04(3)	-	0.05(4)
MgO	0.6(2)	0.75(8)	0.90(4)	-	0.51(6)	1.0(2)	0.35(7)
CaO	0.3(1)	0.4()	0.52(2)	0.62(7)	0.46(5)	0.49(6)	0.59(7)
Na_2O	-	0.02(2)	<0.01	<0.01	<0.01	<0.01	0.12(9)
K_2O	-	-	-	-	<0.01	<0.01	-
Sc_2O_3	-	0.03*	0.06*	<0.01*	0.02*	0.06*	0.01*
REE_2O_3	-	0.13*	0.4*	0.045*	0.03*	0.3*	0.6*
V_2O_5	<0.01*	<0.01*	<0.01*	-	<0.01*	<0.01*	<0.01*
Cr_2O_3	-	<0.01*	<0.01*	<0.01*	<0.01*	<0.01*	<0.01*
ZnO	0.02	0.012	<0.01*	0.048*	0.01*	<0.01*	0.016
Y_2O_3	-	0.25*	0.4*	0.052*	0.09*	0.6*	1.1
TOTAL	100.1	100.9	100.7	100.3	100.2	100.3	100.3
Formula proportions based on 12 oxygen (apfu)							
Si apfu	2.97	2.96	2.96	2.9	2.98	2.95	2.93
Al	0.03	0.04	0.04	0.1	0.02	0.05	0.07
Σ T	3.00	3.00	3	3	3	3	3
V	0.00	0.00	0.00	0.00	0.00	0.00	0.00
Ti	0.01	0.01	0.00	0.00	0.00	0.01	0.00
Cr	0.00	0.00	0.00	0.00	0.00	0.00	0.00
Al	1.90	1.90	0.01	0.00	0.00	0.01	0.00
Fe3+	0.07	0.10	0.08	0.12	0.06	0.08	0.08
Fe2+	0.02	0.00	0.00	0.00	0.00	0.00	0.00
Σ B	2.00	2.00	2.00	2.00	0.00	2.00	2.00
Y	0.02	0.01	0.00	0.00	0.00	0.03	0.00
REE	0.00	0.00	0.02	0.00	0.00	0.00	0.00
Fe2+	1.0	1.16	1.1	0.05	1.76	1.3	1.07
Fe3+	0.00	0.02	0.00	0.10	1.76	0.00	0.00

Sc	0.00	0.00	0.01	0.00	0.00	0.00	0.00
Mn	1.7	1.6	1.59	2.79	1.11	1.43	1.72
Mg	0.08	0.09	0.00	0.00	0.00	0.00	0.00
Ca	0.03	0.04	0.11	0.00	0.06	0.13	0.04
Na	0.01	0.00	0.05	0.06	0.04	0.04	0.05
K	0.00	0.00	0.01	0.00	0.00	0.01	0.02
Σ A	3.00	3.00	0.00	0.00	0.00	0.00	0.00
End-member component (%)							
Yttrogarnet	0.00	0.4	0.82	0.1	0.18	1	1.86
Sc garnet	0.33	0.2	0.34	0.00	0.14	0.36	0.06
Spessartine	58	55	53.16	92.99	36.87	47.86	57.54
Pyrope	2	3	3.68	0.00	2.12	4.21	1.44
Almandine	33	35	38.04	0.6	57.83	42.6	35.12
Grossular	0.00	0.00	0.00	0.00	0.00	0.00	0.00
Andradite	0.00	0.6	0.94	1.7	1.09	0.67	1.42
Skiagite	2	3	2.01	0.88	0.93	1.82	0.8

Table 2 cont.

Sample	MS2-9 Solås	MSB-5 Slobrekka	25444 Håvarstad	KH-3 Hovåsen	25447 Rkb.	28372 Mølland	25375 Ivedal
n	4	6	6	4	4	6	6
SiO_2 wt%	35.2(4)	34.8(1)	35(1)	35.4(3)	34.7(1)	35.9(3)	35.3(3)
Al_2O_3	19.9(2)	20.5(1)	19.9(7)	19.61(6)	20.2(1)	19.9(2)	20.3(3)
FeO	12(1)	17.4(6)	19(2)	9.8(1)	0.9(7)	18(2)	16(2)
Fe_2O_3	2(1)	1.0(6)	-	2.9(2)	3.5(8)	1.7(6)	1.6(9)
MnO	28.1(4)	21.3(5)	20.6(6)	31.4(3)	39.0(6)	21(2)	22(1)
TiO_2	0.10(6)	0.05(2)	0.1(1)	0.13(3)	0.06(1)	0.10(5)	0.05(4)
MgO	0.29(2)	0.77(4)	0.6(1)	0.18(5)	-	0.8(1)	0.66(9)
CaO	0.26(4)	0.62(3)	0.4(2)	0.23(2)	0.76(5)	0.5(1)	0.9(1)
Na_2O	0.08(4)	0.12(4)	-	0.02(2)	-	-	0.1(5)
K_2O	-	-	-	-	-	-	-
Sc_2O_3	0.011*	0.084*	0.13*	<0.01*	<0.01*	0.01*	0.08*
REE_2O_3	0.36*	1.41*	0.17*	0.05*	0.067*	-	1.2*
V_2O_5	<0.01*	<0.01*	<0.01*	<0.01*	-	<0.01*	-
Cr_2O_3	-	-	-	-	-	-	-
ZnO	0.028*	<0.01*	<0.01*	0.021*	0.0261*	0.01*	0.012*
Y_2O_3	1.3*	1.5*	0.45*	0.041*	0.07*	-	1.4*
TOTAL	100.1	99.7	99.1	99.7	99.1	99.5	100.2
Formula proportions based on 12 oxygen (apfu)							
Si apfu	2.93	2.92	2.90	2.94	2.89	2.97	2.91
Al	0.07	0.08	0.10	0.06	0.11	0.03	0.09

Σ T	3.00	3.00	3.00	3.00	3.00	3.00	3.00
V	0.00	0.00	0.00	0.00	0.00	0.00	0.00
Ti	0.00	0.01	0.00	0.01	0.00	0.01	0.00
Cr	0.00	0.00	0.00	0.00	0.00	0.00	0.00
Al	1.91	1.87	1.91	1.89	1.88	1.91	1.90
Fe^{3+}	0.08	0.12	0.07	0.10	0.12	0.09	0.09
Fe^{2+}	0.01	0.01	0.02	0.00	0.00	0.00	0.01
Σ B	2.00	2.00	2.00	2.00	2.00	2.00	2.00
Y	0.06	0.08	0.08	0.03	0.00	0.01	0.06
REE	0.02	0.01	0.04	0.01	0.00	0.00	0.03
Fe^{2+}	1.07	0.85	1.20	1.35	0.06	1.31	1.12
Fe^{3+}	0.01	0.01	0.00	0.03	0.11	0.02	0.01
Sc	0.00	0.00	0.01	0.01	0.00	0.00	0.01
Mn	1.72	1.98	1.50	1.45	2.75	1.50	1.59
Mg	0.04	0.04	0.10	0.08	0.00	0.11	0.08
Ca	0.05	0.02	0.06	0.04	0.07	0.05	0.08
Na	0.02	0.01	0.02	0.02	0.00	0.01	0.02
K	0.00	0.00	0.00	0.00	0.00	0.00	0.00
Σ A	3.00	3.00	3.00	3.00	3.00	3.00	3.00
End-member component (%)							
Yttrogarnet	2.41	2.74	0.85	0.08	0.15	0.19	1.98
Sc garnet	0.07	0.47	0.63	0.01	0.01	0.09	0.46
Spessartine	65.96	50.22	48.39	73.78	91.77	49.97	53.06
Pyrope	1.22	3.21	2.51	0.76	0.00	3.53	2.75
Almandine	24.08	40.35	43.16	18.42	2.01	41.67	37.57
Grossular	0.00	0.32	0.00	0.00	0.14	0.00	0.37
Andradite	0.36	0.96	0.23	0.28	1.93	1.27	1.8
Skiagite	4.44	0.27	1.9	4.38	0.13	1.96	0.15

Table 2 cont.

Sample	25412 Rkb.	25374 Frøyså	25422 Frikstad	MB-3 Brattekleiv	25421 Frikstad	KH-1 Hovåsen	KT-1 Thortveitittgruva
n	6	6	4	4	4	4	5
SiO_2 wt%	36.1(4)	35.4(3)	35.6(5)	35.6(1)	35.2(2)	36.1(3)	36.3(3)
Al_2O_3	20.4(2)	20.5(4)	20.1(2)	20.2(1)	20.5(3)	19.98(7)	19.9(2)
FeO	7(1)	1.7(6)	18.1(6)	21.0(9)	0.7(6)	12.9(2)	14.3(9)
Fe_2O_3	1(1)	2.8(7)	2.0(3)	1.3(4)	3.2(6)	1.6(1)	1.8(4)
MnO	34.5(5)	38.9(4)	21.8(2)	19.4(8)	39.7(5)	28.6(3)	25(1)
TiO_2	0.01(1)	0.04(1)	0.05(1)	0.09(3)	0.05(1)	0.14(8)	0.17(2)
MgO	-	-	0.8(6)	0.526(8)	-	0.50(4)	1.08(9)
CaO	0.49(3)	0.7(1)	0.57(8)	0.5(1)	0.75(4)	0.28(4)	0.8(3)
Na_2O	0.08(7)	0.04(3)	0.05(1)	0.05(1)	-	0.027(9)	0.06(4)

K_2O	0.4	0.05	-	-	-	-	-
Sc_2O_3	<0.01*	<0.01*	0.06*	0.08*	-	0.03*	0.2*
REE_2O	0.06*	0.08*	0.4*	0.39*	0.6*	0.2*	0.4*
V_2O_5	0	0	0	<0.01*	0	<0.01*	<0.01*
Cr_2O_3	0	0	0	0	0	0	0
ZnO	0.047*	0.025*	0.011*	<0.01*	0.044	0.0131	<0.01*
Y_2O_3	0.31*	0.12*	0.4*	0.45*	0.101*	0.66*	0.6*
TOTAL	100.9	100.4	100.2	99.9	100.2	101	101
Formula proportions based on 12 oxygen (apfu)							
Si apfu	2.96	2.91	2.93	2.95	2.90	2.96	2.95
Al	0.04	0.09	0.07	0.05	0.10	0.04	0.05
Σ T	3.00	3	3.00	3.00	3.00	3.00	3.00
V	0.00	0.00	0.00	0.00	0.00	0.00	0.00
Ti	0.00	0.00	0.00	0.01	0.00	0.01	0.01
Cr	0.00	0.00	0.00	0.00	0.00	0.00	0.00
Al	1.93	1.91	1.87	1.92	1.89	1.88	1.86
Fe3+	0.07	0.09	0.12	0.07	0.11	0.10	0.11
Fe2+	0.00	0.00	0.00	0.00	0.00	0.01	0.02
Σ B	2.00	2.00	2.00	2.00	2.00	2.00	2.00
Y	0.02	0.01	0.03	0.03	0.01	0.04	0.03
REE	0.00	0.00	0.02	0.01	0.00	0.01	0.01
Fe2+	0.48	0.12	1.24	1.45	0.05	0.88	0.95
Fe3+	0.04	0.08	0.01	0.01	0.10	0.00	0.00
Sc	0.00	0.00	0.01	0.01	0.00	0.00	0.02
Mn	2.39	2.71	1.53	1.37	2.77	1.98	1.76
Mg	0.00	0.00	0.10	0.06	0.00	0.06	0.13
Ca	0.04	0.07	0.05	0.05	0.07	0.02	0.07
Na	0.01	0.01	0.01	0.01	0.00	0.00	0.01
K	0.01	0.00	0.00	0.00	0.00	0.00	0.00
Σ A	3.00	3.00	3.00	3.00	3.00	3.00	3.00
End-member component (%)							
Yttrogarnet	0.55	0.23	0.84	0.88	0.19	0.58	0.29
Sc garnet	0.00	0.00	0.38	0.49	0.00	0.45	0.19
Spessartine	79.79	90.29	50.86	45.66	92.31	58.39	59.06
Pyrope	0.03	0.00	3.36	2.15	0.03	2.38	3.01
Almandine	15.77	4.07	39.93	47.74	1.79	33.61	32.56
Grossular	0.39	0.76	0.00	0.00	0.23	0.00	0.00
Andradite	1.00	1.43	1.14	0.83	1.72	0.12	0.53
Skiagite	0.23	0.00	1.73	0.73	0.01	2.95	2.90

Table 2 cont.

Sample	MS-6 Solås	KG2-5 Granatgruva	KG-4 Granatgruva	22330 Torvelona
n	4	4	6	4
SiO_2	35.7(4)	35.4(1)	36.1(8)	35.4(3)
Al_2O_3	19.9(3)	19.7(3)	20.1(1)	19.3(1)
FeO	16(1)	15(1)	17(1)	11.3(4)
Fe_2O_3	1(1)	2.10(6)	1.4(6)	2.5(8)
MnO	24.2(1)	25(1)	23.4(7)	28.4(2)
TiO_2	0.07(3)	0.22(6)	0.16(8)	0.20(3)
MgO	0.59(9)	0.66(8)	0.81(2)	0.70(2)
CaO	0.32(2)	0.43(2)	0.5(1)	0.65(6)
Na_2O	-	0.10(9)	-	0.07(2)
K_2O	0.14	-	0.04	-
Sc_2O_3	0.014*	0.11*	0.11*	0.19*
REE_2O_3	0.2*	0.3*	0.1*	0.4*
V_2O_5	<0.01*	<0.01*	<0.01*	<0.01*
Cr_2O_3	<0.01*	<0.01*	<0.01*	<0.01*
ZnO	0.023*	0.016*	<0.01*	<0.01*
Y_2O_3	0.5*	0.7*	0.2*	0.58*
TOTAL	99.6	99.8	100	99.6
Formula proportions based on 12 oxygen				
Si apfu	2.96	2.93	2.96	2.94
Al	0.04	0.07	0.04	0.06
Σ T	3.00	3.00	3.00	3.00
V	0.00	0.00	0.00	0.00
Ti	0.00	0.01	0.01	0.01
Cr	0.00	0.00	0.00	0.00
Al	1.91	1.86	1.91	1.83
Fe3+	0.09	0.12	0.08	0.15
Fe2+	0.00	0.00	0.00	0.01
Σ B	2.00	2.00	2.00	2.00
Y	0.03	0.04	0.01	0.03
REE	0.01	0.01	0.00	0.01
Fe2+	1.11	1.04	1.18	0.78
Fe3+	0.02	0.01	0.01	0.00
Sc	0.00	0.01	0.01	0.02
Mn	1.70	1.75	1.63	1.99
Mg	0.07	0.08	0.10	0.09
Ca	0.03	0.04	0.05	0.06
Na	0.02	0.02	0.01	0.01
K	0.00	0.00	0.00	0.00

Σ A	3.00	3.00	3.00	3.00
End-member component (%)				
Yttrogarnet	0.64	0.58	0.16	0.42
Sc garnet	0.17	0.27	0.09	0.14
Spessartine	52.62	63.26	65.6	39.29
Pyrope	3.34	2.76	1.01	2.61
Almandine	38.48	29.05	28.51	54.44
Grossular	0.00	0.00	0.00	0.00
Andradite	0.75	1.19	1.4	0.97
Skiagite	2.86	1.27	0.94	1.06

Values marked with "*"are obtained from LA-ICP-MS analysis.

Calculation of Fe^{3+} is based on Droop (1987).

Fe-Mn

All of the collected garnets belong to the almandine-spessartine series with the latter being the most abundant (Figure 9). **Error! Reference source not found.** shows that *25421Frikstad* (92.3% spessartine, 1.7% almandine), *MS-9Solås* (92.2% spessartine, 0% almandine) and *25447Røykvartsbruddet* (91.7 % spessartine, 2% almandine) are the garnets that have the highest spessartine component. On the other side of the solid solution lies *25427Steli* (57% almandine, 36% spessartine), which is closest to the almandine end-member. *MB-3Brattekleiv* (47% almandine, 45% spessartine) is another sample closer to the almandine than the spessartine end-member.
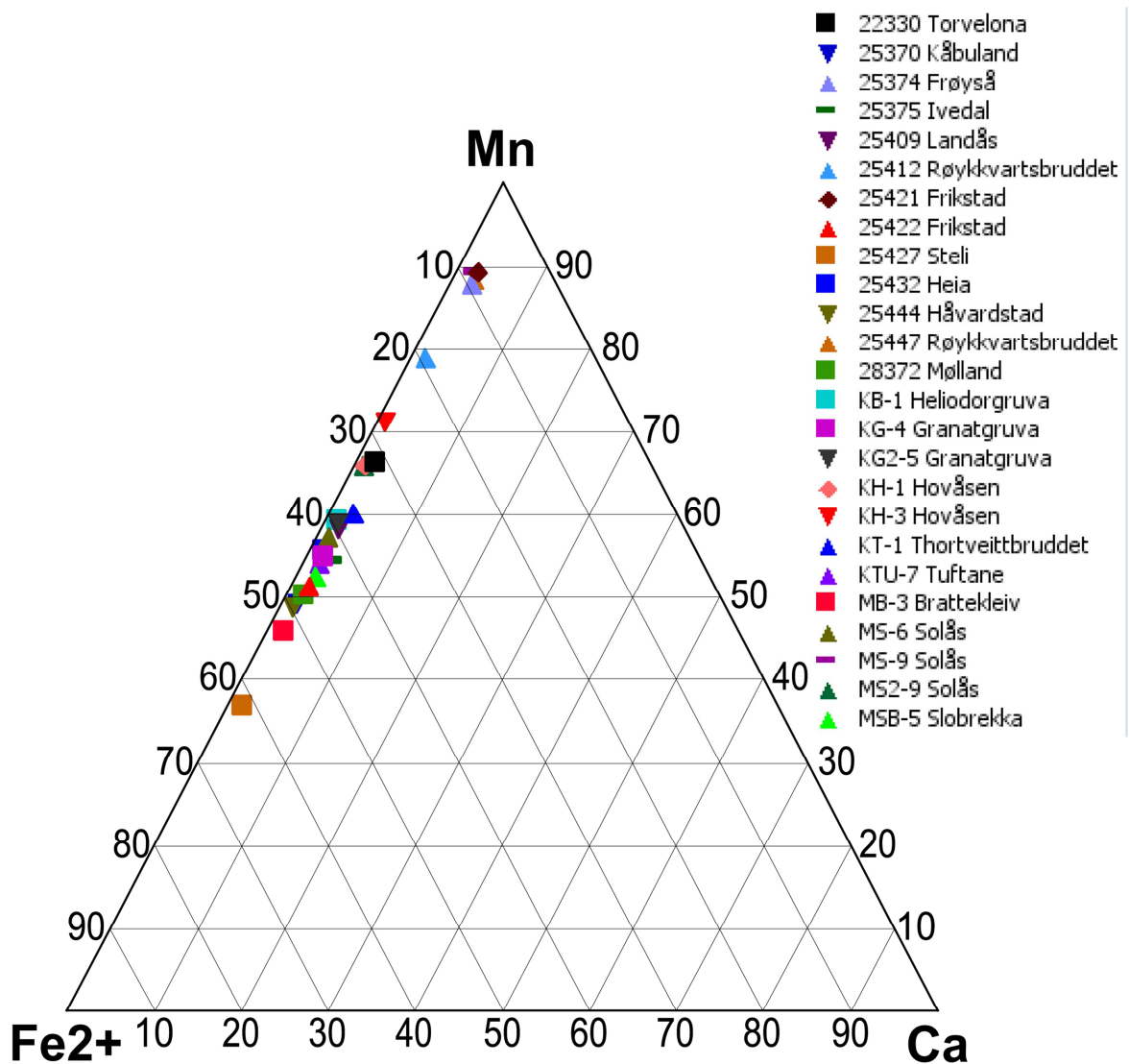
Figure 9: Ternary plot between Mn, Ca and Fe in the collected garnets

Ca and Mg

The pyrope and Ca-end-members (andradite and grossular) components in the collected garnets are minimal compared to the spessartine-almandine components (Figure 10). *KTU-7Tuftane* has the highest pyrope content (3.6% pyrope), however *KT-1Thortveitittbruddet* is closest to the pyrope end-member relative to the spessartine-almandine and grossular end-members. The sample *25375Ivedal* has the highest grossular content, relative to the other garnets, in a spessartine-almandine versus pyrop and grossular plot.
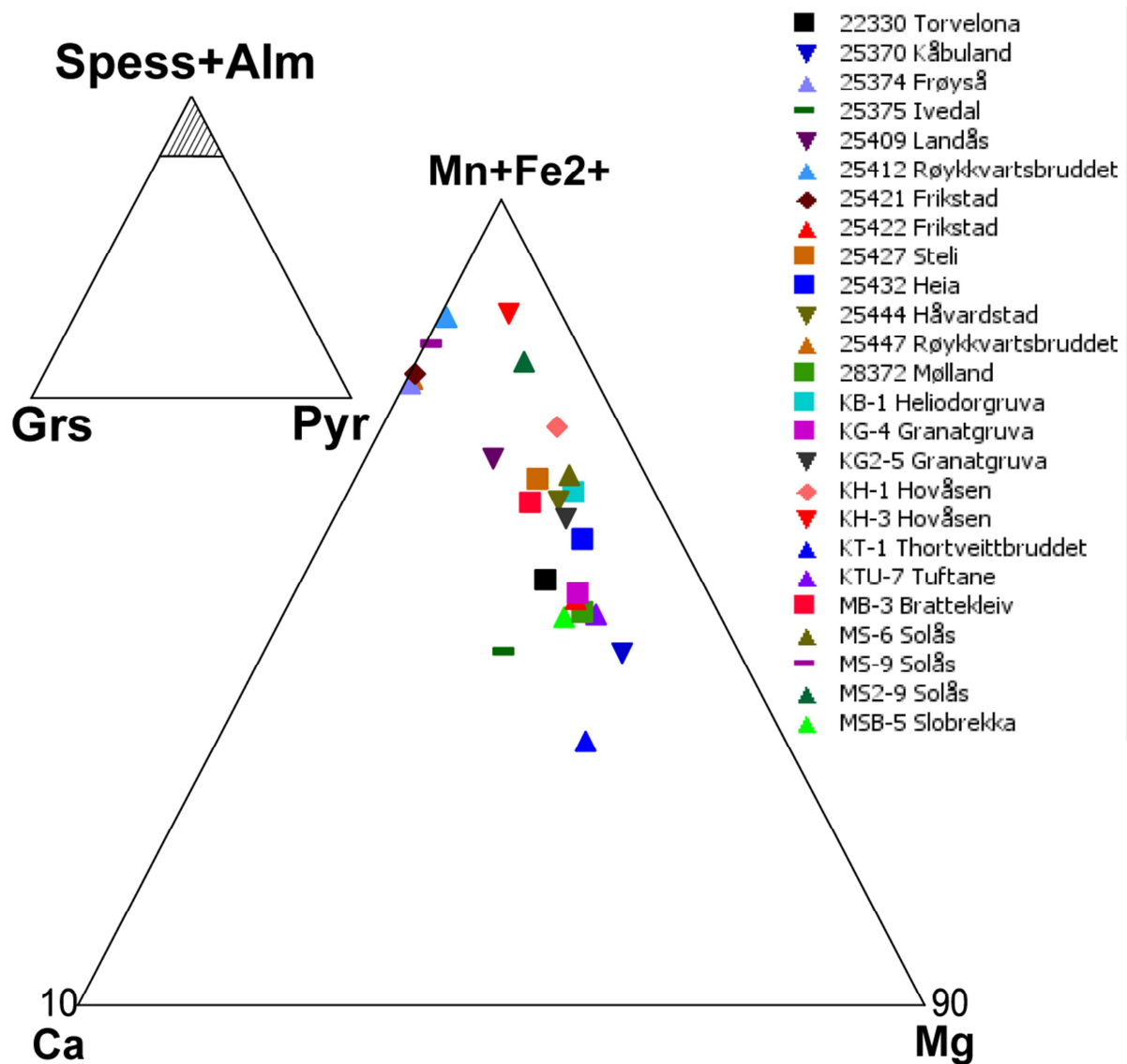
Figure 10: Ternary plot showing the distribution of the garnets between the spessartine-almandine, grossular and pyrope end-members.

Trace element chemistry

Yttrium, scandium and REE

The garnets with the highest Y content are *MSB-5Slobrekka* (1.50 w.t% Y_2O_3), *MS2-9Solås* (1.3 wt.% Y_2O_3), *25409Landås* (1.1 w.t% Y_2O_3) and *25375Ivedal* (1.1 wt.% Y_2O_3), in which *MSB-5Slobrekka* has the highest Y component (2.73% yttrogarnet) (Table 2). The Sc content is considerably lower than Y in the garnets, where *KT-1Thortveitittbruddet* (0.20 wt.% Sc_2O_3), *22330Torvelona* (0.19 wt.% Sc_2O_3) and *25444Håvarstad* (0.13 wt.% Sc_2O_3) have the highest Sc content. *25444Håvarstad* has the highest Sc-component (0.62% Sc garnet) (Table 2).
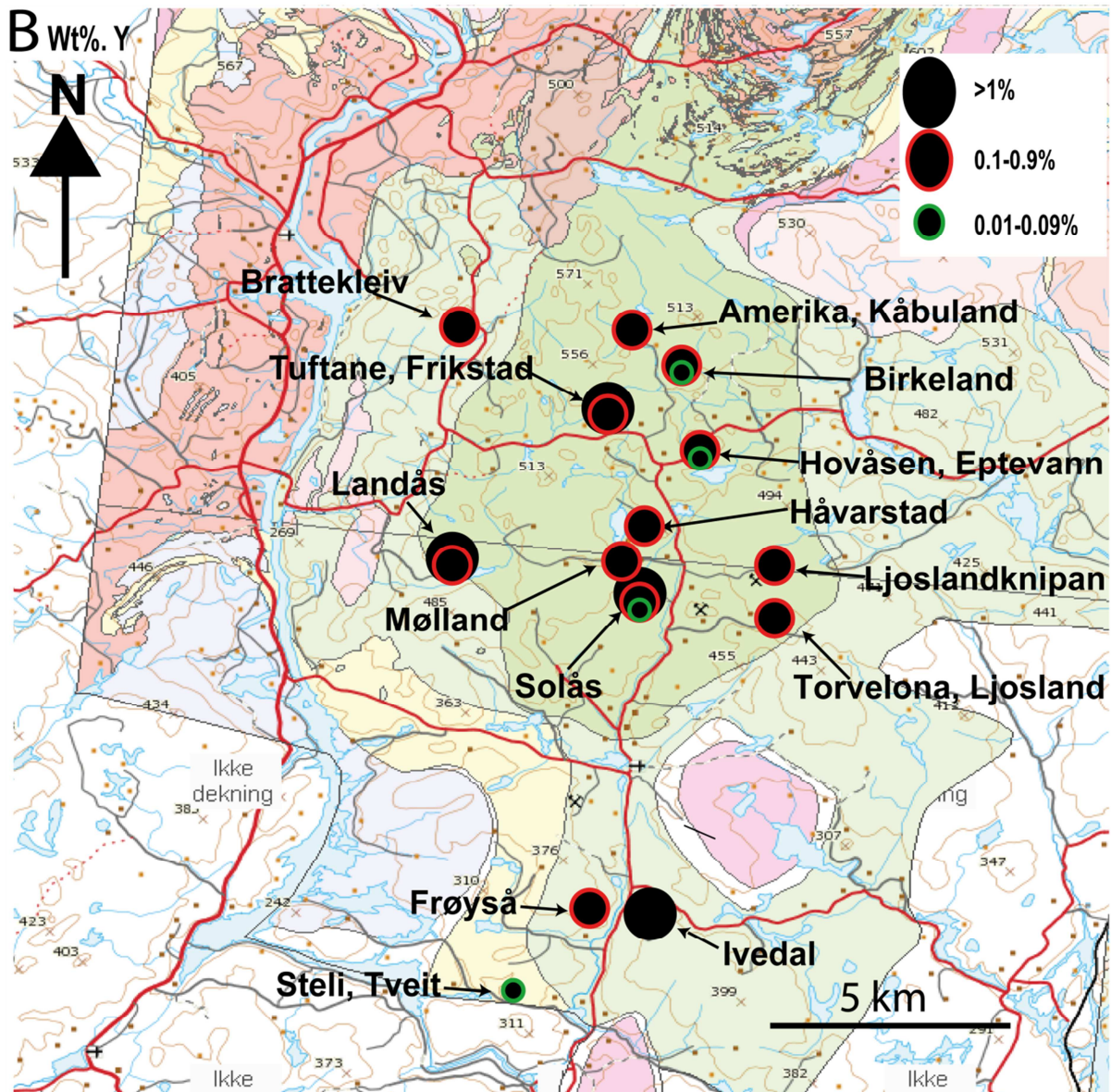
Figure 11:Map showing the distribution of Y in the collected garnets.
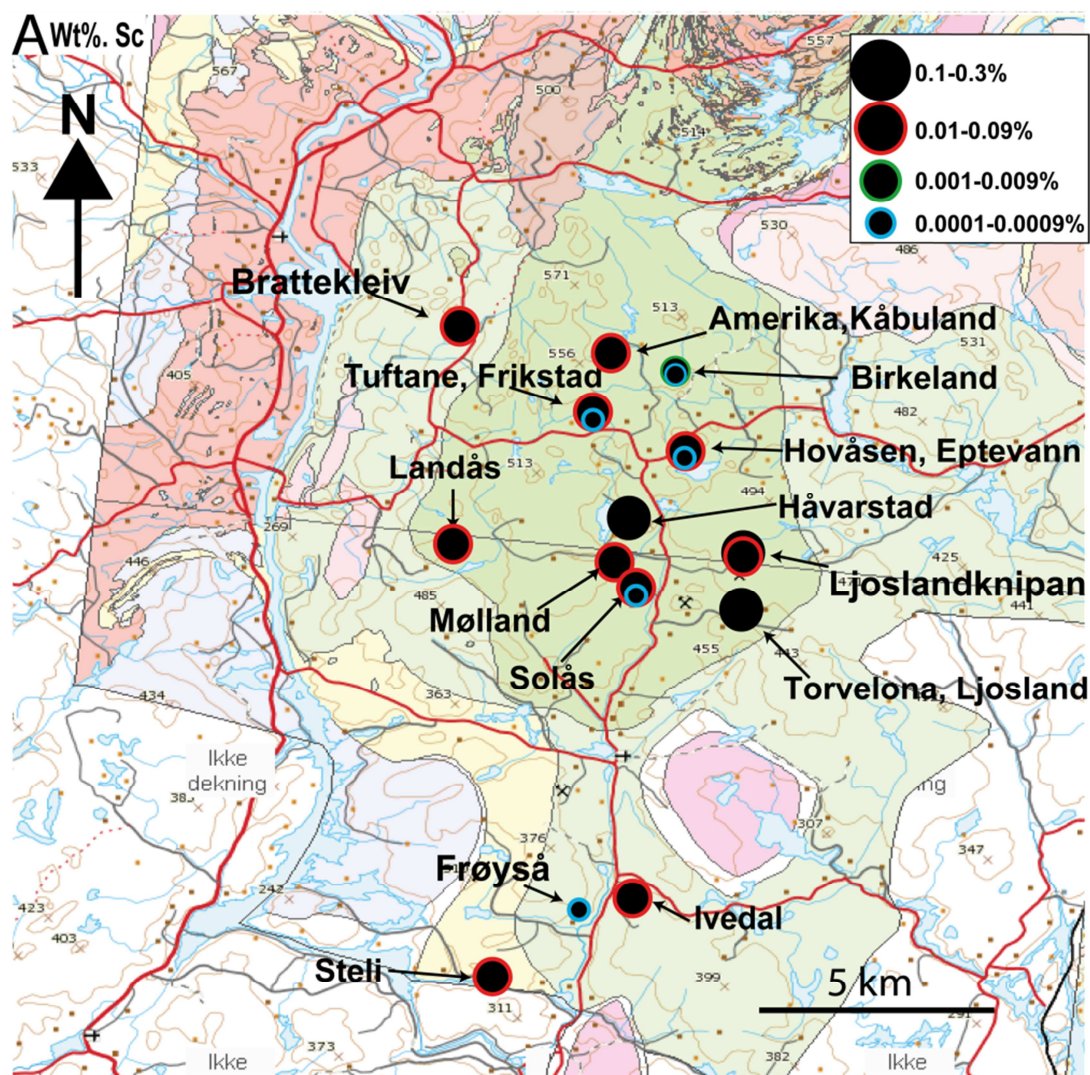
Figure 12:Map showing the distribution of Sc (wt.%) in the collected garnets.

The garnets with the highest Sc content (in wt.%) are from within the Iveland-Gautestad complex (Figure 12), which is also the case for the majority of the garnets when it comes to Y. Garnets collected from the areas of Ljosland, Ljoslandknipan and Håvarstad contains the highes Sc content. Some of the garnets with the highest Y content, e.g. *25375Ivedal*, are from outside the Iveland-Gautestad Complex (Figure 11)

Table 3: Table showing the Mn/(Fe+Mn), Sc and Y (apfu) from core to rim and average in the garnets.

		Mn/(Fe+Mn)	Sc	Y
	Core	0.61	0.005	0.013
	Rim	0.56	0.0024	0.015
25432Heia	Avg.	0.59	0.003	0.014

	Core	0.39	0.0036	0.0067
	Rim	0.37	0.002	0.003
25427 Steli	Avg.	0.38	0.002	0.005
	Core	0.54	0.004	0.042
	Rim	0.48	0.01	0.02
25370 Kåbuland	Avg.	0.51	0.007	0.03
	Core	0.63	0.0012	0.089
	Rim	0.6	0.001	0.03
25409 Landås	Avg	0.63	0.0011	0.06
	Core	0.54	0.0094	0.086
	Rim	0.55	0.0094	0.082
MSB-5 Slobrekka	Avg.	0.54	0.0094	0.084
	Core	0.55	0.011	0.025
	Rim	0.5	0.018	0.025
25444 Håvardstad	Avg.	0.52	0.014	0.025
	Core	0.76	0.00	0.0024
	Rim	0.76	0.00	0.002
KH-3 Hovåsen	Avg.	0.76	0.00	0.0022
	Core	0.97	0.00	0.0047
25447	Rim	0.97	0.00	0.0041
Røykkvartsbruddet	Avg.	0.97	0.00	0.0044
	Core	0.83	0.00	0.018
25412	Rim	0.85	0.00	0.016
Røykkvartsbruddet	Avg.	0.83	0.00	0.017
	Core	0.96	0.00	0.0074
	Rim	0.95	0.00	0.0062
25374 Frøyså	Avg.	0.95	0.00	0.006
	Core	0.56	0.0021	0.0097
	Rim	0.5	0.00	0.00
28372 Mølland	Avg.	0.51	0.001	0.00
	Core	0.56	0.01043	0.053
	Rim	0.6	0.00802	0.07
25375 Ivedal	Avg.	0.58	0.009	0.06
	Core	0.58	0.005	0.026
	Rim	0.59	0.0172	0.0076
KG-4 Granatgruva	Avg.	0.57	0.013	0.01
22330 Torvelona	Avg.	0.71	0.022	0.033
25422 Frikstad	Avg.	0.55	0.007	0.025
MB-3 Brattekleiv	Avg.	0.48	0.009	0.025
25421 Frikstad	Avg.	0.98	0.00	0.0056
KH-1 Hovåsen	Avg.	0.69	0.003	0.036
KT-1 Thortveittbruddet	Avg.	0.64	0.021	0.03
MS-6 Solås	Avg.	0.6	0.0016	0.031
MS2-9 Solås	Avg.	0.69	0.0012	0.07
KG2-5 Granatgruva	Avg.	0.62	0.012	0.04
KTU-7 Tuftane	Avg.	0.57	0.006	0.02
MS-9 Solås	Avg	0.98	0.00	0.0028
KB-1 Heliodorgruva	Avg.	0.63	0.00	0.00

The change in Sc and Y content with the variation of Mn/(Fe+Mn)-ratio is shown in Table 3. The samples *25370Kåbuland*, *25444Håvarstad* and *25375Ivedal* have an inverse change in Sc when the Mn/(Fe+Mn)-ratio changes from core to rim. *25432Heia* and *28372Mølland*, *KG-4Grantgruva* and *25427Steli* have the same change in Sc content as the change in the Mn/(Fe+Mn)-ratio.

The samples *MSB-5Slobrekka* and *KG-4Granatgruva* have an inverse change in Y content when the Mn/(Fe+Mn)-ratio changes from core to rim. *254270Steli*, *25370Kåbuland*, *25404Landås*, *28372Mølland*, *25375Ivedal* and *25374Frøyså* have the same change in Y content as the change in the Mn/(Fe+Mn)-ratio from core to rim.

Two trends occur when it comes to REE enrichment of the garnets. The first trend is an enrichment of the HREEs, which is the normal situation in garnets, while the other trend is a reduction or drop in the enrichment of the HREEs (Figure 13). *KH-3Hovåsen* has a major drop in the enrichment of the HREEs compared to the other garnets. Although a low LREE-enrichment in garnets is normal, some of the garnets have a drop in the Ce-enrichment.
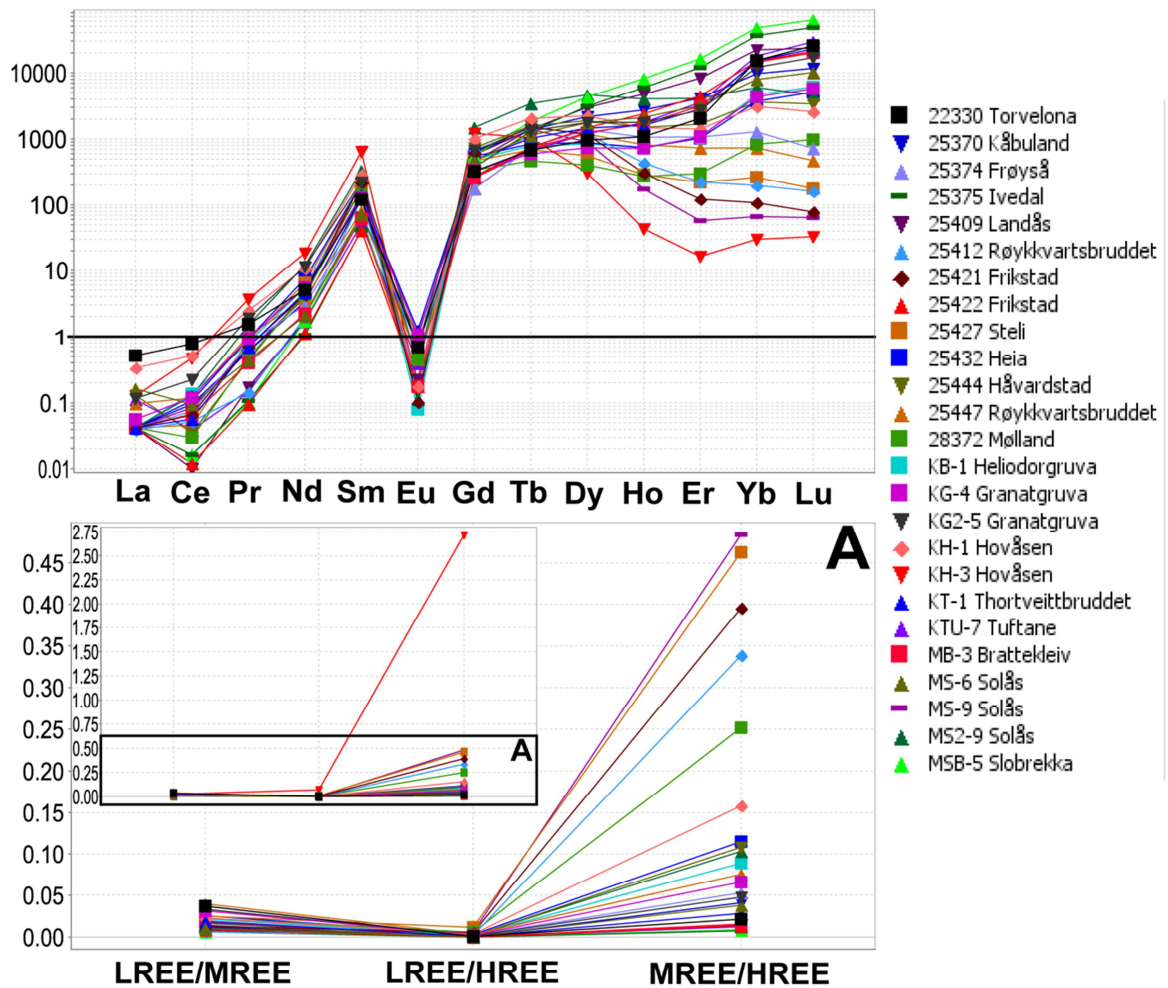
Figure 13: Chondrite normalized REE plot and LREE/MREE, LREE/HREE and MREE/HREE ratio plot for the collected garnets.
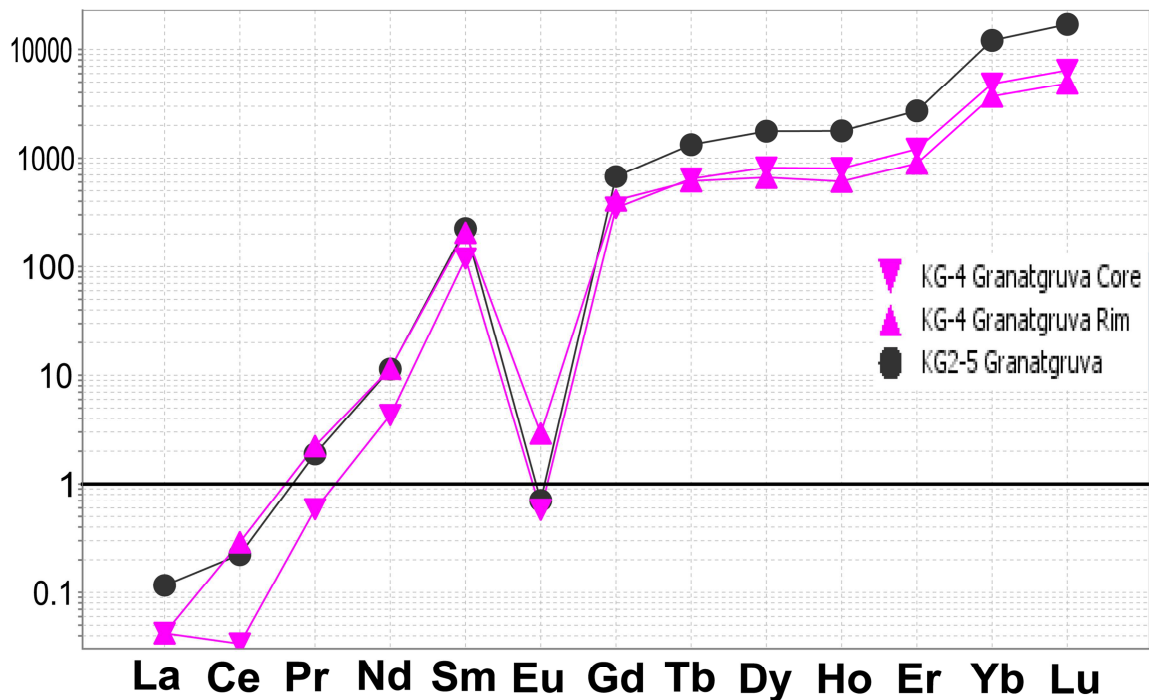
Figure 14:The chondrite normalized REE plot of KG2-5 and the core and rim of KG-4 from Granatgruva.

The two garnets from the Granatgruva pegmatite are also plottet in a separated chondritc plot as this pegmatite was investigated further (Figure 14). Both the core and rim in *KG4* and the average of *KG2-5* have a normal enrichment in the HREEs, while there is a drop in the Ce-enrichment in *KG-4*.

Thortveitite

Occurrence of thortveitite in Evje-Iveland

As the thortveitites are from the collection at NHM, the paragenesis of these samples is obtained by the eventual associated hand specimens, combined with the reported minerals from the same pegmatite. Most of the samples consisted only of a single or multiple crystals of thortveitite. Sample *22292_2Tuftane* was accompanied by plagioclase that separated two thortveitite crystals (Figure 18), while *22239Ljosland* was in a matrix of microcline and mica. *22302Knapen* had grown along the cleavage of a mica crystal. BSE-images (Figure 15) reveals that zircon, muscovite, biotite, quartz and a Y-rich mineral interpreted as allanite usually accompanies as fracture-fillings or overgrowths in the thortveitite samples.
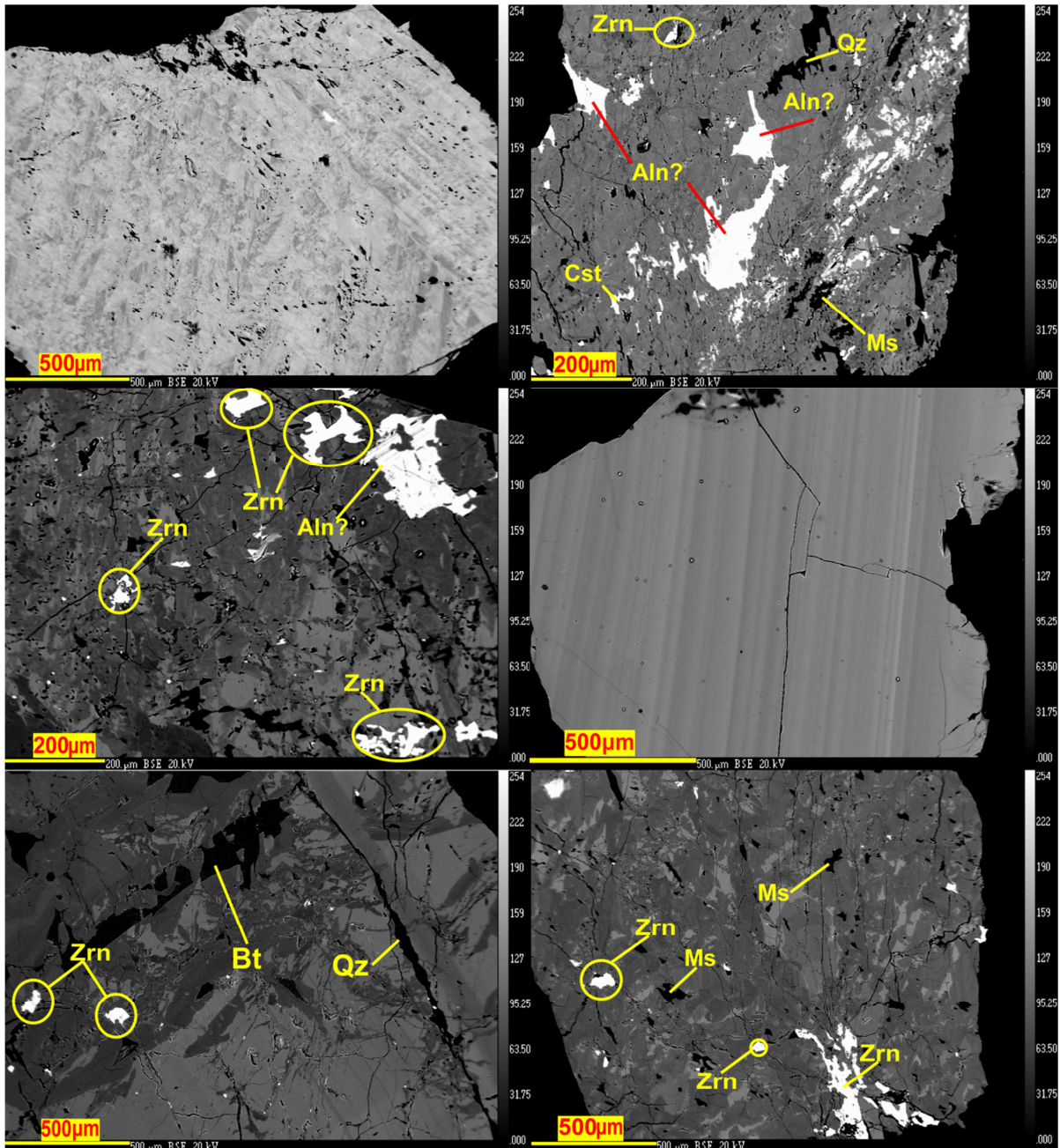
Figure 15: BSE-images of the samples 22286Tuftane (top left), 22330_4-(top right), _1Torvelona (middle left), 22238Tjomstøl (middle right), 22370Eptevann (bottom left) and 22273Håvarstad (bottom right). "Aln?" refers to the question if this is allanite. Zrn= zircon. Ms= muscovite. Cst= cassiterite.

Backscatter of electron (BSE) images shows two generations of oscillatory zoning, in some of the thortveitites, which have a different orientation relative to each other. It is only sample *22302_1Knapen* that show the zones from what probably is the core (dark zone) and outwards in the crystal (Figure 17). The samples with irregular zoning-patterns, e.g. *22330_1Torvelona* and *22273Håvarstad* also have inclusions and fractures filled with zircon (**Error! Reference source not found.**)

Chemistry

The thortveitite group consist of several disilicates (sorosilicates) that have the general formula $M^{3+}_2Si_2O_7$ where M= Sc, Y or Yb. The three end-members of the group are presented in Table 4.

Table 4: The three end-members of the thortveitite group. After Strunz and Nickel (2001)

Mineral	Ideal formula
Thortveitite	$Sc_2Si_2O_7$
Keiviite-(Y)	$Y_2Si_2O_7$
Keiviite-(Yb)	$Yb_2Si_2O_7$

Major element chemistry

The results of the EMP and LA-ICP-MS analysis are presented in Table 8, Appendix 2. Averages of these analyses, for the different samples, are presented in Table 5. As the averages of the samples are from the different zones, the standard deviation is large for some of the samples. Of the collected samples, the highest Sc_2O_3 content is found in the samples *22370Eptevann* (47 wt.% Sc_2O_3) and *22273Håvarstad* (46 wt.% Sc_2O_3). The samples *22292_1Tuftane* (27 wt.% Sc_2O_3)and *22286Tuftane* (27.1 wt.% Sc_2O_3) have the lowest Sc-content. The opposite goes for the Y and REE content, where *22370Eptevann* (0.7 wt.% Y_2O_3 and 1.3 wt.% REE_2O_3) and *22273Håvarstad* (1.7 wt.% Y_2O_3 and 2.3 wt.% REE_2O_3) have the lowest Y and REE content, while *22292_1Tuftane* (15.2 wt.% Y_2O_3 and 14 wt.% REE_2O_3) and *22286Tuftane* (13.84 wt.% Y_2O_3 and 14 wt.% REE_2O_3) have the highest Y and REE content. The ZrO_2 content varies from 1.7 wt.% ZrO_2 for *22239Ljosland*, to 3.9 wt.% ZrO_2 in *22304Eretveit*. The only sample that exceeds 1wt.% MnO is *22304Eretveit* (1.1 wt.% MnO). All the samples have less than 1.00 wt.% oxide when it comes to MgO, CaO and TiO_2. The Hf content varies from 0.18 wt.% HfO_2 in *22239Ljosland* to 0.7 wt.% HfO_2 in *22304Eretveit*.

Table 5: Average wt.% oxide and apfu of the collected thortveitite samples. Values marked with "*" are obtained from LA-ICP-MS analysis. For all the analyzes, see Table 8, Appendix 2

	22302	22304	22370	22273	22286	22330	22238	22239	22292_1	22292_2
n	7	5	5	4	2	9	12	14	4	7
SiO_2	42.3(4)	40.8(7)	44(1)	44.5(	38.9(1)	43(1)	44.1(5)	43.7(7)	38.4(5)	38(1)
Sc_2O_3	38(2)	33(2)	47(3)	46(3)	27.1(2)	41(5)	44(2)	45(2)	27(1)	29(3)
Y_2O_3	5(1)	9.1(8)	0.7(2)	1.7(7)	13.84(2)	4(2)	2.1(2)	2(1)	15.2(8)	13(2)
Fe_2O_3	1.2(2)	1.5(7)	1.2(6)	1.2(5)	2.1(2)	1.1(7)	1.1(5)	1.1(3)	1.1(2)	1.1(5)
FeO	0.4(2)	-	0.4(3)	-	0.1(1)	-	0.6(5)	-	-	-
MnO	0.7(3)	1.1(4)	0.4(4)	0.3(3)	0.68(8)	0.8(7)	0.6(4)	0.09(6)	0.4(1)	0.4(2)
ZrO_2	2.6(5)	3.9(9)	2(1)	2.2(8)	2.9(3)	2(1)	2.8(9)	1.7(2)	2.1(2)	2.1(8)
REE_2O_3	5.6*	6.9*	1.3*	2.3*	14.0*	6*	2.6*	4.0*	14.0*	13*
MgO	0.05*	0.17*	0.09*	-	0.12*	0.05*	0.09*	-	0.06*	0.05*
CaO	0.31*	0.4*	0.14*	0.11*	0.31*	0.1*	0.1*	0.1*	0.23*	-
TiO_2	0.11*	0.18*	0.06*	0.04*	0.17*	-	0.07*	0.03*	0.072*	0.7*
SrO	<0.01*	<0.01*	<0.01	<0.01	<0.01	<0.01	<0.01	<0.01	<0.01	<0.01
HfO_2	0.6*	0.7*	0.3*	0.4*	0.68*	0.5*	0.6*	0.18*	0.5*	0.5*
Ta_2O_5	-	0.016*	<0.01	-	<0.01	-	<0.01	<0.01	<0.01*	<0.01*
PbO	<0.01*	<0.01*	<0.01	-	<0.01	-	<0.01	-	<0.01	-
ThO_2	<0.01*	0.02*	<0.01	<0.01	0.01*	-	<0.01	<0.01	<0.01*	-
UO_2	-	0.03*	-	-	<0.01	-	0.04*	-	<0.01*	<0.01*
Total	99.1(6)	98(1)	99 (1)	100	101.4(3)	100(1	99.6(9)	100.1(9	100(1)	99(1)
Formula proportions based on 7 oxygen										
Si	1.98	1.97	1.98	1.97	1.97	1.98	1.98	1.97	1.96	1.96
Sc	1.58	1.40	1.82	1.83	1.19	1.6	1.73	1.78	1.24	1.2
Y	0.14	0.23	0.012	0.03	0.37	0.11	0.047	0.06	0.41	0.37
Fe3+	0.04	0.05	0.03	0.04	0.07	0.03	0.03	0.03	0.04	0.03
Fe2+	0.00	0.00	0.00	0.00	0.00	0.00	0.00	0.00	0.00	0.00
Mn	0.02	0.04	0.00	0.00	0.02	0.00	0.02	0.00	0.01	0.00
Zr	0.05	0.09	0.05	0.04	0.06	0.04	0.05	0.032	0.047	0.04
REE	0.077	0.10	0.012	0.03	0.21	0.08	0.030	0.05	0.21	0.20
Mg	0.00	0.01	0.00	0.00	0.00	0.00	0.00	0.00	0.00	0.00
Ca	0.01	0.02	0.00	0.00	0.01	0.00	0.00	0.00	0.01	0.00
Ti	0.00	0.00	0.00	0.00	0.00	0.00	0.00	0.00	0.00	0.00
Sr	0.00	0.00	0.00	0.00	0.00	0.00	0.00	0.00	0.00	0.00
Hf	0.00	0.00	0.00	0.00	0.00	0.00	0.00	0.00	0.00	0.00
Ta	0.00	0.00	0.00	0.00	0.00	0.00	0.00	0.00	0.00	0.00
Pb	0.00	0.00	0.00	0.00	0.00	0.00	0.00	0.00	0.00	0.00
Th	0.00	0.00	0.00	0.00	0.00	0.00	0.00	0.00	0.00	0.00
U	0.00	0.00	0.00	0.00	0.00	0.00	0.00	0.00	0.00	0.00
Total	3.9	3.94	3.9	3.9	3.99	3.9	3.9	3.9	3.9	3.7
End-members %										
Thor.	88	82	98.4	96	70.68	90	95.9	94	69	71
K-(Y)	8	13	0.9	2.2	21.9	6	2.8	3	23	21
K-(Yb)	2.7	3.1	0.6	1.08	7.32	2.9	1.1	1.9	7.3	7

Sum	100	100	100	100	100.0	100	100	100	100.0	100

22302 Knapen, Birkeland Avg. 22304 Eretveit Avg. 22370 Eptevann Avg. 22273 Håvarstad22286

Tuftane, Frikstad Avg.22330 Torvelona, Ljosland Avg.22330 Torvelona, Ljosland Avg.Tuftane, Frikstad Avg. 22238 Tjomstøl Avg. 22239 Ljosland Avg. 22239 Ljosland Avg. 22292_1 Tuftane, Frikstad Avg. 22292_2 Tuftane, Frikstad Avg.
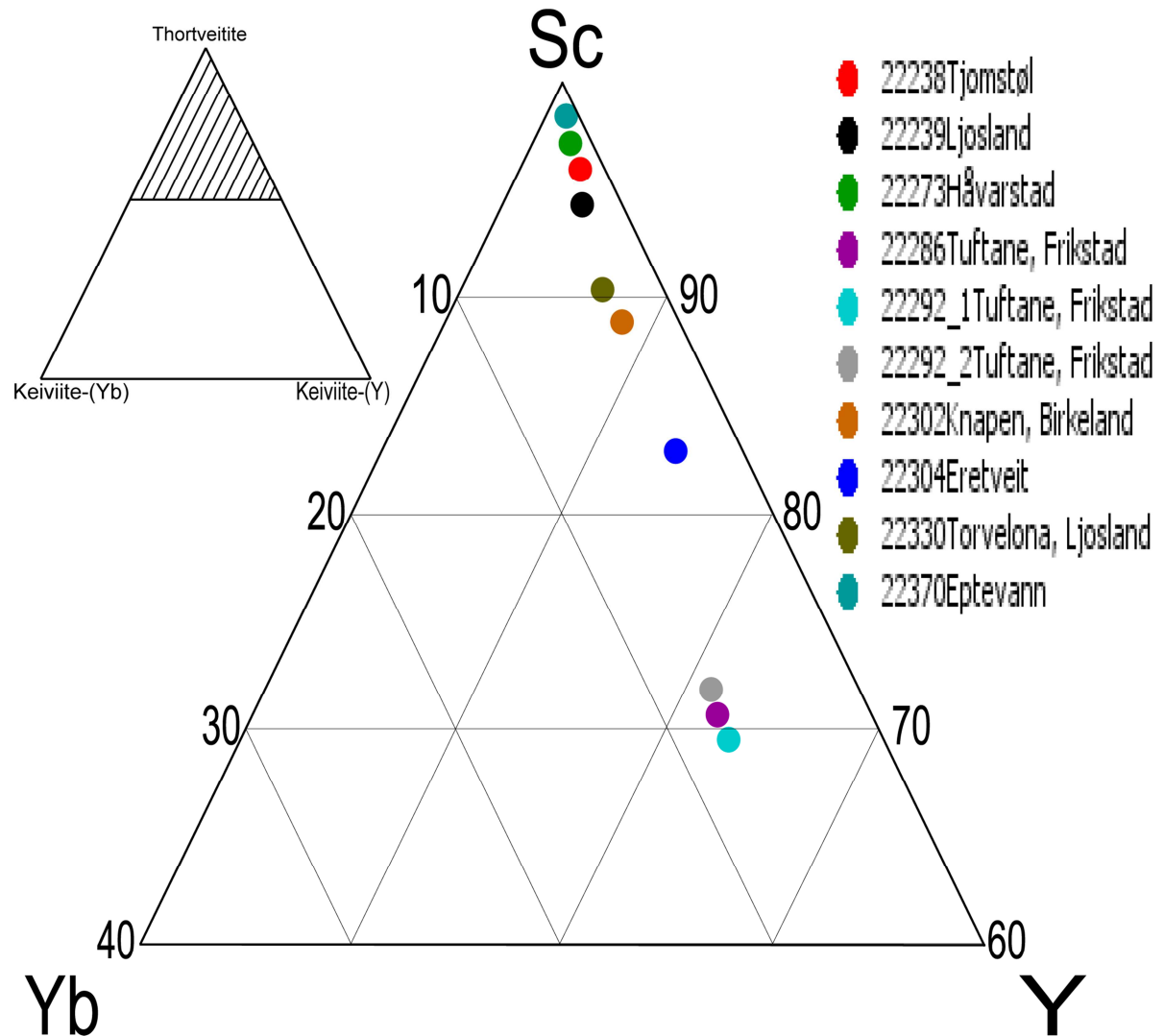
Figure 16: Ternary plot of Sc, Y and Yb distribution on average in the collected thortveitite samples. Note that the plot, due to the high Sc-content in the samples, is over 60% Sc.

The collected samples are within the thortveitite-field, as the atomic Sc content in all is above 50% (Figure 16 and Table 5)

The thortveitite samples are not compositional homogenous (Figure 15), where the darker the zoning, the more Sc content there is. Yttrium and the HREEs tend to have an reveres trend, however, this is not the case for *22370Eptevann* where the Yb content is higher in the dark zoning compared to the medium zoning. The sample *22302_1Knapen*, which was cut perpendicular on its longest axis, is a

example of concentric oscillating zoning in which the Sc content decreases from dark, through medium and to the pale zone (Figure 17 and Table 6)
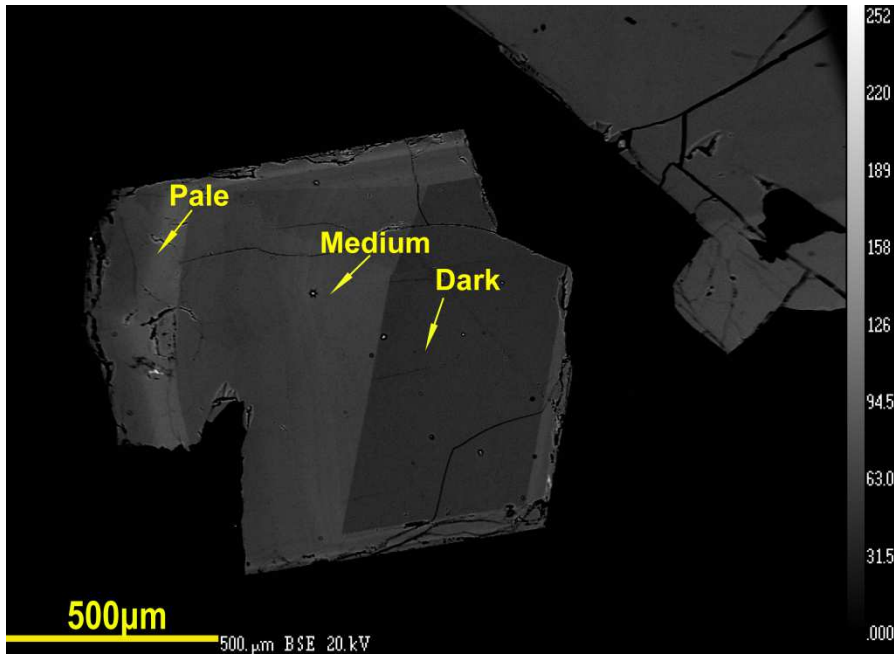
Figure 17: BSE-image of the thortveitite-sample 22302_1Knapen, showing the different zoning patterns that have been measured.

Table 6: Wt.% oxide and apfu based on seven oxygen in the zones in sample 22302_1Knapen

	Pale	Medium	Dark
n	1	1	1
SiO2	42.08	42.52	42.56
Sc2O3	37.09	39.11	39.91
Y2O3	7.00	6.05	5.46
Fe2O3	1.03	1.25	1.23
FeO	0.63	0.36	0.32
MnO	0.89	0.72	0.58
ZrO2	2.77	2.61	2.35
REE2O3	5.78*	5.94*	5.42*
MgO	0.06*	0.05*	0.04*
CaO	0.3*	0.31*	0.35*
TiO2	0.14*	0.1*	0.12*
SrO	<0.01*	<0.01*	<0.01*
HfO2	0.82*	0.64*	0.5*
Ta2O5	0.02*	<0.01*	<0.07*
PbO	<0.01*	<0.01*	<0.01*
ThO2	<0.01*	<0.01*	<0.01*
UO2	0.01*	0.01*	0.01*

	98.627	99.684	98.863
Formula proportions based on 7 oxygen			
Si	2	1.99	1.99
Sc	1.53	1.59	1.62
Y	0.17	0.15	0.13
Fe3+	0.03	0.04	0.04
Fe2+	0.02	0.01	0.01
Mn	0.03	0.02	0.02
Zr	0.06	0.05	0.05
REE	0.08	0.08	0.07
Mg	0.00	0.00	0.00
Ca	0.01	0.01	0.01
Ti	0.00	0.00	0.00
Sr	0.00	0.00	0.00
Hf	0.01	0.00	0.00
Ta	0	0	0
Pb	0	0	0
Th	0	0	0
U	0	0	0
	3.91	3.91	3.92

Sample *22238Tjomstøl* and *22292Tuftane*, which have one of the highest and lowest Sc content, respectively, were chosen as examples on the distribution of Sc, Y and Yb in the zoning-patterns (Figure 18).
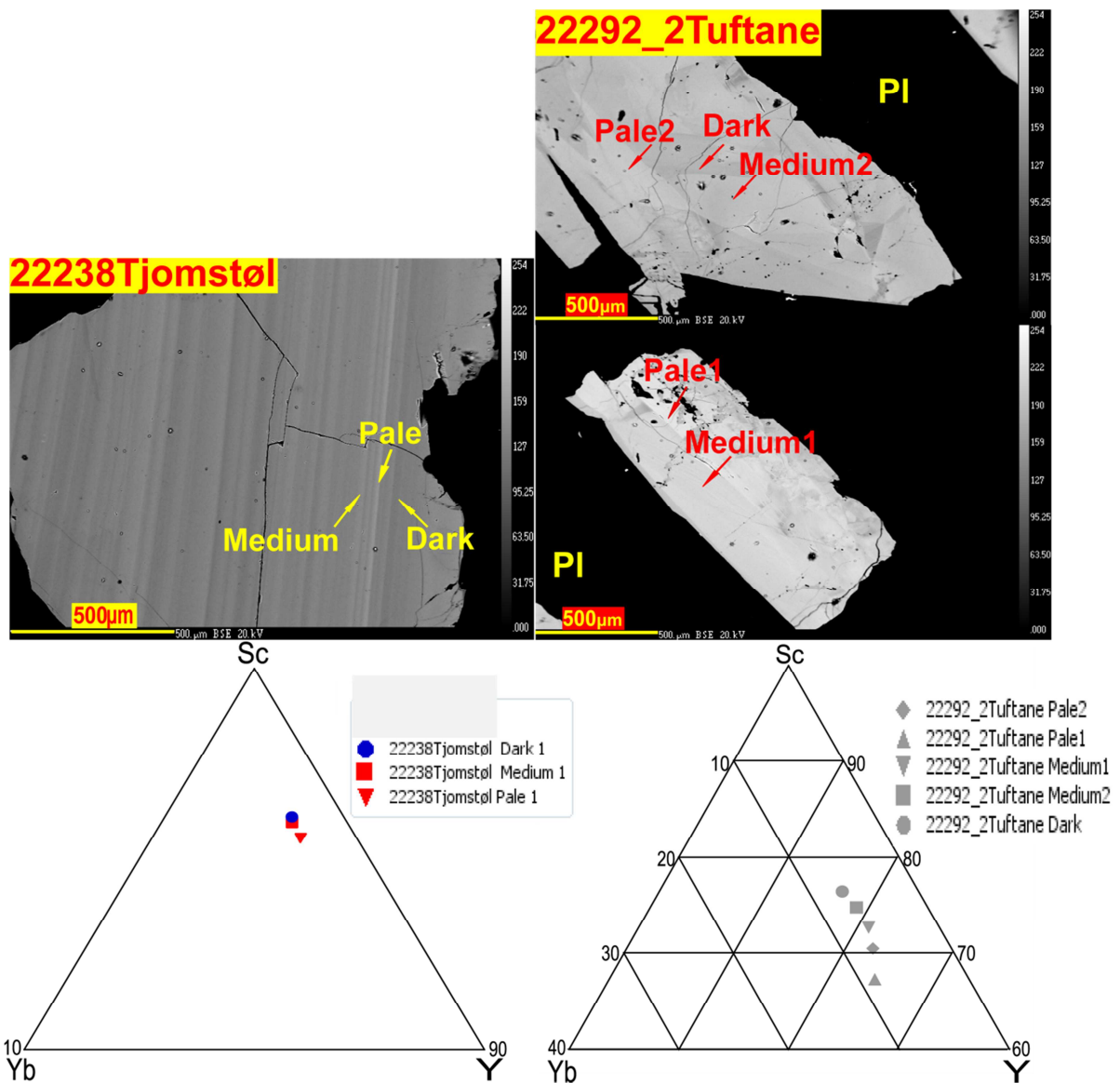
Figure 18:Ternary plot showing zones of 22238Tjomstøl and 22292_2Tuftane. Due to the small differences in Sc, Y and Yb between the zones in 22238Tjomstøl compared to 22292_2Tuftane, the scales on the two plots are different. Pl=plagioclase.

The zones in *22238Tjomstøl* are closer to each other in Sc, Y and Yb composition compared to the zones of *22292_2Tuftane*.
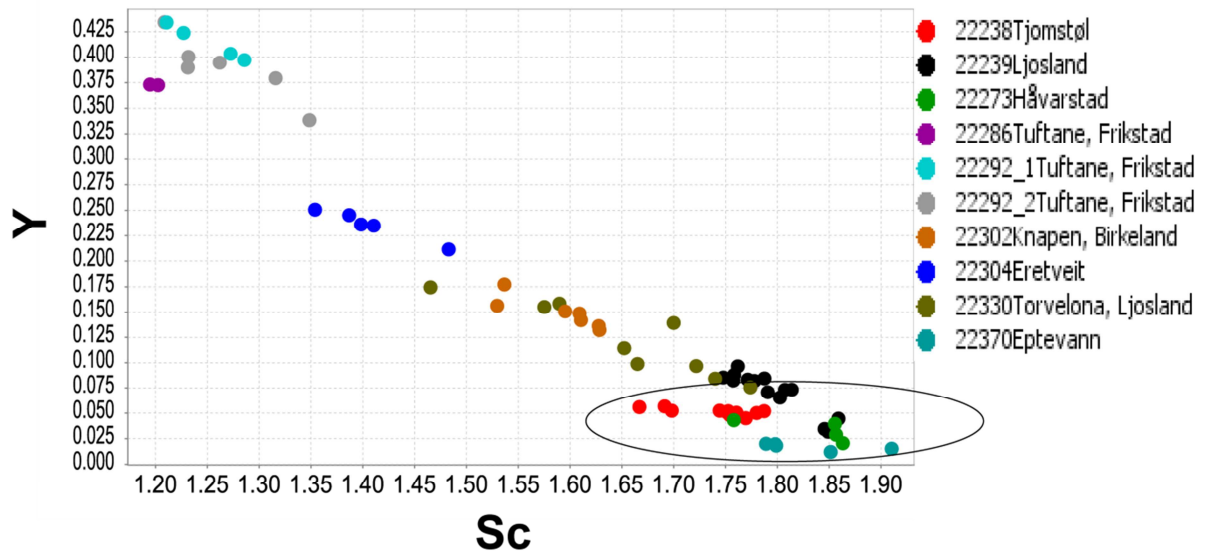
Figure 19:Relation between Sc and Y in the collected thortveitite samples
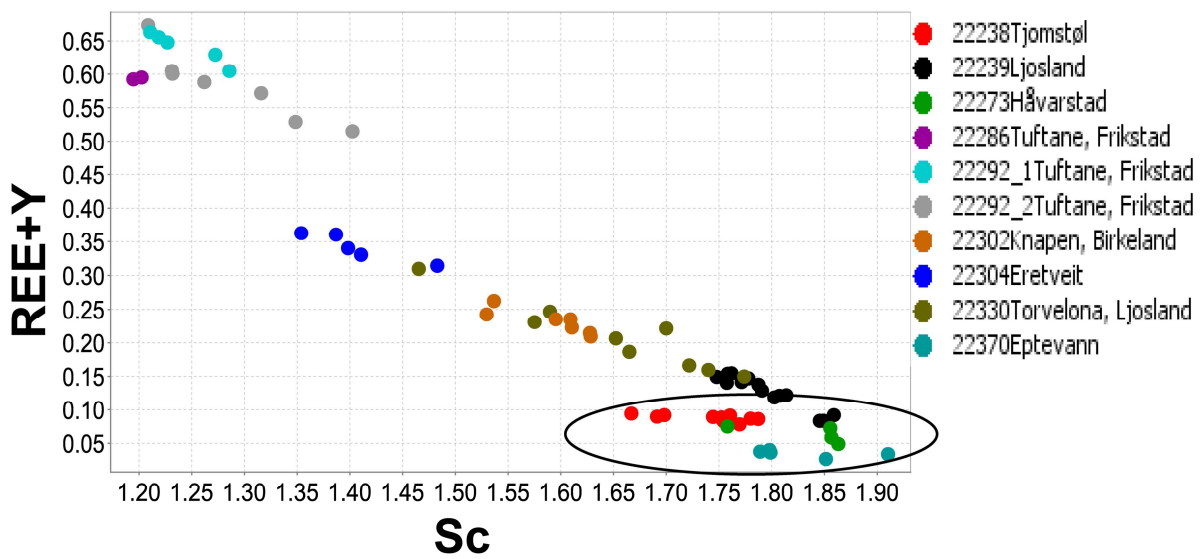
Figure 20: Plot of Sc versus REE+ Y (apfu) in the collected thortveitites. Note the close to zero change in Y+REE in 22238Tjomstøl and 22370 Eptevann.

There is a clear substitution between Y and Sc (Figure 19). However, the plot does not indicate a 1:1 substitution. When combining Y with the REEs, the substitution with Sc moves closer towards a 1:1 substitution (Figure 20).

Figure 20 shows that the REEs and Y decreases when Sc increases in the samples. However, in *22238Tjomstøl* and *22370Eptevann*, there is a minimal change in the already low Y and REE content.
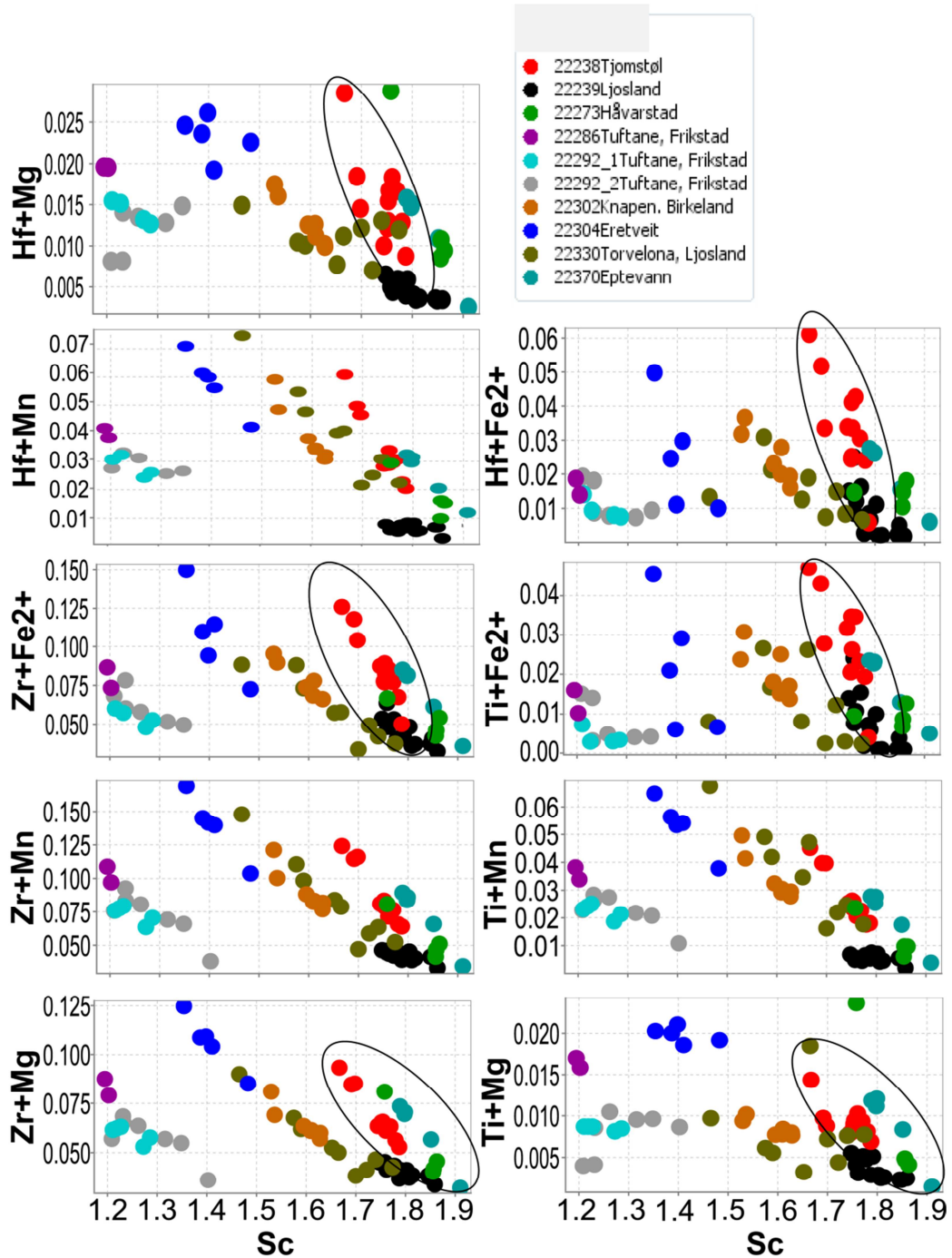
Figure 21: Relation between Sc and other coupled elements (in apfu) that gives a total of 6+ in ionic charge.
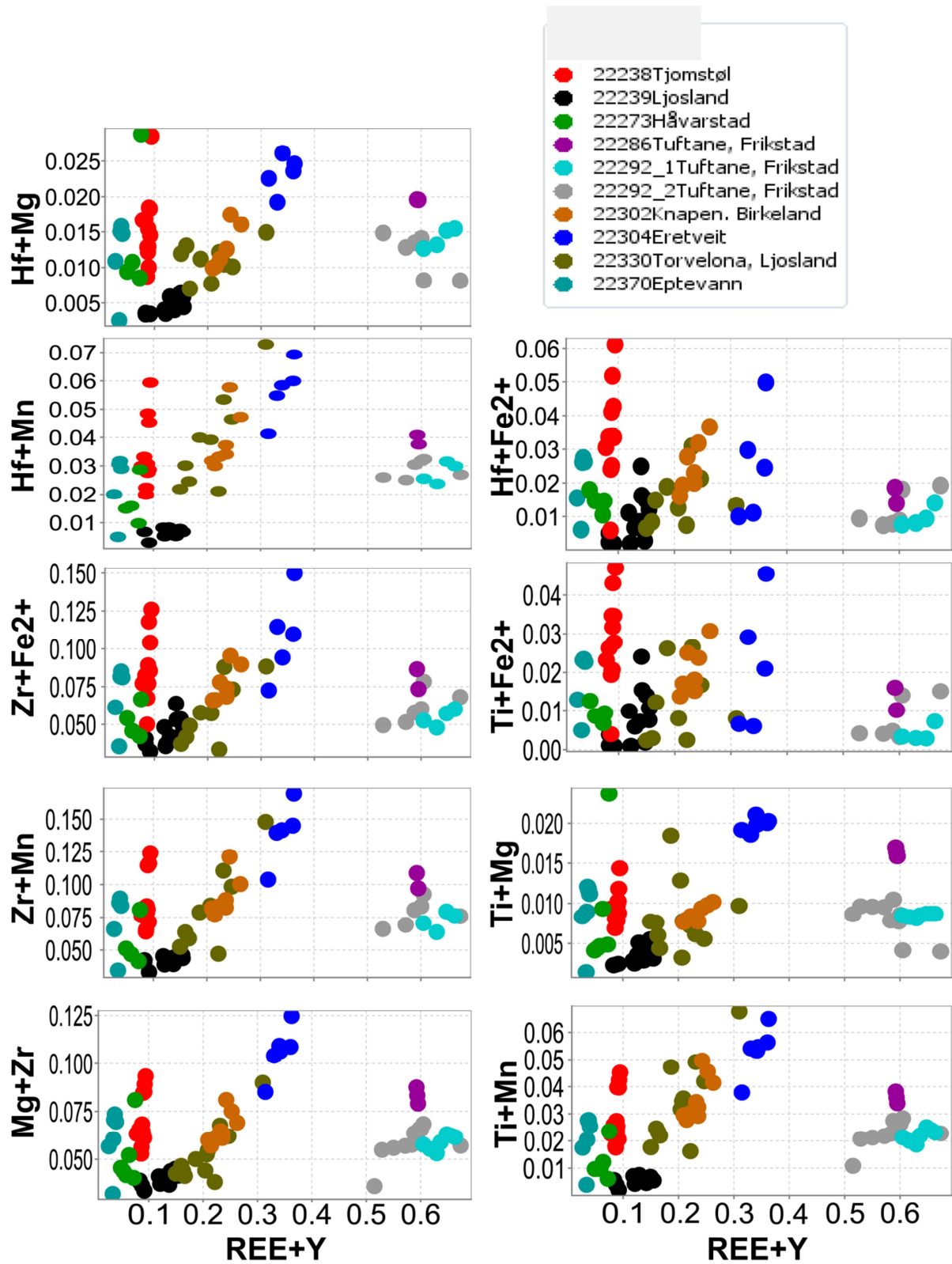
Figure 22: Relation between the REEs+Y and elements that substitutes for Sc in Figure 21.

Combinations of several elements that give a total ionic charge of 6+ are showing a decreasing trend, although variable (e.g. Sc versus Mg+Ti), when the Sc content increases in the thortveitites (Figure

21). The same combinations have an increasing trend when the Y and REE content increase (Figure 22).
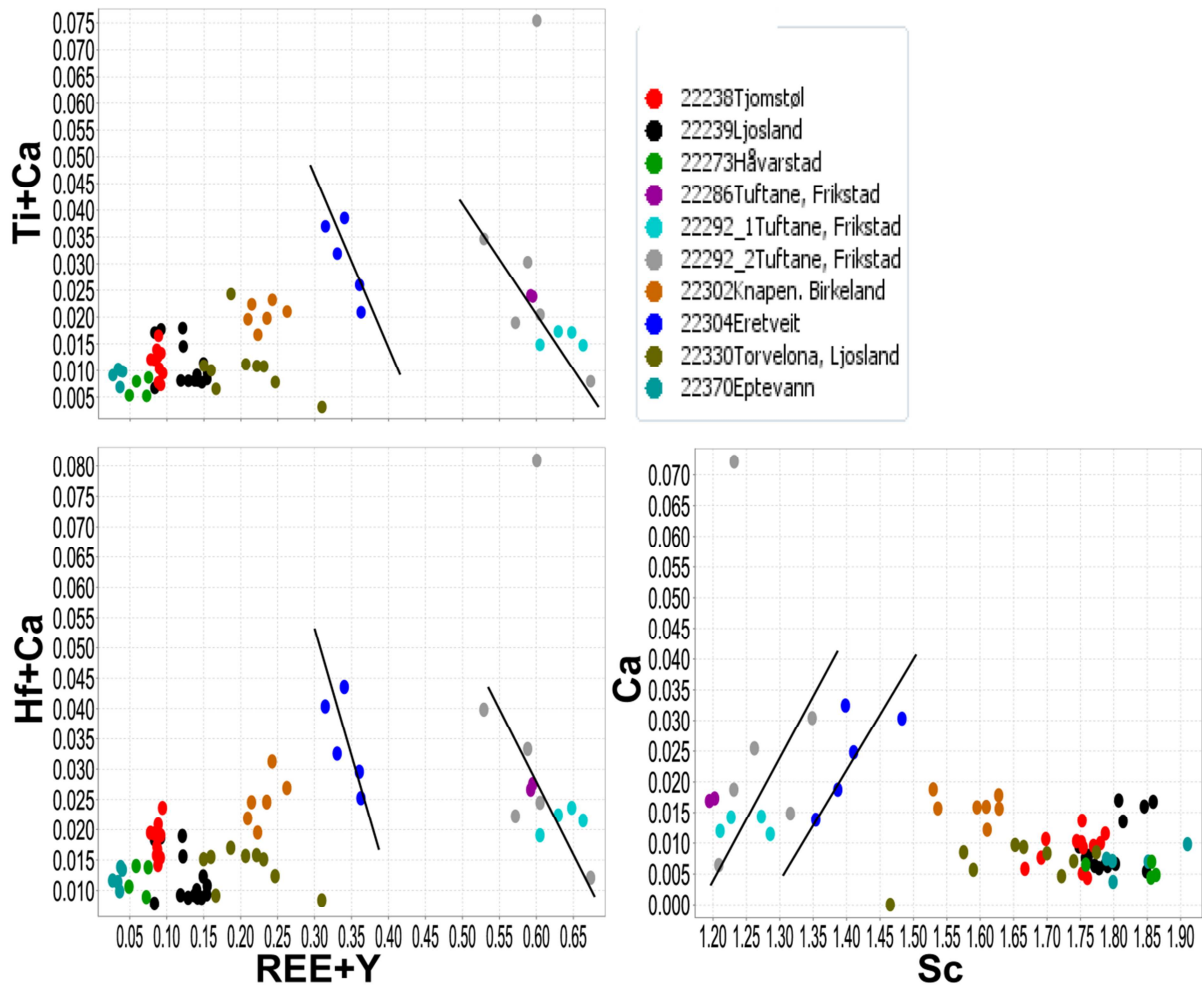
Figure 23: Relation between REE+Y and Ca and Sc and Ca in the thortveitites.

There is an opposite trend when it comes to the Ca content in the samples. Calcium has a positive correlation to the change in Sc while an inverse change compared to REE+Y (Figure 23).

Trace-element chemistry

The chondrite normalized REE plot (Figure 24) shows a strong enrichment in HREE, which is expected as substitution between Sc and the HREEs is possible due to similar ionic radii and ionic charge.
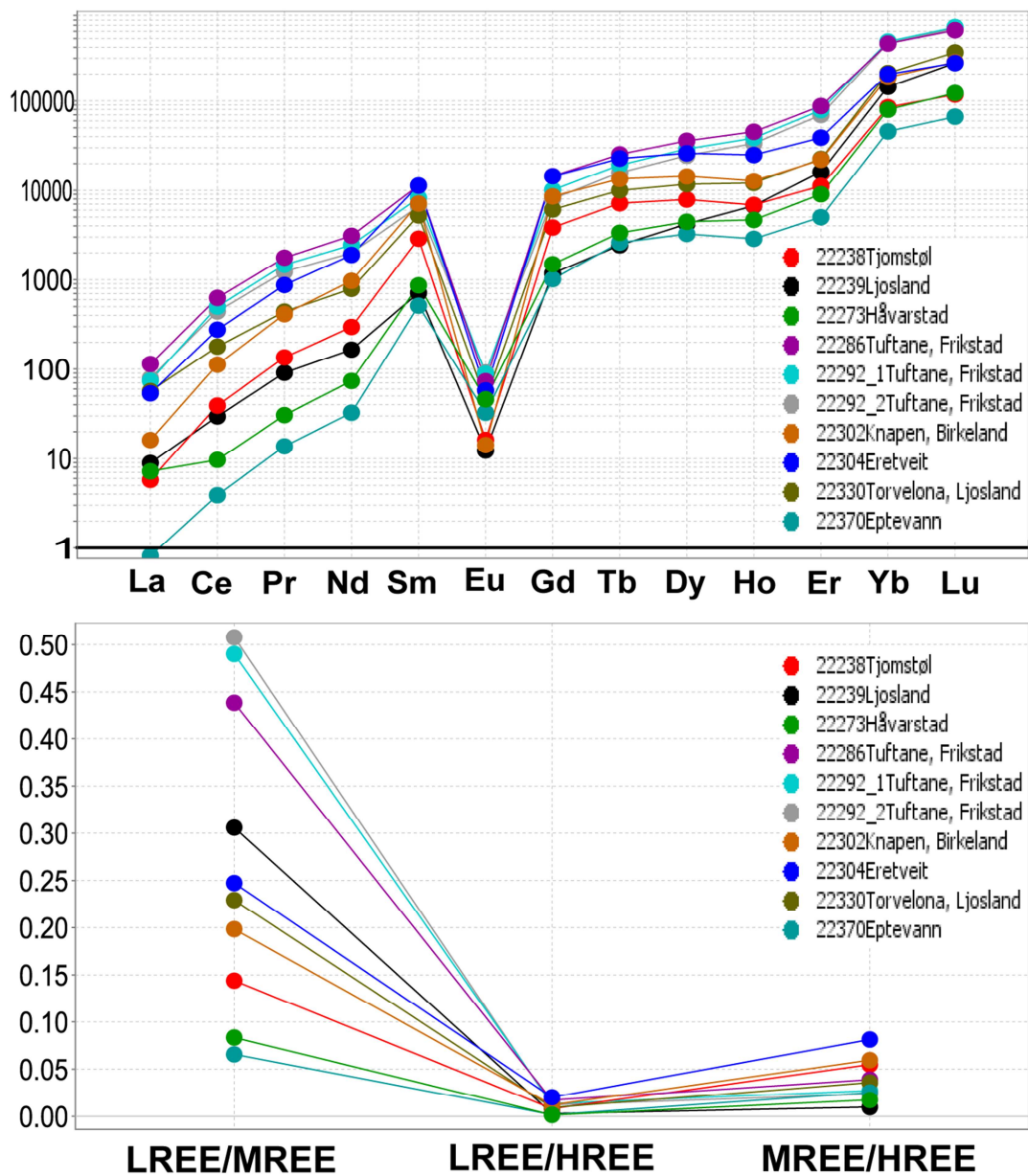
Figure 24:REE chondrite normalized plot for the thortveitite samples (McDonough and Sun, 1995)

Two trends in the chondritic plot can be observed. *22239Ljosland*, *22286Tuftane* and *22292Tuftane* (1 and 2) has the regular enrichment of HREEs. The remaining samples on the other hand, have a lower enrichment in the HREEs. Here, the plot forms a plateau from Tb to Ho before it resumes increasing from Er to Lu.

Discussion

The pegmatites

The abundance of pegmatites in the amphibolite in Evje-Iveland makes this one of Norway's largest pegmatite fields and is part of the Setesdalen pegmatite district. Other large pegmatite fields in the Sveconorwegian pegmatite province are e.g. the Froland pegmatite field in the Bamble district, which is close to Evje-Iveland, and the Østfold-Halland pegmatite district. The Evje-Iveland pegmatite field consists of over 400 pegmatites with a volume of over 1,000m^3, confined in a ca. 30km long and 10km wide, N-S trending area (Müller et al., 2015). This area has been investigated by several authors from the beginning of the 20th century and up to present. Although most of the pegmatites are hosted by amphibolite, the surrounding granitic gneiss and augengneiss also hosts some pegmatites. The pegmatites are classified, after Müller et al. (2012) and Müller et al. (2015), as rare element REE and muscovite rare element REE classes in the classification scheme by Černý and Ercit (2005) (Table 7) (Müller et al.,2012;Müller et al.,2015). A U/Pb dating of one gadolinite gave the age 910 ± 14 Ma (Scherer et al., 2001) while $^{206}Pb/^{238}U$ dating of a monazite gave the age of 906±9 Ma (Seydoux-Guillaume et al., 2012). However, both of these samples were from unspecified pegmatites (Müller et al., 2015). Rb-Sr dating of K-feldspar in pegmatites in the northern part of Evje-Iveland gave an isochron age of 852±2 Ma (Larsen, 2002). Snook (2014) argues that these ages indicate that the pegmatites are too young to be differentiates from the spatially close Høvringsvatnet complex (Figure 25) which was first suggested by Bjørlykke (1937)
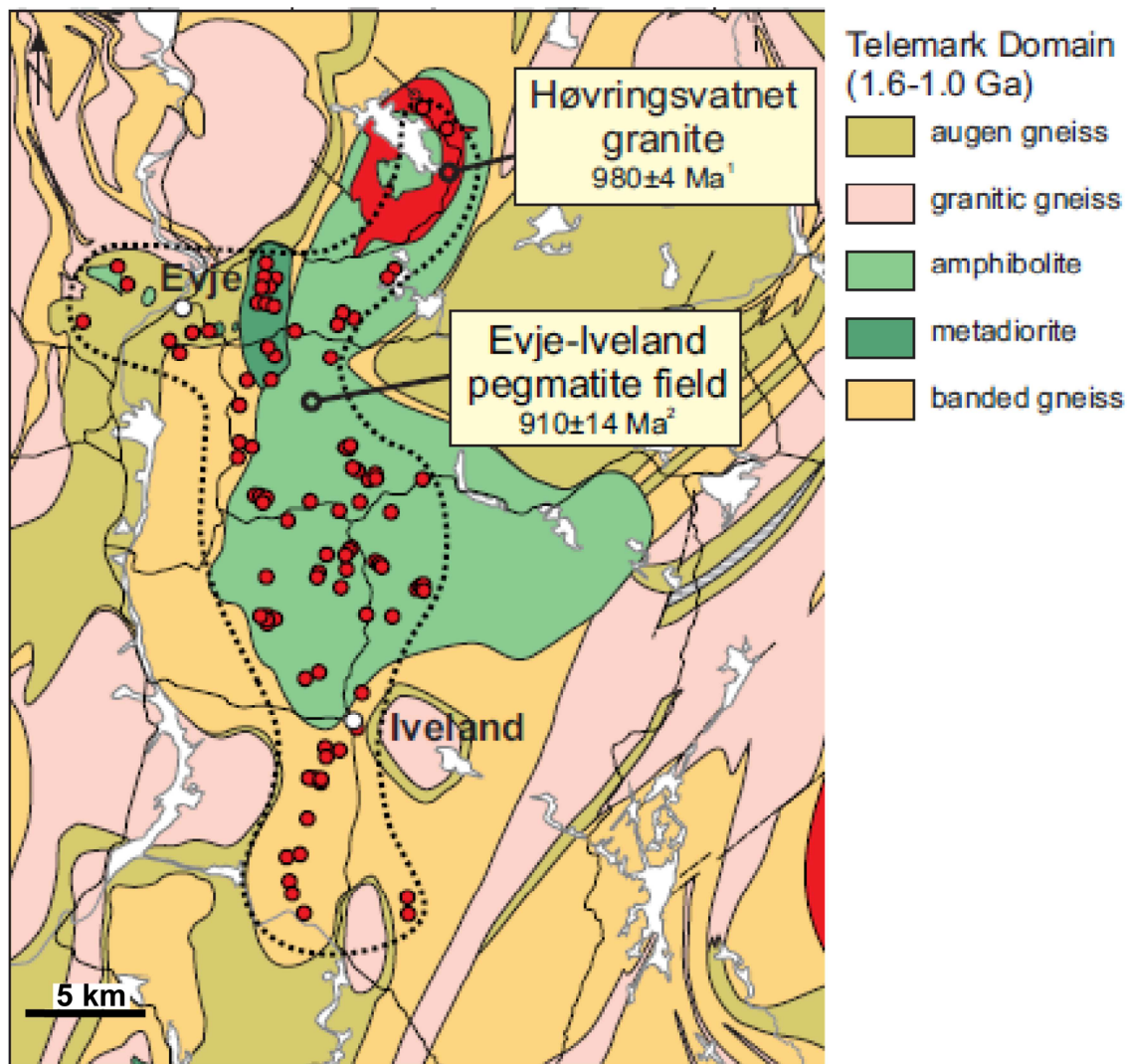
Figure 25: Map of the Evje-Iveland pegmatite field, with the Høvringvatnet complex. (Modified after Müller et al., 2015)

Garnet-chemistry

Major elements

Ca and Mg

The low Ca and Mg contents of the collected garnets, maximum CaO (0.9wt.% CaO) measured in *25375Ivedal* and maximum Mg (ca. 1wt.% MgO) measured in *25370Kåbuland*, could have several reasons. One of these reasons could be the presence of more Ca- and Mg-compatible minerals. Plagioclase, which is Ca-bearing, is one of the most dominant minerals in the pegmatites, while Mg-bearing micas also occur in large amounts in the pegmatites. The variable decrease or increase, which is low (~0.1wt.% or lower for MgO and CaO), for both Mg and Ca from core to rim of the garnets, could also be controlled by the presence or absence of Mg- or Ca- bearing minerals. This is consistent with the work with composition of garnets by Chernoff and Carlson (1997). In their work, they added the compositional control factor by coexisting minerals to the work of Cerny et al. (1985),

who had stated that the melt composition was the major controlling factor of the composition of magmatic garnets (Müller et al., 2012). (Müller et al. 2012) noted that there was a lower Ca content in the Evje-Iveland pegmatites compared to the Froland pegmatites.

Fe-Mn

The domination of the spessartine over the almandine component in the analyzed garnets in this study (Figure 9) is consistent with the findings of Müller et al. (2012) and shows a typical garnet chemistry in pegmatites (London, 2008; Müller et al., 2012)

The generally large Mn/ (Fe+Mn)-ratio in the collected garnets can be explained by the presence of other Fe-bearing minerals that can have formed before the garnets and depleted the melt in Fe. However, this does not explain the decrease in the Mn/Fe-ratio from core to rim in some of the garnets. In the case of the garnets with a decrease in Mn/Fe-ratio, eg *25444Håvarstad* and *25409Landås*, the small decrease could be the result of the Fe and Mn composition of the melt. As the Mn content of the melt is depleted, more Fe is incorporated into the garnet, which agrees with the fact that Mn is more easily incorporated into the garnet than Fe (Feenstra and Engi, 1998). The increasing Mn/(Fe+Mn)-ratio from core to rim in e.g. *MSB-5Slobrekka* and *25375Ivedal* could be explained by the presence of Fe-bearing minerals. Mafic minerals, e.g. columbite, magnetite and biotite that could be more Fe-compatible than garnet, could be formed at the same time as the garnets, leading to the decrease of Fe from core to the rim (Müller et al., 2012). However, Müller et al. (2012) noted that despite the presence of Fe-bearing minerals, the decrease in Fe from core to rim in their garnet sample was low. This could indicate that one or more other factors, alone or in combination with Fe-bearing minerals being present, control the change in the Mn/(Fe+Mn)-ratio.

The samples with the lowest Fe content, *MS-9Solås*, *25447Røykvartsbruddet*, *25421Frikstad*, *25374Frøyså* and *25412Røykvartsbruddet*, in which the latter has the highest Fe content (7 wt.% FeO) of the mentioned samples, could all be from a cleavelandite zone or similar replacement unit. *MS-9Solås* was certainly collected from a cleavelandite zone. According to Müller et al. (2012), the melt that formed the replacement zone at Solås had a low Fe content. This could indicate, if accepting this idea, a systematic trend in Evje-Iveland in which garnets with a low Fe content are from a replacement zone e.g. cleavelandite. By following this theory, a low Fe content in garnets could also help to indicate if whether a pegmatite has experienced replacement, even when the replacement is not directly exposed. *25412Røykvartsbrudded*, which has a higher Fe content than *25447Røykvartsbruddet,* could be from a position closer to the border between the replacement unit and the unaltered part of the pegmatite, than the latter. However, since these samples, except *MS-9Solås*, are from the collection at NHM and was not accompanied by other minerals, this theory cannot be completely verified.

Based on the values for the Mn/(Fe+Mg) ratio of the collected garnets, the Solås- and Røykkvartsruddet pegmatite, along with the pegmatites where samples *25374Frøyså* and *25421Frikstad* are from, are the most fractionated of the investigated pegmatites. This is consistent with the work on an increasing Mn/(Fe+Mg)-ratio during fractionation of a melt, done by Miller and Stoddard (1981)

The Mn/(Fe+Mn) ratio of the collected garnets, based on Müller et al. (2012) also indicates the same fractionation trend as the Mn/(Fe+Mg)-ratio, but the less fractionated pegmatites are more distinguishable. Steli is the least fractionated pegmatite of the less fractionated pegmatites. This is also consistent with Müller et al. (2012), who also mention the Li gruve pegmatites as the relative least fractionated. The remaining primitive pegmatites all have different ratios, but these are negligible. By the ratios of Mn/(Fe+Mg) and Mn/(Fe+Mn), three "fractionation" groups could be observed; fractionated (Solås, Røykkvartsbruddet, Frøyså and *25421Frikstad*), less fractionated (e.g. Mølland and Heia, Ljosland) and least fractionated (Steli, Tveit)   (**Error! Reference source not found.**). The majority of the least fractionated pegmatites have a distribution from east to west in the pegmatite field. This could indicate that these pegmatites lies within a zone confined to a regional zoning pattern that are formed from an igneous or thermal heat source. This regional zoning could have an increasing fractionation trend towards the north or south. However, this "pattern" of distribution is disrupted by the fact that some of the less fractionated pegmatites are from areas that are close to fractionated pegmatites, e.g. *25370Kåbuland* (less fractionated) and *25447Røykkvrartsbruddet, Birkeland* (fractionated) (Figure 26 and Figure 3)
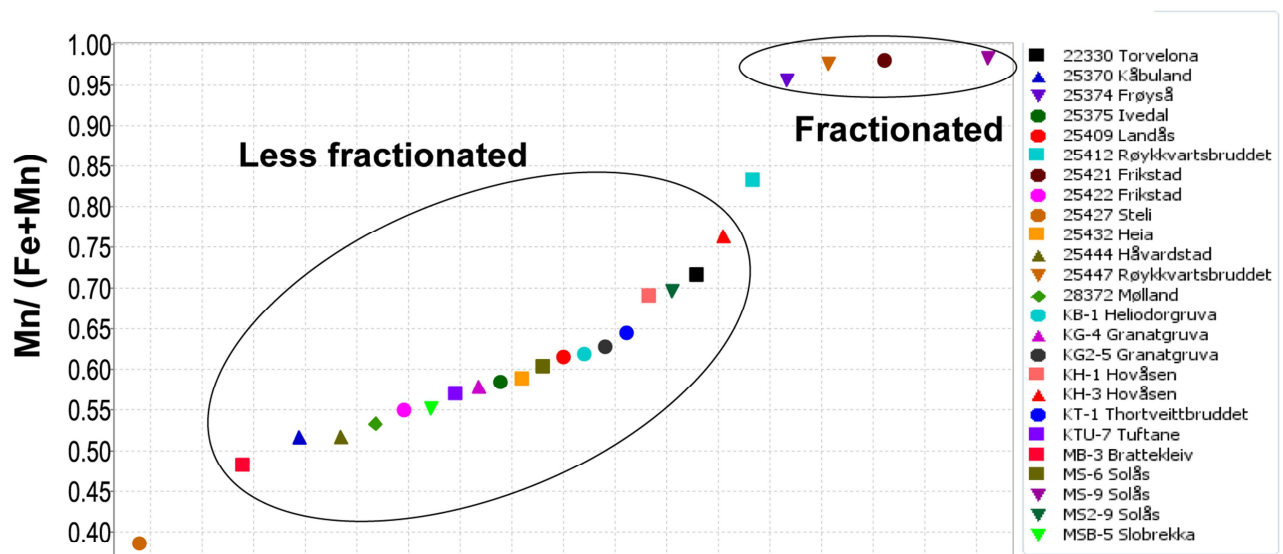
Figure 26: The Mn/(Fe+Mn) ratio in the collected garnets and the interpreted fractionation division.

Trace elements

Yttrium, scandium and REE

The majority of the collected garnets show a trend where the Y content changes with changes in the Mn core to rim composition, which is consistent with the findings of Jaffe (1951) and Geller and Miller (1959) (

and Figure 27**Error! Reference source not found.**). Yttrium can enter garnets through the coupled substitution $Y^{3+}(REE)^{3+}+Al^{3+} = Mn^{2+}+Si^{4+}$ (Jaffe, 1951; Geller and Miller, 1959) to preserve the charge balance. One example of this is *25375Ivedal*, which has a Mn/(Fe+Mn) ratio increase from 0.56 to 0.6 while the Y content increases from 0.053 to 0.07 apfu from core to rim. The same goes *25409Landås*, which has a decrease in Y content from 0.089 to 0.03 apfu while the Mn/(Fe+Mn)-ratio decreases from 0.63 to 0.60.
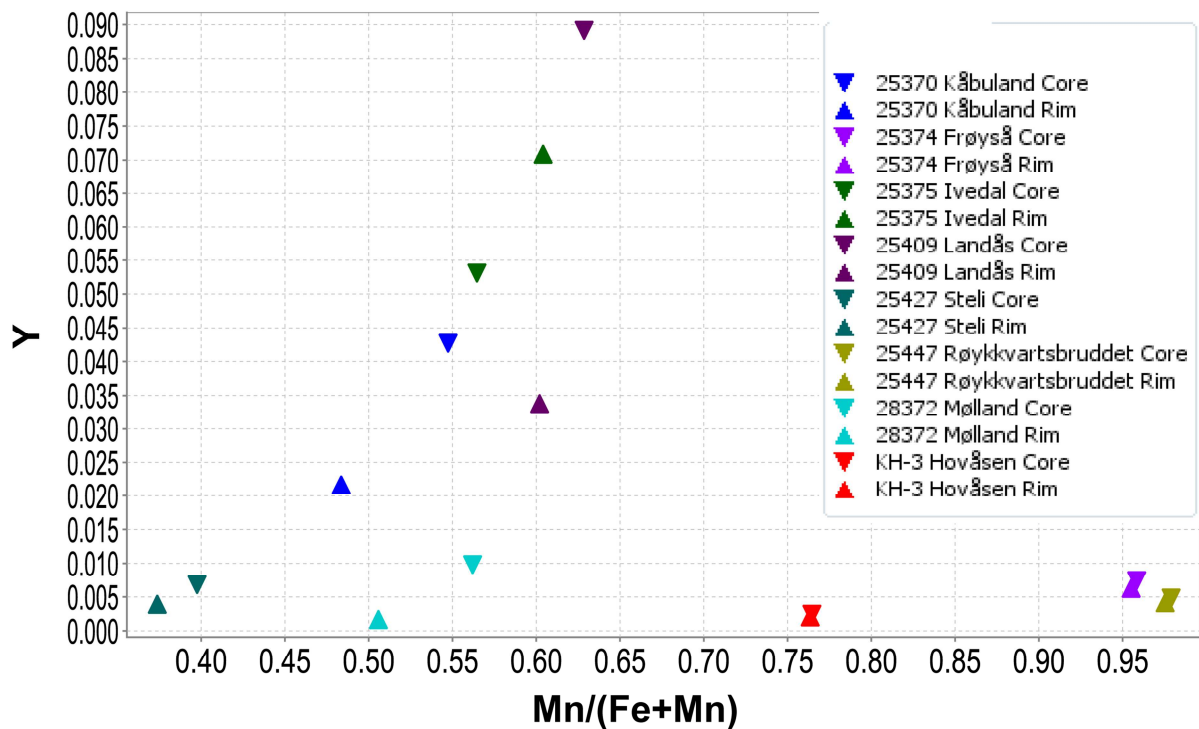
Figure 27: Plot showing a positive correlation between Y (apfu) and the Mn/(Fe+Mn)-ratio.

However, samples like e.g *MSB-5Slobrekka* and *25432Heia*, do not indicate a trend where Y follows Mn (Table 3 andFigure 28). A decrease in Y while the Mn/(Fe+Mn)-ratio increases, e.g. *MSB-5Slobrekka*, can be explained by the coexistence of Y bearing minerals, e.g. xenotime (Pyle and Spear, 1999). Both xenotime and gadolinite have been found at Slobrekka (www.mindat.org , 2016a) Another reason could be the fact that the growth rate of the garnet increased exceeded the diffusion rate of Y, as suggested by Müller et al. (2012).

In *25432Heia*, the increase in Y while the Mn/(Fe+Mn)-ratio decreases can be explained by the relation between the crystal growth rate of the garnet and the diffusion rate along its surface. If the growth rate exceeds the diffusion rate and the compatible element Mn is depleted in the crystal-forming melt, Y and the REEs that have been concentrated in boundary layer around the crystal are much more easily incorporated. The occurrence of oscillatory zoning is usually the result of this situation (Allegre et al. 1981; Müller et al. 2012)
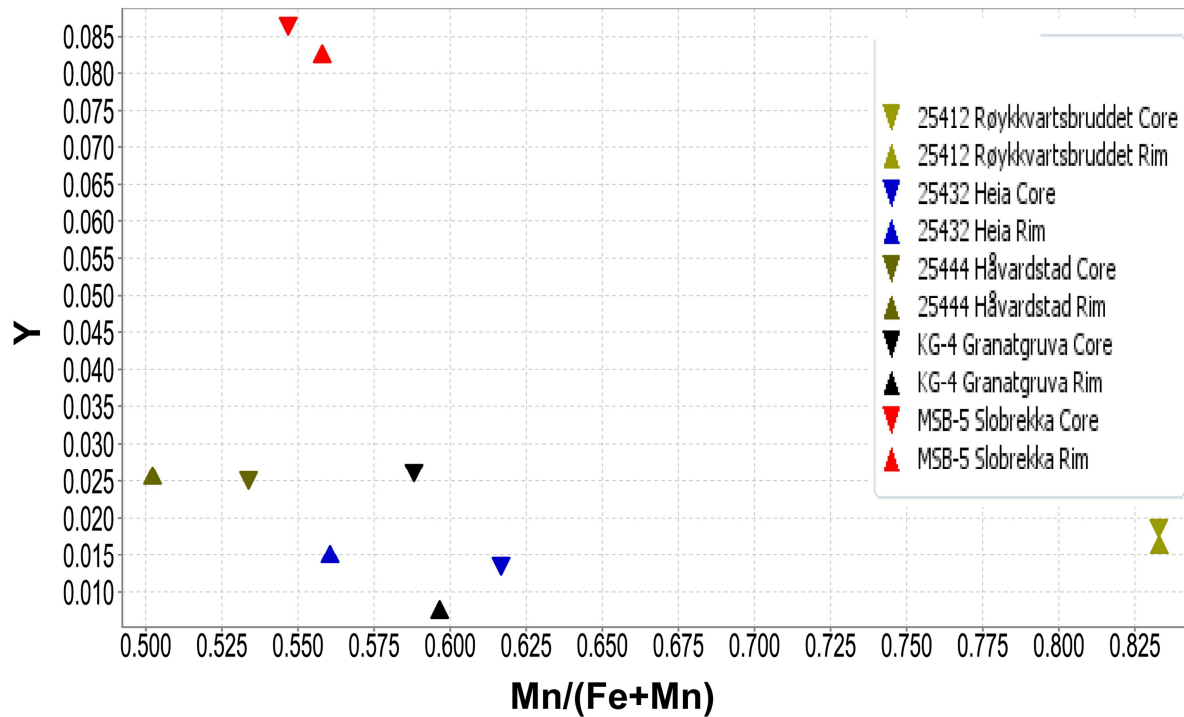
Figure 28: Plot showing an inverse change, or no change, in Y (apfu) compared to the Mn/(Fe+Mn)-ratio change.

The majority of the garnets have a change in the total REE that follows the changes of Y content from core to rim. This is observed in the enrichment of the HREEs, which increases or decreases with Y. The differences from core to rim are small in most of the garnets, however *28372Mølland*, which has a decrease from 0.097 to 0 apfu Y is a good example of this trend (Figure 29).
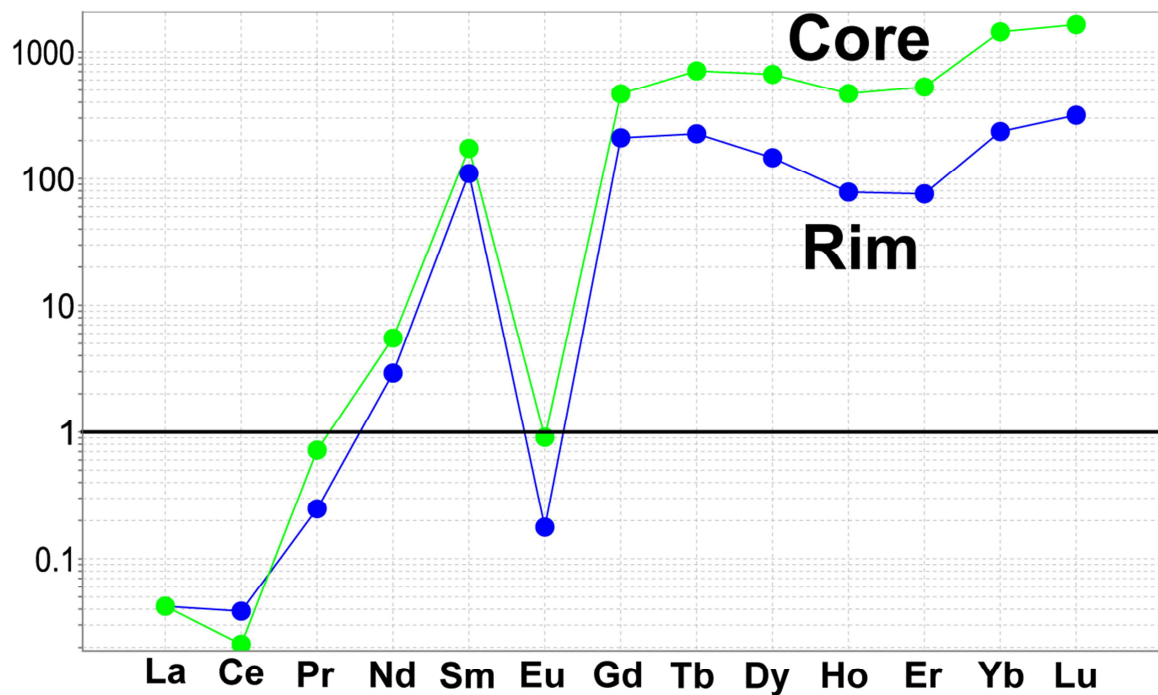
Figure 29: Chondrite normalized REE pattern for the core and rim in 28372Mølland.

In a wider view, when looking at the Y and REE-content of two garnets with different Mn/(Fe+Mn) ratios from the same pegmatite, the Y-content and HREE-enrichment are also inverse to the change in the Mn/(Fe+Mn)-ratio. One example this trend can be observed in the garnets from the Hovåsen pegmatite at Eptevann. *KH-3Hovåsen* shows a more fractionated trend (Mn/(Fe+Mn) = 0.76) than *KH-1Hovåsen* (Mn/(Fe+Mn) =0.69). The Y content in *KH-3* is 0.002 apfu and *KH-1* has a Y content of 0.036 apfu. While the REE curve for *KH-3* shows a drop of the HREEs of both core and rim, *KH-1* has a flattening curve of the HREE. The lower Y content and the drop in the HREEs could suggest that *KH-3*, which was collected a regular wall zone, was situated closer to a replacement zone than *KH-1*. This theory is consistent with the work of Müller et al. (2012) on the same pegmatite, who suggests the presence of a replacement zone that has not been excavated.

The chemistry of the garnets from the Røykkvartsbruddet pegmatite at Birkeland follows the same theory. Both of the garnet samples from the Røykkvartsbruddet show a fractionated, high Mn/(Fe+Mn) ratio. The high Mn/(Fe+Mn)-ratio and lower Y content in *25447Røykkvartsbruddet* (ratio= 0.97, 0.0044 apfu Y) compared to *25412Røykkvartsbruddet* (ratio= 0.97, 0.017 apfu Y), along with a flattening (*25412*) and a drop (*25447*) in the enrichment of the HREEs, could suggest that *25477* was situated deeper into a replacement zone than *25412*. This drop of Y-content between two garnets where the Mn content is stable could be explained by the occurrence of Y-bearing minerals between them. However, the transition from a Y-rich melt to the Y-poor LCT fluid that formed the replacement zone can also be an explanation.

The three garnet samples from Solås, *MS-6Solås, MS2-9Solås* and *MS-9Solås* could reflect an internal fractionation of the pegmatite. *MS-6Solås* was collected from the graphic granite with a Y content of 0.031 apfu and Mn/(Fe+Mn)-ratio of 0.60. *MS2-9Solås* was collected from the "buffer zone" between the cleavlandite zone and the wall zone, with a higher Y (0.07 apfu) and Mn/(Fe+Mn)-ratio (0.69) content than *MS-6Solås*. *MS-9Solås* on the other hand was collected from the cleavelandite zone of the pegmatite and has a low Y content 0.0028 apfu and a high Mn/(Fe+Mn)-ratio (0.98) compared to the two other garnets.

The trend of a low Y content in garnets from the least fractionated (Steli) and more fractionated (*25374Frøyså* and *25421Frikstad*) pegmatites compared to the less fractionated pegmatites (Figure 30), was also reported by Smeds (1994) on the NYF pegmatites in Falun. Pegmatites derived from aluminous sources tend to host garnets as an accessory mineral. The LCT-family of RE pegmatites, along with the common and less evolved pegmatites with I- or S-type granitic magmas as sources, usually hosts peraluminous minerals and therefore also garnets. The opposite is usually the case for pegmatites of the NYF-family and their source, A-granites, since they are usually metaluminous (London, 2008). However, according to Smeds (1994), garnets in peraluminous NYF pegmatites are unusually enriched in Y. This theory is based on the works of Jaffe (1951) and Geller and Miller (1959), who shows that Y is compatible in garnet (London, 2008). This is consistent with Frigstad (1999) on the pegmatite-forming melt being peraluminous. The low Y content in the garnets with a fractionated chemistry could be explained by the presence of Y-bearing minerals, or the fact that the environment these garnets are situated in, the replacement zones, are generated by an Y-poor fluid (Smeds, 1994; Müller et al., 2012).
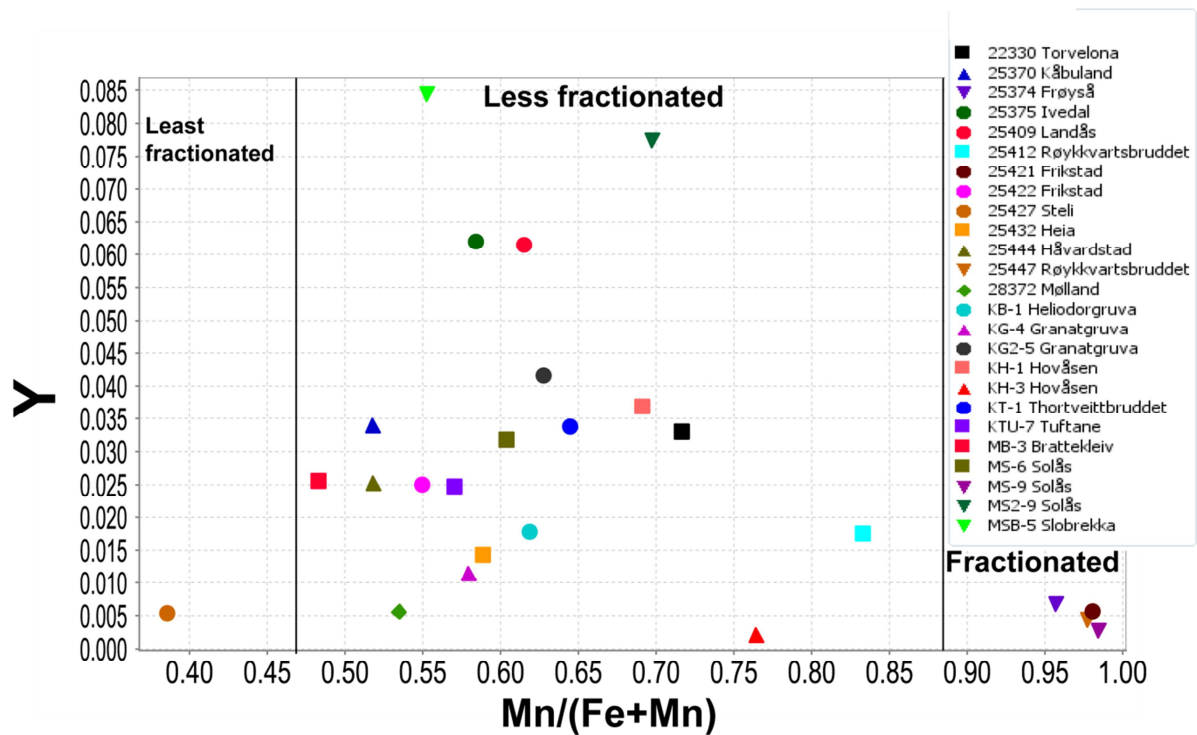
Figure 30: Distribution of Y (apfu) in garnets with least-, less- and fractionated chemistry.

The change of the Sc content in the garnets do not follow, either with an inverse of positive change, the Mn/(Fe+Mn)-ratio to the same degree as the Y content (

). In *25432Heia*, *28372Mølland* and *25427Steli*, the Sc content decreases with decreasing Mn/(Fe+Mn)-ratio from core to rim. However, the Sc content only increases with an increase in the Mn/(Mn+Fe)-ratio in *KG-4Granatgruva* from core (0.58 and 0.005 apfu Sc) to rim (0.59 and 0.017apfu Sc). As the garnets with the highest Mn/(Fe+Mn)-ratio, *KH-3Hovåsen, 25374Frøyså 25412-* and *25447Røykvartsbruddet*, has low or no Sc content, this could indicate that the melt fluid forming these garnets was depleted in Sc. The distribution of Sc in garnets when it comes to total Mn/(Fe+Mn)-ratio follows the same distribution as Y, in which the majority of the garnets with the less fractionated chemistry host more Sc than the least and fractionated garnets (Figure 31).
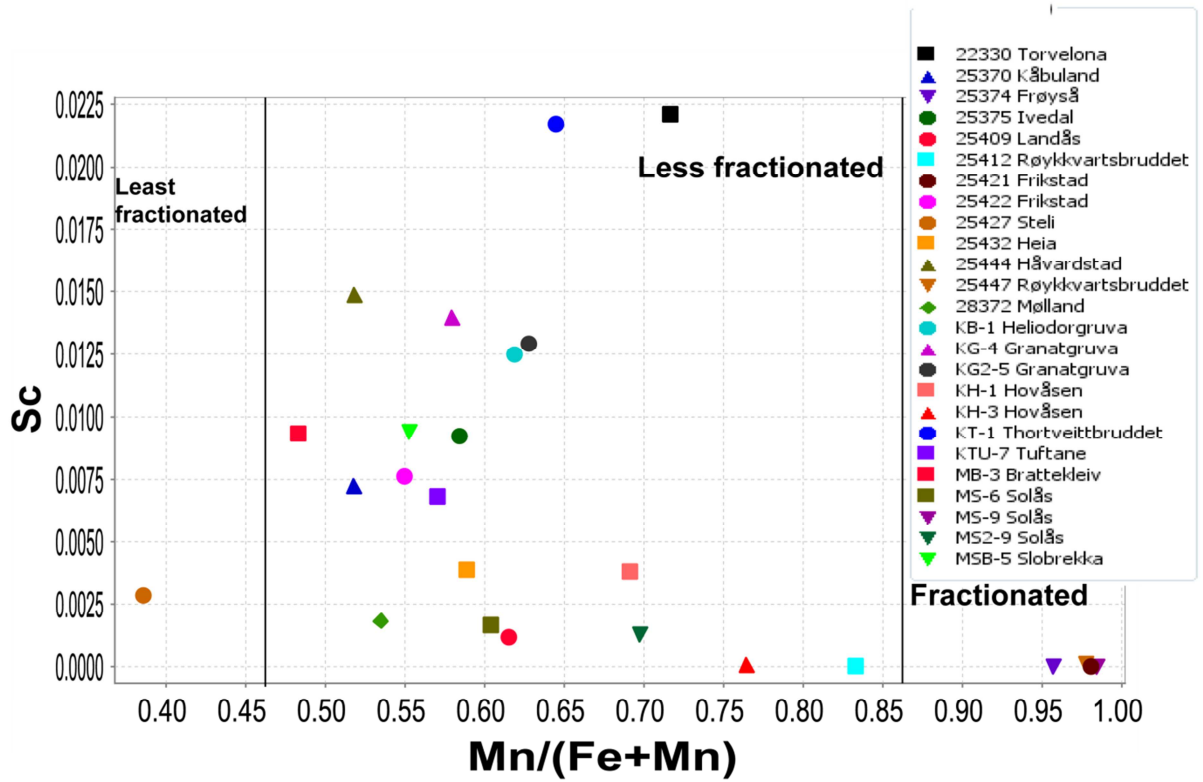
Figure 31: Distribution of Sc (apfu) in the garnets with least-, less- and fractionated chemistry.

According to Klein and Dutrow (2007), the B site in garnets is occupied by trivalent ions in six-coordination. This puts Sc^{3+} in the B site (Table 2). As Sc enters the garnet structure by substitution, it would be interesting to investigate if this is by simple or coupled substitution. The other two trivalent ions in the B site, which Sc could have a simple substitution with are Al^{3+} and Fe^{3+}.
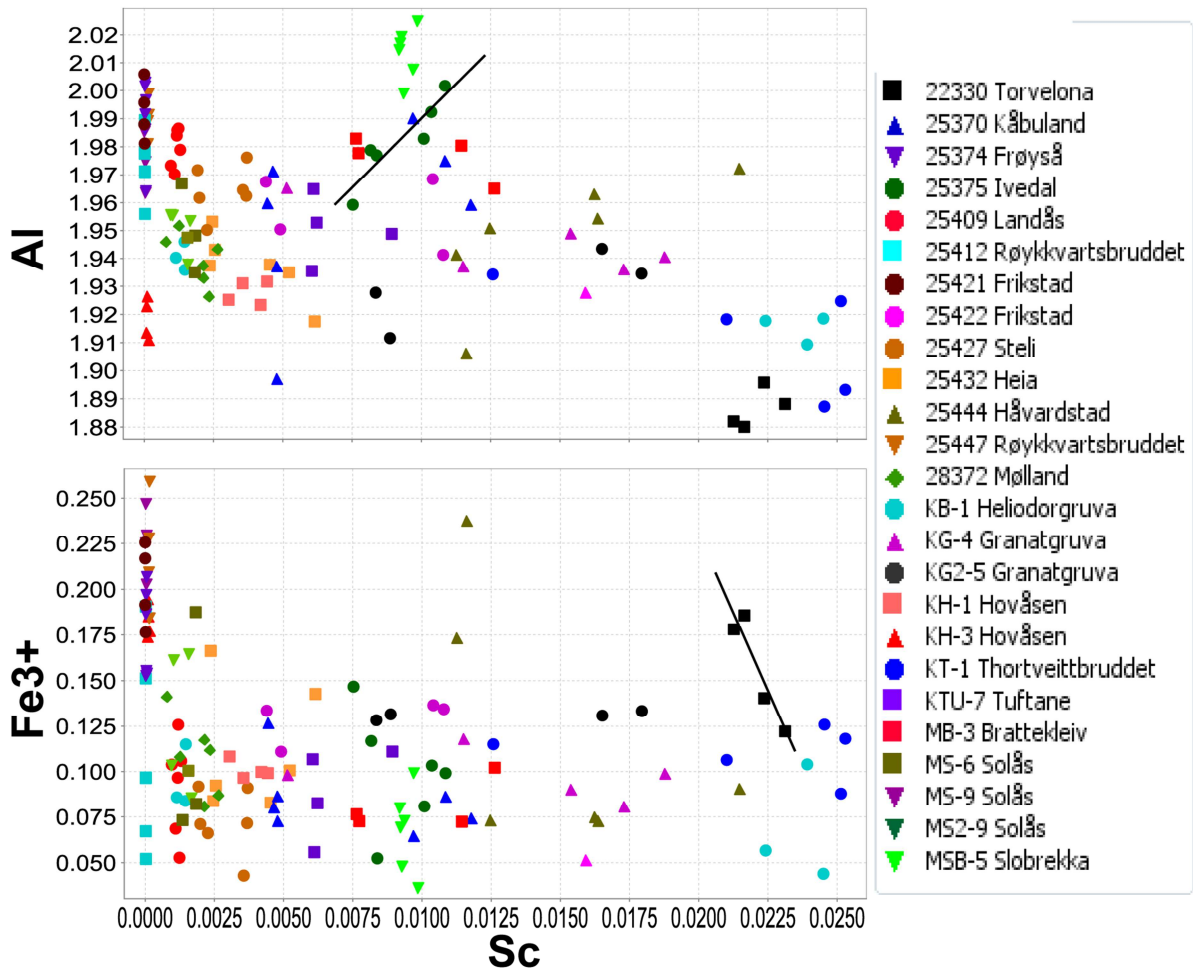
Figure 32: Relation between Sc and Fe3+ and Al, which all enters the B site of the garnet and have an ionic charge of 3+

Figure 32 indicate that simple substitution between Sc and Al and Sc and Fe^{3+} is not the case here, except for *22330Torvelona* between Sc and Fe^{3+}. In the sample *25375Ivedal*, Al is increasing with Sc, which may indicate that they both are on one side of a coupled substitution. Goldschmidt and Peters (1931) and later Shama (1936) suggested that Sc^{3+} may enter garnets by the substitution of Fe^{2+} or Mg^{2+} based on the similarities in their size. While Mg^{2+} is only situated in the A site, Fe^{2+} can occupy both A and B. In the A site, Mg^{2+} and Fe^{2+} are 8-coordinated and have a size of 0.89 Å and 0.92Å respectively, while Fe^{2+} in the B site hase a size of 0.780Å (Shannon, 1976; Klein and Dutrow, 2007). Scandium has a size of 0.870Å in 8-coordination and 0.745Å in 6-coordination (Shannon, 1976). As of this, Sc is 2.2% smaller than Mg^{2+} and 5.4% smaller than Fe^{2+} in 8-coordination, which indicate a possible substitution according to Klein and Dutrow (2007). Between Sc and Fe^{2+} in the B

site, there is a possible substitution as Sc is 4.4% smaller than Fe2$^+$. However, since there is a difference in ionic charge, a coupled substitution involving Sc^{3+} and Fe^{2+} or Mg^{2+} must occur. As Al could follow Sc (Figure 32), Al could substitute for Ti^{4+} in the B site or Si^{4+} in the T site. Also, Fe^{3+} could substitute for Ti^{4+} in the B site due to similarities in size (0.605 for Ti^{4+}, which is 6.2% smaller than Fe^{3+}). Combinations of two trivalent ions versus one divalent and one ion with 4+ in charge will give coupled substitutions where the total charge of 6+ is preserved.
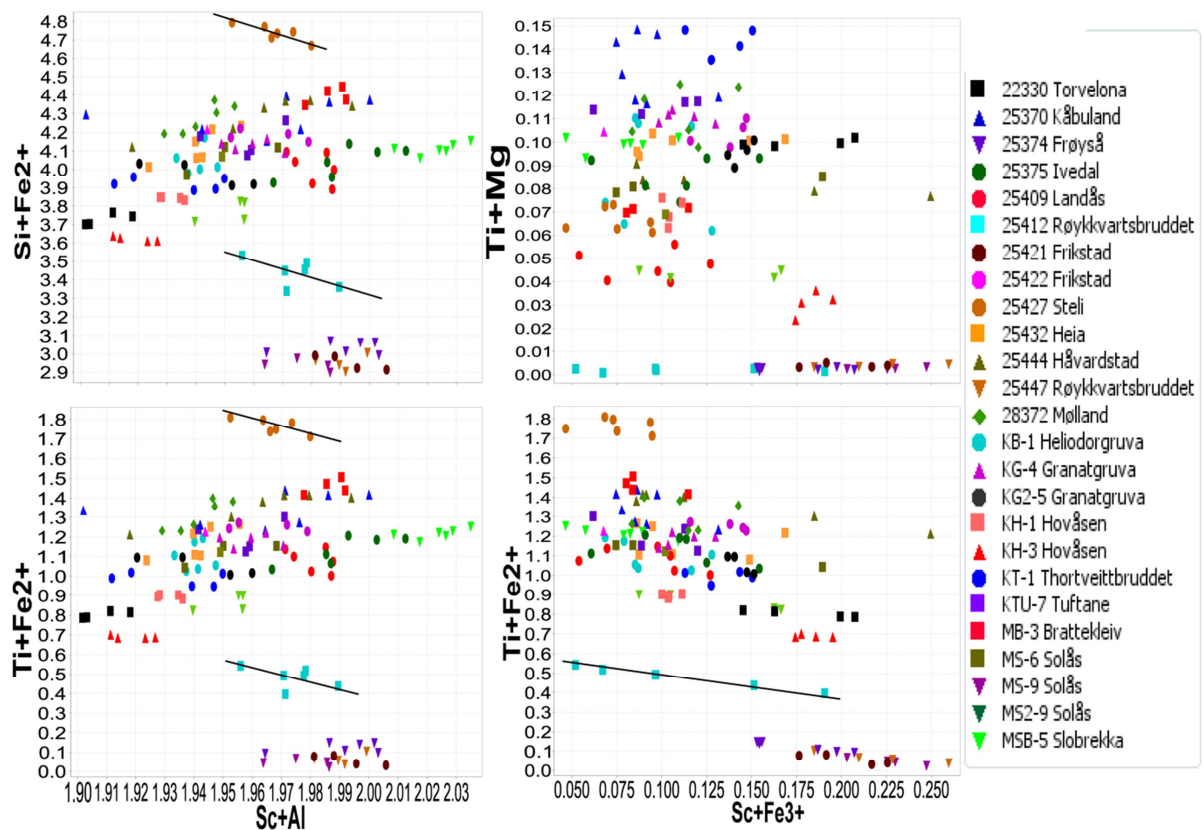
Figure 33: Relation between Sc+Al and Ti+Fe2+, Sc+Al and Si+Fe2+, Sc+Fe3+ and Ti+Fe2+, and Sc+Fe3+ and Ti+Mg. The total ionic charge of 6+ is preserved in all cases.

Figure 33 indicate some trends where Sc and Al substitutes for Ti and Fe^{2+} or Si and Fe^{2+}, e.g. *25427Steli* and *25412Røykkvartsbruddet*. The latter garnet sample can also show a trend where Sc and Fe^{3+} substitutes for Ti and Fe^{2+} however no trend where Sc and Fe^{3+} substitutes for Ti and Mg. The absence of a substituting trend between Mg and Sc could be explained by the low Mg versus Fe^{2+} ratio in the garnets. According to Jaffe (1951), Sc tends to substitute for Fe^{2+} when the garnets are low in Mg. Since there is no clear substitution trend involving Sc, this could suggest that other factors play a part in the incorporation of Sc in garnets.

The Ce-anomaly in some of the garnets, e.g. *25422Frigstad* and *MSB-5Slobrekka*, could be explained by a low Ce-content of the pegmatite-forming melt or the presence of Ce-bearing minerals such as

allanite-(Ce). The same drop in Ce can be observed in the chondritic plots from both the Evje-Iveland and Froland pegmatites in Müller et al (2012).

Petrogenesis of the pegmatites

The chemistry of the investigated garnets (Mn/(Fe+Mn)-ratio, Y-content and REE-plots) suggests that some of the pegmatites are more chemically evolved than others, however the regional distribution of the least-, less- and fractionated pegmatites do not confine to the regional zoning pattern from a source. This is consistent with previous research done on the pegmatites in Evje-Iveland by Frigstad (1968), Müller et al. (2012) and Snook (2014). A regional zoning pattern of pegmatites from a parental pluton, or thermal source, would show an increase in chemical complexity in the pegmatites further away from the source (London, 2014) (Figure 34).
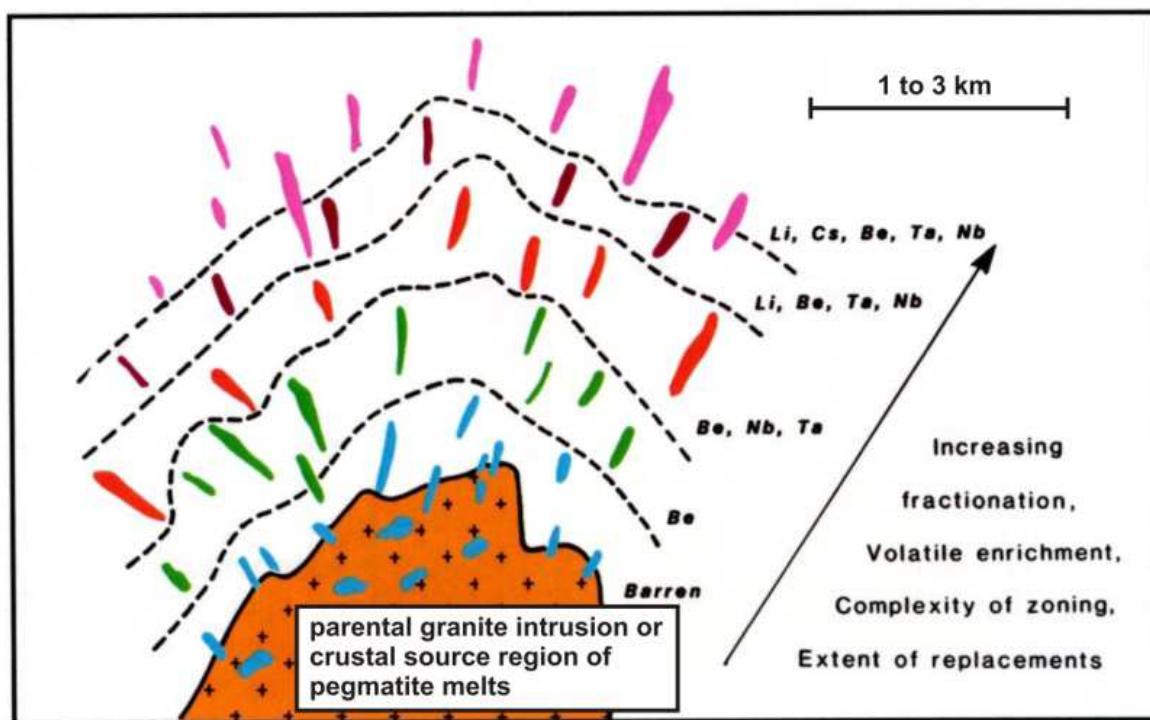
Figure 34: Regional zoning of pegmatites from their cogenetic intrusion.(Modified by Axel Müller after Cerny 1991):

In the extensive work done on the Evje-Iveland pegmatites, Snook (2014) proposed partial melting of the country rocks to be source of the pegmatite-forming melts. The mechanism that created the Rogaland Igneous Province, underplating, crustal tongues or a combination of the two, is both close in age and geographically to have partial melted the crustal rocks in Evje-Iveland (Snook, 2014). This theory has later been widely accepted due to the lack of evidence of other possible pegmatite-forming mechanisms and as the Iveland Wall (Figure 35) indicates partial melting of the crustal rocks with resulting pegmatite-forming melts.

The low Y and HREE content and high Mn/(Fe+Mn)-ratio in the garnets from replacement zones in the pegmatites suggests that the parental fluid was Y depleted and having a LCT- component instead of a NYF- component based on the works of Müller et al (2012) and Baldwin and von Knorring (1983). As garnets from outside the replacement zone in this study (e.g. Solås) are Y- and HREE-enriched (NYF), suggests that these pegmatites are a mix of the NYF- and LCT-families. This is consistent with Müller et al. (2015). The major part of the pegmatite can have been formed by a melt with the NYF-component while the final stage resulted in a fluid enriched in the LCT-component.

Granatgruva

Texture and formation

Based on the macroscopic texture of the pegmatite, the Granatgruva pegmatite appears to be of the simple zoned type according to the scheme of internal anatomy in pegmatites by Cameron et al. (1949) (London, 2014) The pegmatite has several zones with different dominant geochemistry and size of crystals, however no late stage metasomatic replacement unit is observed.

The outer zones in the Granatgruva pegmatite, the border zone and the wall zone, is dominated by graphic granite. Graphic granite is a texture of intertwined crystals of quartz and feldspar, which resembles the ancient Egyptian cuneiform script. While London (2005) and London and Morgan (2012) stated that graphic granite is formed during rapid liquidus undercooling, Martin and DeVito (

2005) suggested that this is not necessary and proposes that graphic granite can also form as a result of anatexis. In the case of rapid liquidus undercooling, the texture forms as a result of slow rates of elemental diffusion from a flux-bearing medium which has been substantially undercooled. In the case of anatexis, rapid nucleation and growth of the graphic texture may have been initiated by degassing of the pegmatite-forming melt (Martin and DeVito, 2005).

The coarser grain size (up to over 1m) and more euhedral crystals in the inner zones in the Granatgruva compared to that of the wall zone could be the result of a process called constitutional zone refining (CZR). This process, where a layer of liquid accompanies the crystallization along the border of the crystal growth front, was argued in favor of by London (1992, 1999 and 2005) for the formation of large well-developed crystals (Bartels el al., 2011). The liquid hosts a fluxing of components, which prevents impurities of incompatible elements in the forming crystal (**Error! Reference source not found.**). As the liquid has a low viscosity and is flux-enriched, this lead to more rapid diffusion, which in turn enhances the increase of grain size (London and Morgan, 2012).
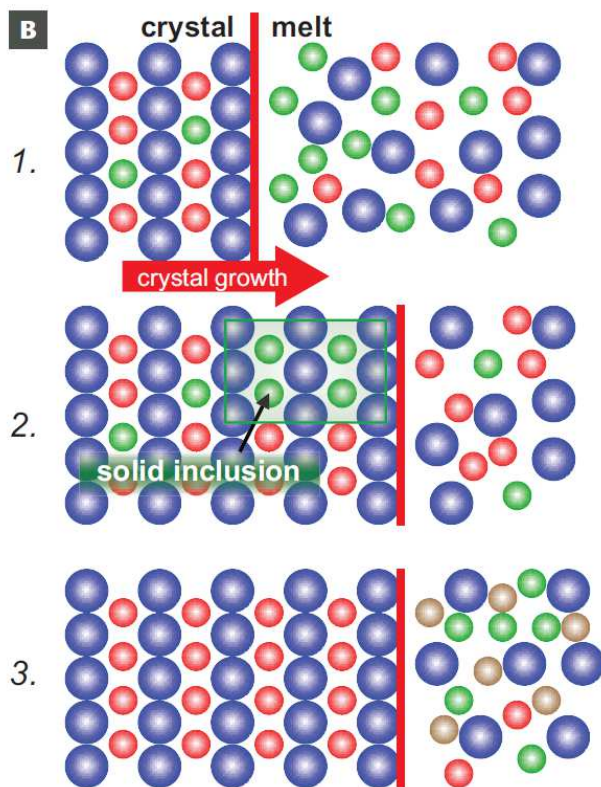
Figure 36:Schematic figure showing the growth of a crystal with (3) and without (1 and 2) CZR. Green= incompatible elements, brown= fluxing and incompatible component. (London and Morgan, 2012).

Two of the three observed intermediate zones, the plagioclase and the microcline, appear to be in the same sequential position of the pegmatite. This is not uncommon in pegmatites, as London (2008)

states that intermediate zones do not need to be symmetrical distributed or continuous throughout the pegmatite (London, 2008). London (2008) also notes that more developed zones are usually in the thicker part of a pegmatite. This can be observed in the Granatgruva pegmatite. The plagioclase-intermediate zone, in what appear to be a thinner part (eastern part of the pegmatite) has a smaller grain size and less anhedral crystals than the other two. In the western and thicker part of the pegmatite, the microcline phase dominates the intermediate zone. The third intermediate zone, with its mix of large (>1m) and well-developed plagioclase and microcline crystals, lies in the thickest part of the pegmatite.

The BSE imaging of *KG-4* (Figure 8) show an oscillatory zoning pattern, although not as good as in *MS-6Solås*. Oscillatory zoning of garnet is usually attributed to hydrothermal garnet from open-system environments according to Jamtveit et al (1993) and Müller et al. (2012). In this scenario, the garnet will get a new rim enriched in compatible elements (Mn, Fe) each time the crystal-forming melt is supplemented by pulses of new melt before it incorporates less compatible elements. Müller et al. (2012) noted the same oscillating zoning in a garnet from the Slobrekka pegmatite, but did not find any evidence this being an open-system. This may be the same case for the Granatgruva pegmatite (find evidence) or for the other pegmatites for that matter. The analyses of *KG-4* indicate that the Mn, Fe and Al content have a negligible change throughout the garnet. In the case of the Slobrekka garnet investigated by Müller et al. (2012), they suggested, based on the works of Allègre et al. (1981), that the oscillatory zoning was a result of self-organized diffusion controlled crystal growth (Müller et al., 2012). The growth of the garnet is controlled by the relation between the growth rate of the garnet and the diffusion rate of Mn, Fe, Al and Si, where the diffusion rate is the dominant factor. As the reaction zone between crystal and melt is enriched in these elements, the growth rate increases. When the growth rate increases enough to deplete the reaction zone for major elements, it will exceed the diffusion rate which in turn will slow down the growth rate. Yttrium and the HREEs, that also have been concentrated in the reaction zone, are also more easily incorporated in the garnet when it has a high growth rate. Recovery of the major elements in the reaction zone will help to resume the growth rate (Müller et al., 2012). The sample *KG-4* is from the microcline intermediate zone, while *KG2-5* is from the plagioclase intermediate zone and has no oscillatory zoning. This could indicate a difference in garnet growth or that the melt forming the plagioclase zone was so enriched in Mn, Fe, Al and Si that the growth rate did not exceed the diffusion rate.

The white rim observed in the innermost part of the mine is interpreted as an infill between the large quartz and microcline crystals. Fluids, with a low content of nucleation-inhibiting fluxes, had probably went through this space and fractures in the microcline and formed a matrix of plagioclase-dominated feldspar and quartz.

Classification

Comparison of the Mn/(Fe+Mn)-ratio in the collected garnets, 0.55 for *KG-4* and 0.6 for *KG2-5*, in Grantgruva with the other pegmatites in this study, suggest that the Granatgruva pegmatite belongs to the less fractionated pegmatites in Evje-Iveland (Figure 26). Based on the relative Mn versus Fe+Mn components of the Grantgruva pegmatite and the Slobrekka and Hovåsen pegmatites in this study and the work by Müller et al. (2012) on the latter two, the data could suggest that the Granatgruva pegmatite is equally fractionated as these two. Based on the observation of replacement zones being absent, and that both of the garnets, from the plagioclase and microcline intermediate zones, have an enrichment of the HREEs (Figure 14), results in the interpretation of the Granatgruva pegmatite being one of the regular NYF-pegmatites in Evje-Iveland. *KG4* has an average Y content of 0.23 wt.% Y_2O_3 and a increase of 0.008 to 0.026 apfu Y from core to rim, while *KG2-5* has an average Y content of 0.74wt.% Y_2O_3. As no REE-bearing minerals, except a few euxenite-(Y) or polycrase-(Y) crystals, have been found in the Granatgruva, this could indicate that the pegmatite is a primitive REL REE euxenite type. However, it is more likely to be of the Abyssal HREE class and subclass of the Cerny and Ercit (2005) classification scheme (Table 7)

Table 7: Classification scheme for pegmatites by Cerny and Ercit (2005).

Class	Subclass	Type	Subtype	Family
Abyssal	HREE			NYF
	LREE			
	U			NYF
	BBe			LCT
Muscovite				
Muscovite-rare element	REE			NYF
	Li			LCT
Rare element	REE	allanite-monazite Euxenite Gadolinite		NYF
	Li	Beryl	beryl-columbite beryl-columbite-phosphate	LCT
		Complex	Spodumene Petalite Lepidolite Elbaite Amblygonite	
		albite-spodumene Albite		
Miarolitic	REE	topaz-beryl gadolinite-fergusonite		NYF

Li	beryl-topaz	LCT
	spodumene	
	petalite	
	lepidolite	

Thortveitite

Zoning

In the samples with a low Sc content (e.g. *22292_2Tuftane*), there is a larger difference in the Sc versus Y versus Yb content between the zones, compared to the samples with a high Sc content (e.g. *22238Tjomstøl*) (Figure 18). This could be explained by the Sc composition of the melt and the boundary layer around the forming crystal. For *22238Tjomstøl*, the boundary layer could have got a more rapid supplement of Sc, explaining the thin nature of the zones, in which the Sc content was not severely depleted before new material was added. For *22292_2Tuftane*, there could have been a longer duration between the additions to the boundary layer or the melt was already low in Sc content. However, the patchy zoning of *22292_2Tuftane* could also indicate other factors controlling the diffusion and crystal growth of the crystal. The observed zoning can also be explained by in which angel the crystal was cut, which is most likely the case for *22286Tuftane* (Figure 15). The sample *22292_1Tuftane* could indicate that fractures can be the reason behind patchy zoning (Figure 37).
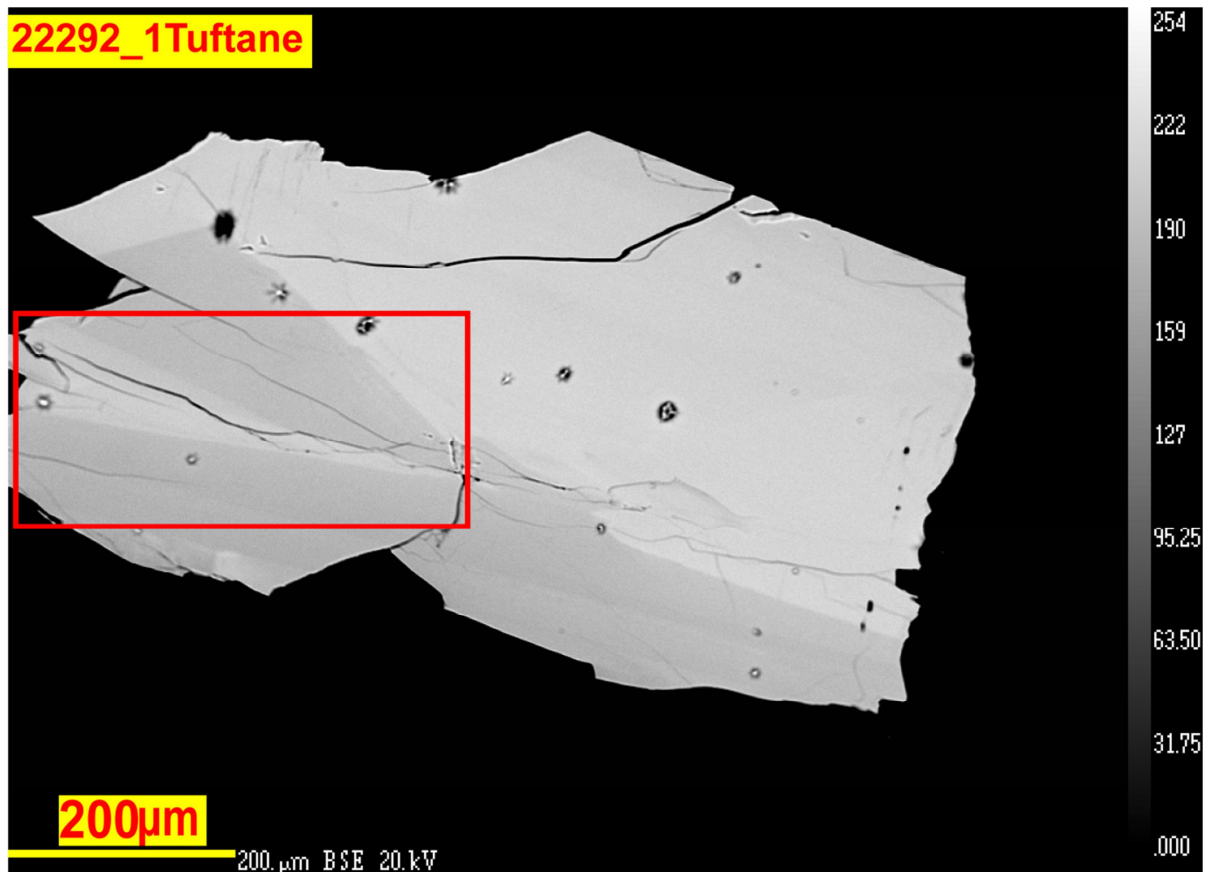
Figure 37:BSE-image of sample 22292_1Tuftane.

This elongated (ca. 1 cm long and <1 mm wide) crystal was cut perpendicular on its longest axis. A very weak oscillatory zoning pattern can be observed from the medium zone towards the top-right corner. To the left in the figure (red square), a part of the medium zone could have been displaced by a fracture after crystallization, in which a new and more Sc-poor material has refilled the gap. However, the angle of the gap and displacement of the medium zoning are not of the same degree. Alternatively, this could be part of a sector zoning, which unfortunately is not fully exposed as this is only a fragment.

Another example, in which fractures with fluids could have contributed to the zoning pattern, is the sample *22273Håvarstad* (Figure 15). In the middle of this sample, beneath top right "Ms", a "flow-pattern" of dark, medium and pale zoning can be observed following the fractures. However, a relation between the fractures and the zoning cannot be confirmed.

Some of the samples have a darker zoning pattern, with oscillatory zoning inside, which is surrounded by patchy zoning. One example on this can be observed in *22330Torvelona* (**Error!**
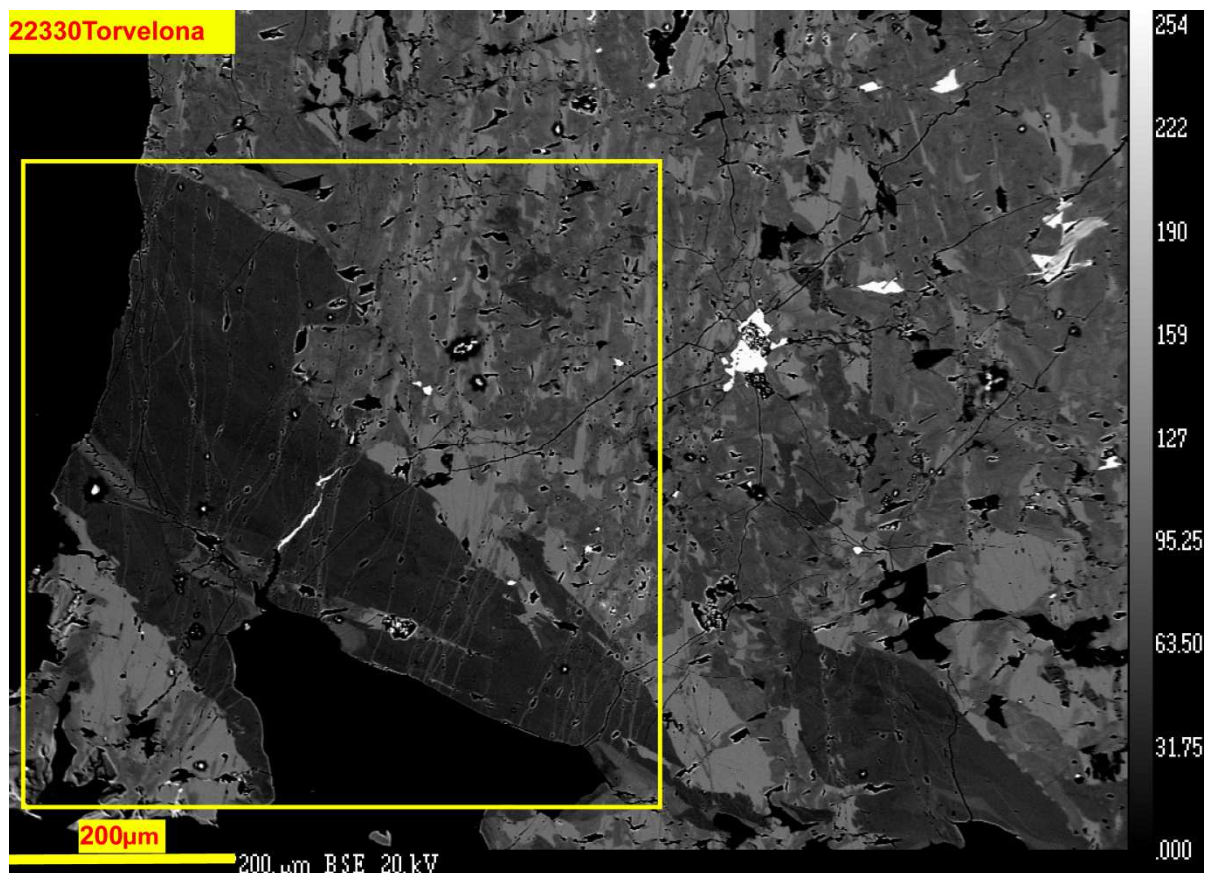
Figure 38: BSE-image of another part of 22330Torvelona.

This pattern can be the result of a Sc-rich melt that have filled the gap between two thortveitite crystals (top right and bottom left in yellow square).

The darker zone surrounding what is interpreted to be allanite (semi-quantitative analyzes gave Y, Fe, Ca, Sc and Al content in decreasing order), may indicate that an iron-rich fluid have filled a fracture in the thortveitite and incorporated Y and probably REE from the host mineral.

Substitution

All of the collected thortveitites, both from sample to sample and in the zoning in each sample, indicate that Y increases when Sc decreases (**Error! Reference source not found.**). Several factors apply when determining a substitution of elements in minerals (Klein and Dutrow, 2007). A substitution between Sc^{3+} and Y^{3+} is possible due to equal ionic charge and similarities in size. Both Sc^{3+} and Y^{3+} are six-coordinated in the thortveitite structure, which give them a size of 0.745Å and 0.900Å respectively according to Shannon (1976). The same goes for the substitution between Sc and the REEs (**Error! Reference source not found.**). The chondrite normalized REE plots (**Error! Reference source not found.**) show enrichment in the HREEs, especially in Yb and Lu, in the collected thortveitites. This is expected due to the similarities in size and charge between Sc and the

HREEs (Moriyasu and Nishikawa, 1991; Foord et al., 1993). Ytterbium and lutetium (Yb^{3+} and Lu^{3+}) have a size of 0.868Å and 0.861Å respectively according to Shannon (1976), which gives a smaller difference in size between them and Sc compared to Sc and Y. This indicates that Sc is more likely to form a solid solution with Yb (e.g. kieviite-(Yb)) or Lu than Y (kieviite-(Y)). However, the availability of the substituting elements plays an important role, in which the average amount of Y in the crust (33 ppm) is much higher than that of Yb (3.4 ppm) and Lu (0.5 ppm) and the other HREEs that have an ionic size closer to Sc than Y (Klein and Dutrow, 2007). One should note that Ohashi et al (2007) have proven a solid-solution between $Sc_2Si_2O_7$ and $Lu_2Si_2O_7$ at 1550°C. The two trends, in which some of the samples are having a lower enrichment rate of Tb, Dy and Ho (higher MREE/HREE- and LREE/HREE- ratio, Figure 24) compared to the other samples, can be explained by the temperature and pressure during crystallization. As one moves from right to left in the chondritic plot, the size of the elements increases, resulting in an increasing limitation of substitution with Sc. However, when the temperature increases, the crystal structure expands and an incorporation of elements with a larger size is more possible. A higher pressure has the opposite effect, however in combination with temperature, the temperature-factor is dominant (Klein and Dutrow, 2007). While the enrichment of the HREEs in *22239Ljosland* and the samples from Tuftane could be only size-dependent, the temperature when *22238Tjomstøl*, *22273Håvarstad*, *22302Knapen*, *22304Eretveit*, *22370Eptevann* and *22330Torvelona* was formed, could have only been high enough to promote the incorporation of Lu, Yb and possibly Er of the HREEs into the thortveitite. Another reason for these two trends can also be the presence or absence of other REE-bearing minerals that incorporates Tb, Dy and Ho much more easily than thortveitite.

The Zr, Fe^{2+}, Mg, Mn, Ti and Hf contents have also an inverse change compared to the change of Sc in the thortveitite samples. However, as these elements have an different ionic charge than Sc^{3+} (Zr^{4+}, Fe^{2+}, Mg^{2+}, Mn^{2+}, Ti^{4+}, Hf^{4+}), coupled substitution is are more likely to be the cause. The relation between Sc and combinations of these elements that give a balanced charge of 6+, indicate that substitution between Sc and the combinations are present (Figure 21). While Y and the REEs decrease with increasing Sc in most of the samples, there is a minimal change in *22238Tjomstøl* and *22370Eptevann* (circle in **Error! Reference source not found.**). The total REE+Y in these samples could have met a larger competition from especially $Mg^{2+}+Ti^{4+}$ and $Fe^{2+}+Zr^{4+}$, and other combinations when it comes to substitution of Sc (circles in **Error! Reference source not found.**). The relation between the REEs and Y and the previous mentioned combinations (Figure 22) indicates that these substitutions only applies for Sc and not Y and the REEs. One reason for that Y and the REEs still dominate in *22238Tjomstøl* and *22370Eptevann* could be the occurrence of minerals that much easily incorporates the elements in the combinations (eg. micas for Mg^{2+} and ilmenite for Fe^{2+} and Ti^{4+}). The differences in the amount of the mentioned minerals between pegmatites could explain the variable coupled substitutions between the samples. Further emphasizing that the coupled

substitutions are more controlled by what is available when thortveitite than being essential for the stability of the thortveitite structure.

When plotting Sc versus Ca, no apparent correlation is shown when all the analysis-points are plotted (except to some degree, a positive correlation for *22304Eretveit* and *22292_2Tuftane*). This could be explained by the difference in charge between the Sc^{3+} and Ca^{2+}, but no obvious substitution trends were found between Sc and Ca in combination with any of the 4+ elements (Hf^{4+}, Ti^{4+} and Zr^{4+}), in which Ca played a part. "Obvious" refers to that although eg. Ca+Zr decreases with increasing Sc, it is suspected that Zr is the controlling factor here. The size of Ca in six-coordination is 1.00Å according to Shannon (1976), which puts it closer in size to Y and the other REEs. When plotting Y+REE versus Ca in combination with elements that gives a balanced charge of 6+, there is indication on a substitution trend (**Error! Reference source not found.**). The best correlation here can be observed in *22304Eretveit* and *22292_2Tuftane*, where Ca increases with Sc, but substitutes for Y+REE in combination with Hf and Ti (circles in **Error! Reference source not found.**). For *22304Eretveit*, the one outlier in the plots is excluded in this case. For the remaining samples where there are no trends between Ca and Sc or Ca and REE+Y, this could be explained by the presence of plagioclase that is a major controlling factor of Ca in a melt.

From our data it is clear that all analyzed samples are thortveitite, but with a large keiveiite-(Y) component and to a smaller degree also keiveiite-(Yb). The analyzed samples contained minor amounts of elements such as Ca, Mg, and Zr, which often form coupled substitutions with trivalent cations (e.g. $Zr^{4+}+Mg^{2+} = 2Sc^{3+}$) However, the coupled substitutions are not the same for those involving Sc and those with Y, indicating that the size of the cations plays an important role and changes the substitution mechanism throughout the thortveitite-keiviite-(Y) solid-solution.

Formation of thortveitite

Several authors have investigated the formation of thortveitite, both in Norway and abroad (e.g. Oftedal, 1943; Foord et al., 1993). Foord et al. (1993), who investigated the thortveitites found in the Crystal Mountain fluorite complex in North America, suggested that the thortveitites found in the metagabbro host-rock was formed as a result of Sc exceeding the solid solution limit of the amphiboles. This is based on the behavior of Sc in melts, in which Sc is usually incorporated into mafic minerals such as the amphibole-, pyroxene- and biotite groups (Norman and Haskin, 1967; Foord et al., 1993, Klein and Dutrow, 2007). However, this does not explain the occurrence of thortveitite or other Sc-bearing minerals in granitic pegmatites, unless they are derived from a Sc-rich granitic system where a late stage formation of pegmatites may become enriched in Sc (Foord et al., 1993).

Several authors have studied the correlation between the Sc content in a pegmatite and the occurrence of thortveitite. This has been done by analyzing the Sc content in minerals from thortveitite-bearing pegmatites and compared the results with the same minerals from non-thortveitite-bearing pegmatites. Oftedal (1943) measured Sc content in biotites, where the four biotites from thortveitite-bearing pegmatites had between 500 and 1000ppm Sc while the biotites from non-thortveitite-bearing pegmatites had less than 100 ppm Sc. Neumann (1961) reached similar results on other minerals from thortveitite-bearing and non-thortveitite-bearing pegmatites and so does the current study concerning biotites and garnets. Consequently, pegmatites containing thortveitite have elevated Sc contents not only expressed in the presence of thortveitite, but also by higher levels of Sc in the associated minerals.

Some of the collected garnets that are from the pegmatites or areas where thortveitite has been found, *KT-1Thortveitittbruddet* (2005 ppm Sc), *22330Torvelona* (1995 ppm Sc), *25444Håvarstad* (1347 ppm Sc), *25375Ivedal* (831ppm Sc), *25370Kåbuland* (695ppm Sc) and *25422 Frikstad* (523ppm Sc) also have an elevated Sc content. These samples, along with the relative low Sc content in the garnets from non-thortveitite-bearing pegmatites, e.g. *25427Steli* (267ppm Sc), *25409Landås* (102ppm Sc) and *28372Mølland* (183ppm Sc), could indicate that the melts forming the thortveitite-bearing pegmatites had a higher Sc content compared to non-thortveitite-bearing pegmatite-forming melts.

The high Sc-content in the pegmatites, as proposed by Goldschmidt (1934), could have been extracted by the granitic magma forming the pegmatites, from the surrounding amphibolite. The Iveland-Gautestad metagabbro can be a suitable source that was enriched in Sc due to its overall mafic composition. However, Goldschmidt (1934) could have based his theory on the granitic magma being differentiates of a plutonic source, rather than a result of anatexis, which is wider accepted today (Müller et al., 2015). How the Sc content was transported from the remaining mafic part to the resulting granitic melts during partial melting still opposes a question. In the case of the plutonic-differentiate model, Oftedal (1943) suggested that if amphiboles in the contact between the host rock and pegmatite melt were altered to biotite at a high temperature, only a part of the Sc content from the amphiboles was able to enter the biotites. The remaining free Sc content entered the pegmatite melt and was either incorporated into micas formed at lower temperature or formed Sc-minerals (Oftedal, 1943). A transporting mechanism for Sc in the anatexis-model could be the presence of fluorine. The work done by Gramenitskiy and Shchekina (2001) on the behavior of Sc in fluorine-bearing melts indicates that Sc would rather enter the fluoride phase, due to higher affinity to F, than the aluminousilicate phase of a melt. By this, Gramenitskiy and Shchekina (2001) argued that the segregation of salt melts from a granitic magma during its differentiation is the only explanation to the enrichment of Sc in pegmatites. If we ignore the fact that Gramenitskiy and Shchekina (2001) based their findings on magmatic differential, fluorine could still have been the transporting agent of scandium in the form of aqueous complexes, e.g. M_3ScF_6 (M = Na, Na+K or Na+K+Li), in the

pegmatites in Evje-Iveland. If fluorine complexes have transported scandium into the pegmatites where a reaction with other minerals had released the Sc, there should be F-bearing or F enriched minerals in these pegmatites. Even though the pegmatites are of NYF-character, they are poor in F (Müller et al., 2015). However, biotite $(K(Mg,Fe^{2+})_3(AlSi_3O_{10})(OH,F)_2)$ is a very common mineral in most of the pegmatites and other F-bearing minerals like bastnäsite-(Ce) $(Ce(CO_3)F$, fluorite (CaF_2) and/or topaz $(Al_2(SiO_4)(F,OH)_2$ have been found at Slobrekka, one of the thortveitite-bearing pegmatites (www.mindat.org, 2016a). Since topaz is also reported from Solås (www.mindat.org, 2016b), where the collected garnets have a low Sc content (the highest being in *MS-6Solås* with 148 ppm) and other non-thortveitite-bearing pegmatites, the presence of F to transport Sc cannot alone explain the occurrence of thortveitite.

However, there are anomalies in the correlation between Sc enrichment and the occurrence of thortveitite. One example of a pegmatite with an elevated Sc content in the garnets but where no thortveitite has been found is Granatgruva at Ljoslandknipan. Here, the two collected garnets *KG-4* and *KG2-5* have elevated Sc content (1181 ppm and 1169 ppm), but no thortveitite has been found. Another example is the garnet sample *25374Frøyså*. This garnet is from an area where thortveitite (Pegmatite locality 19 in www..org (2016c)) has been found, but it has a low scandium content (2 ppm). There could be several reasons for these anomalies. One reason could be that thortveitites or other Sc-bearing minerals have formed prior to this garnet and incorporated most of the Sc. The possibility remains that thortveitite may have formed in this pegmatite, although it has never been found (or sampled) there.

In the case of *25374Frøyså*, fractionation of the pegmatite melt could be the reason for low Sc content. This sample has a Mn/(Fe+Mn)-ratio of 0.9, which is relative high compared to other samples. Other garnet samples with high Mn/(Fe+Mn)-ratio, eg. *25447Røykvartsbruddet* (0.97) and *MS-9Solås* (0.98), show a fractionated trend and have a low Sc content (12 ppm in *25447* and 1 ppm in *MS-9Solås*). *MS-9Solås* was collected from a cleavelandite zone, which could indicate that the melt forming the replacement unit was depleted in scandium. However, both *MS-6Solås* and *MS2-9Solås*, from the graphic granite and the reaction zone of the cleavelandite zone respectively, have a low Sc content (148 ppm and 117 ppm respectively). This could indicate that the melt forming this pegmatite had too low scandium content for thortveitite to form. Müller et al. (2012) on the other hand, report of a drop in Sc content from core (1067 ppm) to rim (169 ppm) in their garnet from Solås. The difference between the samples in this study and the large drop in Sc from core to rim in Müller et al. (2012), may indicate that other Sc-bearing minerals have formed during and after the crystallization of the latter garnet. Also, the high Sc content in the core of the garnet in Müller et al. (2012) could indicate that the melt that formed the Solås pegmatite was depleted in Sc. The garnet sample from the cleavelandite zone at Solås and the other samples that have a high Mn/(Fe+Mn)-ratio, eg. *25421Frikstad*, *25447Røykkvartsbruddet* and *24374Frøyså*, all have low scandium content.

Also, the garnet sample *25427Steli* have a low Sc content (266 ppm). The low Sc content in these samples could indicate that only the pegmatites that are less fractionated hosts thortveitite. However, according to www.mindat.org (2016c), both the occurrence of thortveitite and the amazonite variety of microcline at the Landsverk 3 pegmatite, could suggest that thortveitite can occur in more fractionated pegmatites with replacement zones. Another example indicating that Sc content in garnets alone cannot be used as an indicator of thortveitite being present is Slobrekka. The garnet from Slobrekka in this study, *MSB-5Slobrekka*, has a Sc content of 848 ppm, while the garnet in Müller (2012) from the same pegmatite has a Sc content under 40 ppm.

The high Sc content in the garnet from Thortveitittbruddet (2005 ppm), along with *KG-4* and *KG2-5* (1181 ppm and 1169 ppm) from Granatgruva, could either suggest that the crustal rocks in the area of Ljoslandknipan were rich in Sc before pegmatite formation, or that the pegmatites here originate from a scandium rich parental source. The latter theory is more plausible based on Snook (2014), who suggested that the pegmatites have been transported away from their source.

Oftedal (1943) may have been on to something when he worked with the enrichment of Sc in biotite as the temperature decreases. Oftedal (1943) theorized with the substitution of the Fe-content of the micas, especially biotite, to be the reason for this enrichment. However, as the iron in biotite is divalent, this substitution must be coupled to maintain the charge balance. A general equation for the coupled substitution between Sc^{3+} and Fe^{2+} is:

$$Sc^{3+} + X^{3+} = Fe^{2+} + Z^{4+}$$
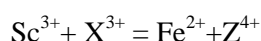
where X can be an additional Sc.

Simple substitution is easier to accomplish than coupled substitution and one of the elements of which Sc^{3+} are commonly substituted with is Al^{3+}. The other element is Fe^{3+} (Raade et al., 2002). Muscovite ($KAl_2(Si_3Al)O_{10}(OH,F)_2$) has three times more Al than biotite ($K(Mg,Fe^{2+})_3AlSi_3O_{10}(OH,F)_2$) in its formula. This could indicate that although biotite can pick up much Sc, muscovite can pick up even more. The works of Yang and Rivers (2000) on partitioning of trace elements between coexisting biotite and muscovite support this theory. By following Bowen's reaction series, muscovite will start to crystallize at lower temperature then biotite. By following the work of Corneliussen (2016), most of the thortveitite-bearing pegmatites, if not all, are dominated by biotite while some of the non-thortveitite bearing pegmatites are dominated by muscovite or are classified as cleavelandite pegmatites. The work done by Müller et al. (2015) on Ti-in quartz geothermobarometry in the Evje-Iveland and Froland pegmatite field, indicate that the crystallization temperature for quartz in the intermediate zones of the pegmatites ranged from 442° to 731°C. This could indicate, that the variable degree in temperature in the pegmatites (**Error! Reference source not found.**), could explain the occurrence of biotite- or muscovite dominated pegmatites. The

thortveitite-bearing pegmatites could have reached a higher temperature, promoting crystallization of biotite, than the non-thortveitite-bearing pegmatites where crystallization of muscovite was promoted. However, as the temperatures in the pegmatites are based on quartz, which crystallize at lower temperatures than muscovite and biotite, this may cause a problem with the theory. It is uncertain if the pegmatite-forming melts reached high enough temperatures in which the difference in temperature between biotite- and muscovite dominated pegmatites was large enough to only promote one of the micas. Other factors may also play a part when it comes to promote the crystallization of biotite or muscovite. If the temperature is the major determining factor on the crystallization of biotite or muscovite, which further controls the formation of thortveitite, this could explain the lack of thortveitite in the Granatgruva pegmatite at Ljoslandknipane (**Error! Reference source not found.**). Here there is a thin "sliver" of a colder isobar in which the Granatgruva pegmatite could be located, while the Thortveitite pegmatite could be located at the warmer isobar. Some of the thortveitite-bearing pegmatites that are located in the same or colder isobar than the Granatgruva pegmatite may have not been included in the works of Müller et al. (2015) and could have had a higher crystallization temperature.

A higher biotite content relative to the muscovite content, which may be controlled by temperature, could be the reason for the formation of thortveitite in a pegmatite.
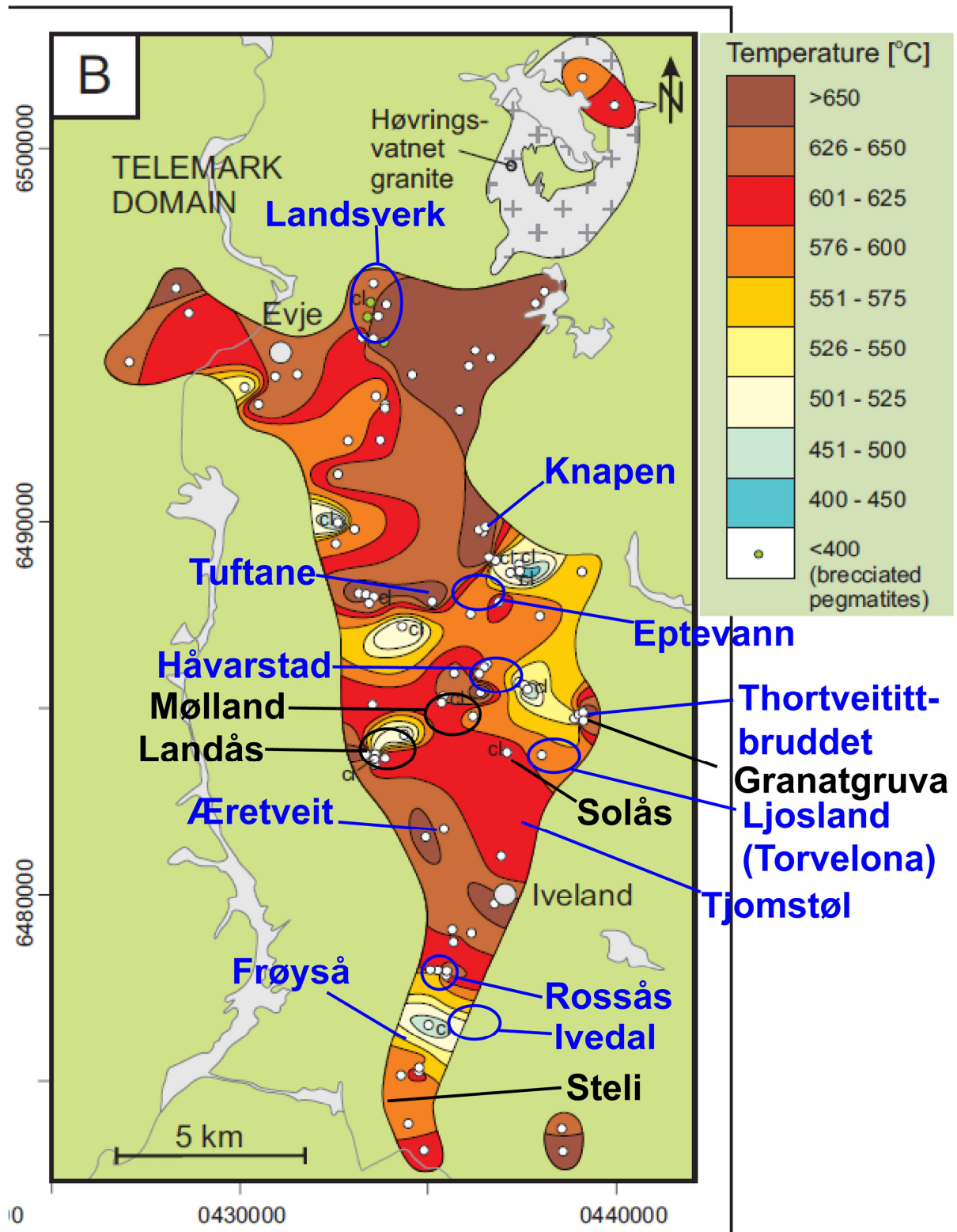
Figure 39: Map showing the distribution of some thortveitite-bearing (blue) and non-thortveitite-bearing (black) pegmatites. (Modified after Müller et al., 2015)

Conclusion

The different Mn/(Fe+Mn)-ratios in garnets, both between core and rim and from crystal to crystal, can be used to identify an eventual internal and/or regional chemical fractionation pattern. Combination of analyzing the Mn/(Fe+Mn)-ratio and Y and REE content in garnets from a pegmatite, may help to indicate if a replacement zone is present but not excavated. However, it is important to collect garnets from several zones of the pegmatites to get a precise result.

The formation of thortveitite in Evje-Iveland could be dependent on the temperature in the pegmatite-forming melt from a possible Sc-rich source, was high enough to promote crystallization of biotite over muscovite, in which more available Sc could be present to form thortveitite.

Future work

It could be of interest to investigate the Sc content in biotites and muscovites from thortveitite-bearing and non-thortveitite-bearing pegmatites in Evje-Iveland, to see if the muscovites are richer in Sc than the biotites and if there is a trend between thortveitite-bearing and non-thortveititebearing pegmatites.

Bibliography

Allègre, C. J., Provost, A., and Jaupart, J. (1981). Oscillatory zoning: a pathological case of crystal growth. *Nature* , 223-227.

Allendorf, B., and Sendelbach, M. (n.d.). Thortveitit ein sehr seltenes Scandiummineral.

Andersen, T. (2005). Terrane analysis, regional nomenclature and crustal evolution in the Southwest Scandinavian Domain of the Fennoscandian Shield. *GFF, 127* , 159-168.

Baldwin, J. R., and von Knorring, O. (1983). Compositional range of Mn-garne in zoned granitic pegmatites. *Canadian Mineralogist , 21*, 683-688.

Bartels, A., Vetere, F., Holtz, F., Behrens, H., and Linnen, R. L. (2011). Viscosity of flux-rich pegmatitic melts. *Contrib Mineral Petrol , 162*, 51-60.

Barth, T. F. (1947). The nickeliferous Iveland-Evje amphibolite and its relation. *Norwegian Geological Survey* , 71.

Bergstøl, S., and Juve, G. (1988). Scandian Ixiolite, Pyrochlor and Bzzite in Granite Pegmatite in Tørdal, Telemark, Norway. A Contribution to the Mineralogy and Geochemistry of Scandium and Tin. *Mineralogy and Petrology , 38*, 229-243.

Bingen, B., Giulio, V., and Nordgulen, Ø. (2008). A four-phase model for the Sveconorwegian orogeny, SW Scandinavia. *Norvegian Journal of Geology , 88*, 43-72.

Bjørlykke, H. (1947). Flaat Nickel. *Norwegian Geological Survey , 168*.

Bjørlykke, H. (1937). The granitic pegmatites of Southern Norway. *Journal of the Mineralogical Society of America , 22*, 241-255.

Cameron, E. N., Jahns, R. H., McNair, A. H., and Page, L. R. (1949). Internal structure of granitic pegmatites. *Economic Geology* .

Černý, P. (1991). Rare-element Granitic Pegmatites. Part 2: Regional to Global Environments and Petrogenesis,. *Geoscience Canada , 18*, 68-81.

Černý, P., and Ercit, S. (2005). The classification of granitic pegmatites revisited. *Canadian Mineralogis , 43*, 2005-2026.

Černý, P., Meintzer, R. E., and Anderson, A. J. (1985). Extreme fractionation in rare-element granitic pegmatites: selected examples of data and mechanism. *Can. Mineral , 23*, 381-421.

Chernoff, C. B., and Carlson, W. D. (1997). Disequilibrium for Ca during growth of pelitic garnet. *Journal of Metamorphic Geology , 15*, 421-438.

Coint, N., Slagstad, T., Roberts, N. M., Marker, M., Røhr, T., and Sørensen, B. E. (2015). The Late Mesoproterozoic Sirdal Magmatic Belt, SW Norway:Relationships between magmatism and metamorphism and implications for Sveconorwegian orogenesis,. *Precambrian Research , 265*, 57-77.

Corneliussen, A. (2012). *Prosjektet Gruver i Iveland/Evje*. Retrieved December 2015, from Pegmatite.no: http://pegmatite.no/

Feenstra, A., and Engi, M. (1998). An experimental study of the Fe-Mn exchange between garnet and ilmenite. *Contrib. Mineral. Petrol. , 131*, 379-392.

Foord, E. E., Birmingham, S. D., Demartin, F., Pilati, T., Gramaccioli, C. M., and Lichte, F. E. (1993). Thortveitite and associated Sc-bearing minerals from Ravalli County, Montana. *Canadian Mineralogist , 31*, 337-346.

Frigstad, O. F. (1999). Amazonittpegmatitter i Iveland-Evje. *Bergverksmuseets Skrift , 15*, 60-73.

Frigstad, O. F. (1968). En undersøkelse av cleavelanditsonerte pegmatittganger i Iveland-Evje, Nedre Setesdal. *Unpublished thesis?*

Fryklund Jr., V., and Fleischer, M. (1963). The abundance of scandium in volcanic rock, a preliminary estimate. *Geochimica et Cosmochimica Acta , 27*, 643-664.

Geller, S., and Miller, C. E. (1959). Silicate garnet-yttrium-iron garnet solid solutions. *The American Mineralogist , 44*, 1115-1120.

Goldschmidt, V. M. (1934). Drei Vorträge über Geochemie. *Geol. Fören. Förh. , 56*.

Goldschmidt, V. M., and Peters, C. (1931). Zur geochemie des scandiums. *Nachr.Gess.Wiss, Gøttingen, Math-Phys* , 264-267.

Gramenitskiy, E. N., and Shchekina, T. I. (2003, July 15). The experimental investigation of scndium behavior in fluorine-bearing melts. *Informational Bulletin of the Annual Seminar of Experimental Mineralogy, Petrology and Geochemistry , 21* . Moscow, Russia. Retrieved 2015, from http://www.scgis.ru/russian/cp1251/h_dgggms/1-2003/informbul-1_2003/magm-25e.pdf

Griffin, W. L., Powell, W., Pearson, N., and O´Reilly, S. Y. (2008). GLITTER: data reduction software for laser ablation ICP-MS. In: Sylvester, P. (Ed.), Laser Ablation–ICP–MS in the Earth Sciences. *Mineralogical Association of Canada Short Course Series , 40*.

Henderson, I. H., and Ihlen, P. M. (2004). Emplacement of polygeneration pegmatites in relation to Sveco-Norwegian contractional tectonics: examples from southern Norway. *Precambrian Research , 133*, 207-222.

Jaffe, H. W. (1951). The role of yttrium and other minor elements in the garnet group.

Jamtveit, B., Wogelius, R. A., and Fraser, D. (1993). Zonation patterns of skarn garnets: records of hydrothermal evolution. *Geology , 21*, 113-116.

Jarosewich, E., and Boatner, L. A. (1991). Rare-earth element reference samples for electron microprobe analysis. *Geostandards Newsletter , 15*, 397-399.

Jarosewich, e., Nelen, J. A., and Norberg, J. A. (1980). Refrence Samples for Electron Microprobe Analysis. *Geostand. Newsletter , 4*, 43-47.

Klein, C., and Dutrow, B. (2007). *Mineral Science* (23 ed.). John Wiley and sons, Inc.

Larsen, R. B. (2002). The distribution of Rare-earth elements in K-feldspar as an indicator of petrogenetic processes in granitic pegmatites: Examples from two pegmatite fields in southern Norway. *The Canadian Mineralogist , 40*, 137-151.

Locock, A. J. (2008). An Excel spreadsheet to recast analyses of garnet into end-member components, and a synopsis of the crystal chemistry of natural silicate garnets. *Computers and Geosciences , 34*, 1769-1780.

London, D. (2014). A petrologic assessment of internal zonation in granitic pegmatites. *Lithos* , 74-104.

London, D. (2005). Granitic pegmatites: an assesment of current concepts anddirections for the future. *Lithos , 80*, 281-303.

London, D. (2005). Granitic pegmatites: an assessment of current concepts and directions for the future. *Lithos , 80*, 281-303.

London, D. (2008). *Pegmatites.* Quebec: Mineralogical Association of Canada.

London, D. (1999). Stability of tourmaline in peraluminous granite systems: the boron cycle from anatexis to hydrothermal aureoles. *Eur. J. Mineral , 11*, 253-262.

London, D. (1992). The application of experimental petrology to the genesis and crystallization of granitic pegmatites. *Canadian Mineralogist , 30*, 499-540.

London, D., and Morgan, G. B. (2012). The Pegmatite Puzzle. *Elements , 8*, 263-268.

Lund, M. (2016). Columbite-tantalite and garnet geochemistry in Evje-Iveland. *Unpublished thesis* .

Martin, R., and DeVito, C. (2005). The patterns of enrichment in felsic pegmatites ultimately depend on tectonic setting. *The Canadian Mineralogist , 43*, 2027-2048.

McDonough, W. F., and Sun, S. S. (1995). Composition of the Earth. *Chemical Geology* , 223-253.

McDonough, W. F., and Sun, S.-s. (1995). The composition of the Earth. *Chemical Geology , 120*, 223-253.

Miller, C. F., and Stoddard, E. F. (1981). The role of manganese in the petrogenesis of magmatic garnet: an example from the Old-Woman-Piute Range, California. *J.Geol , 89*, 233-246.

Mindat. (2016a). Retrieved 01. 23, 2016, from http://www.mindat.org/loc-49248.html

Mindat. (2016b). Retrieved 01 23., 2016b, from http://www.mindat.org/loc-32623.html

Mindat. (2016c). Retrieved 01 22, 2016c, from http://www.mindat.org/loc-49349.html

Moriyasu, K., and Nishikawa, Y. (1991). Chemical Analysis of Thortveitite from Oro, Mineyama-cho, Naka-gun, Kyoto Prefecture, Japan. *Bulletin of the Chemica Society of Japan , 64*, 2908-2911.

Mulch, A., Cosca, M. A., Andresen, A., and Fiebig, J. (2005). Time scale of deformation and exhumation in extensional detachemnt systems determine by high-spatial resolution in situ UV-laser 40Ar/40Ar. *Earth and Planetary Science Letters , 233*, 375-390.

Müller, A., Hearsley, A., Spratt, J., and Seltmann, R. (2012). Petrogenetic implications of magmatic garnet in granitic pegmatites from southern Norway. *The Canadian Mineralogist , 50*, 1095-1115.

Müller, A., Ihlen, P. M., Snook, B., Larsen, R., Flem, B., Bingen, B., et al. (2015). The Chemistry of Quartz in Granitic Pegmatites of Southern Norway: Petrogenetic and Economic Implications. *Economic Geology , 110*, 1-100.

Neumann, H. (1961). The scandium content of some Norwegian Minerals and the formation of Thortveitite, A reconnaissance survey. *Norsk geologisk tidskrift , 41*, 197-210.

Nijland, T. G., Harlov, D. E., and Andersen, T. (2014). The Bamble Sector, South Norway: A review. *Geoscience Frontiers , 5*, 635-638.

Norman, J. C., and Haskin, L. A. (1967). The geochemistry of Sc: A comparison to the rare earths and Fe. *Geochemica et Cosmochimica Acta , 32*, 93-108.

Oftedal, I. (1943). Scandium in Biotite as a geologic thermometer. *Norsk geologisk tidskrift , 23*, 202-213.

Ohashi, H., Alba, M. D., Becerro, A. I., Chain, P., and Escudero, A. (2007). Structural study of the Lu2Si2O7-Sc2Si2O7 system. *Journal of Physics and Chemistry of Solids , 68*, 464-469.

Pedersen, and Konnerup-Madsen. (2000). Geology of the Setesdalen area, South Norway: Implications for the Sveconorwegian evolution of South Norway. *Bulletin of the Geological Society of Denmark , 46*, 181-201.

Pedersen, S., Andersen, T., Konnerup-Madsen, J., and Griffin, W. (2009). Recurrent mesoproterozoic continental magmatism in South-Central Norway. *Int. J Earth Sci* (98), 1151-1171.

Pouchou, and Pichoir. (1985). "PAP" (phi-rho-z)procedure for improved quatitative microanalysis. In: Armstrong JT(ed) Microbeam Analysis. San Francisco Press, San Francisco, 104-106

Pyle, J. M., and Spear, F. S. (1999). Yttrium zoning in garnet: Coupling of major and accessory phases during metamorphic reactions. *Geological Materials Research , 1*, 1-49.

Raade, G., Ferraris, G., Gula, A., Ivaldi, G., and Bernhard, F. (2002). Kristiansenite, a new calcium-scandium-tin sorosilicate from granitic pegmatite in Tørdal, Telemark, Norway. *Mineralogy and Petrology , 75*, 89.99.

Ramberg, I. B., Bryhni, I., and Nøttvedt, A. (2007). *The making of the land.* Norsk Geologisk Forening.

Sahama, T. G. (1936). Akzessorische Elements in den Granulitin von Finnisch-Lappland. *Bull.Geol.de Finl , 115*.

Scherer, E., Münker, C., and Mezger, K. (2001). Callibration of the lutetium-hafnium clock. *Science*, *293*, 683-687.

Schetelig, J. (1922). Thortveitite. A silicate of scandium, (Sc,Y)2Si2O7. *Norsk geologisk tidskrift , 6*, 233-234.

Schetelig, J. (1911). Ueber Thortveitite ein neues Mineral. *Centrblatt Min.* , 721-726.

Selbekk, R. (2012). Thortveititt og litt om scandium. *Stein* (2), 4-7.

Seydoux-Guillame, A.-M., Montel, J.-M., Bingen, B., Bosse, V., de Parceval, P., Paquette, J.-L., et al. (2012). Low-temperature alteration of monazite: Fluid mediated coupled dissolution-precipitation, irradiation damage, and disturbance of the U-Pb and Th-Pb chronometers . *Chemical Geology* , 140-158.

Shannon, R. D. (1976). Revised Effective Ionic Radii and Systematic Studies of Interatomic Distances in Halides and Chalcogenides. *Acta Cryst , 32*, 751-767.

Smeds, S.-A. (1994). Zoning and fractionation trends of a peraluminous NYF granitic pegmatite field at Falun, south-central Sweden. *GFF , 116* (3), 175-184.

Snook, B. R. (2014). Towards exploration tools for high purity quartz: An example from the South Norwegian Evje-Iveland pegmatite belt. *PhD thesis* .

Strunz, H., and Nickel, E. H. (2001). *Strunz Mineralogical Tables. Chemical Structural Mineral Classification System* (9 ed.). E. Schweizerbart'sch Verlangsbuchhandlung.

Yang, P., and Rivers, T. (2000). Trace element partitioning between coexisting biotite and muscovite from metamorphic rocks, Western Labrador: Structural, compositional and thermal controls. *Geochimica et Cosmochimica Acta , 64* (8), 1451-1472.

Appendix 2: Thortveitite

Table 8: Wt.% oxide and apfu for each analysis-spot in the collected thortveitites.

	22292_2Tuftane						
	Pale 1		Sone2		Medium1	Medium2	Dark
	29/1.	24 / 1 .	30/1.	25 / 1 .	26/1.	27/1.	28/1.
SiO2	38.34	38.13	39.01	38.29	38.51	39.17	40
Sc2O3	26.83	27.7	27.74	28.16	29.62	30.95	32.37
Y2O3	15.79	14.74	14.38	14.42	13.98	12.72	11.54
Fe2O3	0.76	1.27	1.12	1.44	1.24	1.28	0.72
FeO	0.31	-	0.29	-	-	-	-
MnO	0.48	0.53	0.61	0.51	0.4	0.39	0.2
ZrO2	2.16	2.42	2.65	2.31	2.07	2.02	1.22
REE2O3	15.03	12.71	13.74	12.19	12.22	12.35	13.65
MgO	0.03	0.06	0.03	0.07	0.07	0.07	0.08
CaO	0.11	1.31	0.34	0.46	0.27	0.56	0.36
TiO2	0.03	0.08	0.04	0.12	0.1	0.11	0.06
SrO	<0.01	<0.01	<0.01	<0.01	<0.01	<0.01	<0.01
HfO2	0.38	0.6	0.39	0.53	0.5	0.66	0.7
Ta2O5	<0.01	<0.01	<0.01	<0.01	<0.01	<0.01	<0.01
PbO	0.01	<0.01	<0.01	<0.01	<0.01	<0.01	<0.01
ThO2	0.03	0.01	<0.01	0.01	0.01	<0.01	0.01
UO2	<0.01	<0.01	<0.01	<0.01	<0.01	<0.01	<0.01
Total	100.32	99.62	100.41	98.56	99.05	100.35	100.98
Apfu							
Si	1.98	1.94	1.98	1.96	1.96	1.95	1.98
Sc	1.2	1.23	1.23	1.26	1.31	1.34	1.4
Y	0.43	0.40	0.38	0.39	0.37	0.33	0.30
Fe3+	0.02	0.04	0.04	0.05	0.04	0.04	0.02
Fe2+	0.01	0.00	0.01	0.00	0.00	0.00	0.00
Mn	0.02	0.02	0.02	0.02	0.01	0.01	0.00
Zr	0.05	0.06	0.06	0.05	0.05	0.04	0.02
Mg	0.00	0.00	0.00	0.00	0.00	0.00	0.00
Ca	0.00	0.07	0.01	0.02	0.01	0.03	0.01
Ti	0.00	0.00	0.00	0.00	0.00	0.00	0.00
Sr	0.00	0.00	0.00	0.00	0.00	0.00	0.00
La	0.00	0.00	0.00	0.00	0.00	0.00	0.00
Ce	0.00	0.00	0.00	0.00	0.00	0.00	0.00
Pr	0.00	0.00	0.00	0.00	0.00	0.00	0.00
Nd	0.00	0.00	0.00	0.00	0.00	0.00	0.00
Sm	0.00	0.00	0.00	0.00	0.00	0.00	0.00
Eu	0.00	0.00	0.00	0.00	0.00	0.00	0.00

Gd	0.00	0.00	0.00	0.00	0.00	0.00	0.00
Tb	0.00	0.00	0.00	0.00	0.00	0.00	0.00
Dy	0.01	0.01	0.00	0.01	0.01	0.01	0.01
Ho	0.00	0.00	0.00	0.00	0.00	0.00	0.00
Er	0.02	0.02	0.01	0.01	0.02	0.01	0.02
Tm	0.00	0.00	0.00	0.00	0.00	0.00	0.00
Yb	0.15	0.11	0.13	0.11	0.11	0.11	0.12
Lu	0.03	0.02	0.03	0.02	0.02	0.02	0.02
Hf	0.00	0.00	0.00	0.00	0.00	0.00	0.01
Ta	0.00	0.00	0.00	0.00	0.00	0.00	0.00
Pb	0.00	0.00	0.00	0.00	0.00	0.00	0.00
Th	0.00	0.00	0.00	0.00	0.00	0.00	0.00
U	0.00	0.00	0.00	0.00	0.00	0.00	0.00
Total	3.92	3.92	3.9	3.9	3.91	3.89	3.91
%							
Thortveitite	67.32	70.36	69.99	71.18	72.68	74.81	76.46
Kieviite-(Y)	24.19	22.86	22.16	22.26	20.95	18.77	16.65
Kieviite-(Yb)	8.47	6.76	7.84	6.55	6.36	6.4	6.87
Total	99.98	99.98	99.99	99.99	99.99	99.98	99.98

	22292_1Tuftane				22286Tuftane	
	22/1.	23/1.	21/1.	20/1.	17/1.	20/1.
SiO2	38.16	38.17	38.72	38.77	39.01	38.9
Sc2O3	26.85	27.33	28.81	28.95	27.31	27.04
Y2O3	15.77	15.46	14.95	14.64	13.85	13.83
Fe2O3	1.03	1.2	1.09	1.29	2.27	2.07
FeO	0.1	-	-	-	0.08	0.21
MnO	0.46	0.5	0.36	0.41	0.64	0.72
ZrO2	2.2	2.28	1.94	2.11	2.82	3.14
REE2O3	14.33	14.08	14.46	13.2	14.22	13.96
MgO	0.07	0.07	0.06	0.06	0.12	0.13
CaO	0.21	0.25	0.26	0.21	0.32	0.31
TiO2	0.07	0.07	0.07	0.08	0.17	0.18
SrO	<0.01	<0.01	<0.01	<0.01	<0.01	<0.01
HfO2	0.64	0.63	0.55	0.52	0.7	0.67
Ta2O5	<0.01	<0.01	<0.01	<0.01	<0.01	<0.01
PbO	<0.01	<0.01	<0.01	<0.01	<0.01	<0.01
ThO2	0.01	0.01	0.01	0.01	0.01	0.01
UO2	<0.01	<0.01	<0.01	<0.01	<0.01	<0.01
Total	99.98	100.13	101.35	100.32	101.59	101.23
Apfu						
Si	1.97	1.96	1.96	1.97	1.97	1.97
Sc	1.21	1.22	1.27	1.28	1.2	1.19

Y	0.43	0.42	0.4	0.39	0.37	0.37
Fe3+	0.04	0.04	0.04	0.04	0.08	0.07
Fe2+	0.00	0.00	0.00	0.00	0.00	0.00
Mn	0.02	0.02	0.01	0.01	0.02	0.03
Zr	0.05	0.05	0.04	0.05	0.06	0.07
Mg	0.00	0.00	0.00	0.00	0.00	0.00
Ca	0.01	0.01	0.01	0.01	0.01	0.01
Ti	0.00	0.00	0.00	0.00	0.00	0.00
Sr	0.00	0.00	0.00	0.00	0.00	0.00
La	0.00	0.00	0.00	0.00	0.00	0.00
Ce	0.00	0.00	0.00	0.00	0.00	0.00
Pr	0.00	0.00	0.00	0.00	0.00	0.00
Nd	0.00	0.00	0.00	0.00	0.00	0.00
Sm	0.00	0.00	0.00	0.00	0.00	0.00
Eu	0.00	0.00	0.00	0.00	0.00	0.00
Gd	0.00	0.00	0.00	0.00	0.00	0.00
Tb	0.00	0.00	0.00	0.00	0.00	0.00
Dy	0.01	0.01	0.01	0.01	0.01	0.01
Ho	0.00	0.00	0.00	0.00	0.00	0.00
Er	0.02	0.02	0.02	0.02	0.02	0.02
Tm	0.00	0.00	0.00	0.00	0.00	0.00
Yb	0.13	0.13	0.13	0.12	0.12	0.12
Lu	0.02	0.02	0.02	0.02	0.02	0.02
Hf	0.00	0.00	0.00	0.00	0.01	0.00
Ta	0.00	0.00	0.00	0.00	0.00	0.00
Pb	0.00	0.00	0.00	0.00	0.00	0.00
Th	0.00	0.00	0.00	0.00	0.00	0.00
U	0.00	0.00	0.00	0.00	0.00	0.00
Total	3.91	3.9	3.91	3.92	3.89	3.88
%						
Thortveitite	67.96	68.75	70.27	71.15	70.72	70.64
Kieviite-(Y)	24.37	23.75	22.27	21.98	21.9	22.06
Kieviite-(Yb)	7.65	7.49	7.45	6.86	7.36	7.29
	99.98	99.99	99.99	99.99	99.98	99.99

	22239Ljosland					
	Pale 1			Pale 2		
	10/1.	16/1.	6/1.	11/1.	9/1.	17/1.
SiO2	43.26	43.24	43.68	43.58	43.8	43.27
Sc2O3	43.75	44.24	44.27	44.54	44.92	44.94
Y2O3	3.49	3.62	3.39	3.99	3.45	3.39
Fe2O3	1.23	1.44	0.88	1.11	1.1	1.5
FeO	0.31	0.15	0.58	0.24	0.26	-
MnO	0.12	0.09	0.08	0.1	0.07	0.12
ZrO2	1.85	1.89	1.86	1.8	1.79	1.82

REE2O3	4.56	4.73	4.17	4.18	4.36	4.68
MgO	0.05	0.04	0.03	0.02	0.04	0.04
CaO	0.19	0.13	0.15	0.16	0.17	0.12
TiO2	0.05	0.05	0.04	0.04	0.05	0.05
SrO	<0.01	<0.01	<0.01	<0.01	<0.01	<0.01
HfO2	0.21	0.21	0.19	0.22	0.20	0.21
Ta2O5	<0.01	<0.01	<0.01	<0.01	<0.01	<0.01
PbO	<0.01	<0.01	<0.01	<0.01	<0.01	<0.01
ThO2	<0.01	<0.01	<0.01	<0.01	<0.01	<0.01
UO2	0.01	0.01	0.01	<0.01	0.01	0.01
Total	99.15	99.91	99.4	100.03	100.29	100.22
Apfu						
Si	1.98	1.97	1.99	1.97	1.98	1.96
Sc	1.74	1.75	1.75	1.76	1.76	1.77
Y	0.08	0.08	0.08	0.09	0.08	0.08
Fe3+	0.04	0.04	0.03	0.03	0.03	0.05
Fe2+	0.01	0.00	0.02	0.00	0.01	0.00
Mn	0.00	0.00	0.00	0.00	0.00	0.00
Zr	0.04	0.04	0.04	0.03	0.03	0.04
Mg	0.00	0.00	0.00	0.00	0.00	0.00
Ca	0.00	0.00	0.00	0.00	0.00	0.00
Ti	0.00	0.00	0.00	0.00	0.00	0.00
Sr	0.00	0.00	0.00	0.00	0.00	0.00
La	0.00	0.00	0.00	0.00	0.00	0.00
Ce	0.00	0.00	0.00	0.00	0.00	0.00
Pr	0.00	0.00	0.00	0.00	0.00	0.00
Nd	0.00	0.00	0.00	0.00	0.00	0.00
Sm	0.00	0.00	0.00	0.00	0.00	0.00
Eu	0.00	0.00	0.00	0.00	0.00	0.00
Gd	0.00	0.00	0.00	0.00	0.00	0.00
Tb	0.00	0.00	0.00	0.00	0.00	0.00
Dy	0.00	0.00	0.00	0.00	0.00	0.00
Ho	0.00	0.00	0.00	0.00	0.00	0.00
Er	0.00	0.00	0.00	0.00	0.00	0.00
Tm	0.00	0.00	0.00	0.00	0.00	0.00
Yb	0.04	0.04	0.03	0.03	0.03	0.04
Lu	0.01	0.01	0.01	0.01	0.01	0.01
Hf	0.00	0.00	0.00	0.00	0.00	0.00
Ta	0.00	0.00	0.00	0.00	0.00	0.00
Pb	0.00	0.00	0.00	0.00	0.00	0.00
Th	0.00	0.00	0.00	0.00	0.00	0.00
U	0.00	0.00	0.00	0.00	0.00	0.00
Total	3.94	3.93	3.95	3.92	3.93	3.95
%						

Thortveitite	93.2	93.05	93.58	92.93	93.5	93.44
Kieviite-(Y)	4.54	4.65	4.38	5.08	4.39	4.3
Kieviite-(Yb)	2.24	2.29	2.02	1.97	2.09	2.24

	22239Ljosland							
	Medium 1					Medium2	Dark	
	13/1.	14/1.	8/1.	18/1.	12/.1	19/1.	15/1.	7/1.
SiO2	43.88	43.92	43.99	43.56	44.1	43.83	44.23	44.57
Sc2O3	45.61	45.92	45.61	46.18	46.41	47.33	47.59	48.37
Y2O3	2.94	2.72	3.52	3.05	3.07	1.44	1.34	1.89
Fe2O3	1.2	1.04	1.15	1.24	1.18	1.4	1.2	0.86
FeO	0.11	0.19	0.15	-	-	-	0.07	-
MnO	0.15	0.14	0.1	0.09	0.08	0.11	0.11	0.02
ZrO2	1.72	1.8	1.61	1.67	1.63	1.69	1.74	1.49
REE2O3	4.22	3.66	3.85	3.52	3.46	3.56	3.77	3.5
MgO	0.05	0.01	0.02	0.02	0.01	0.01	0.01	0.02
CaO	0.13	0.17	0.13	0.28	0.17	0.33	0.11	0.35
TiO2	0.05	0.03	0.04	0.02	0.03	0.03	0.03	0.02
SrO	<0.01	<0.01	<0.01	<0.01	<0.01	<0.01	<0.01	<0.01
HfO2	0.19	0.18	0.2	0.15	0.17	0.18	0.18	0.15
Ta2O5	<0.01	<0.01	<0.01	<0.01	<0.01	<0.01	<0.01	<0.01
PbO	<0.01	<0.01	<0.01	<0.01	<0.01	<0.01	<0.01	<0.01
ThO2	<0.01	<0.01	<0.01	<0.01	<0.01	<0.01	<0.01	<0.01
UO2	0.01	<0.01	<0.01	<0.01	<0.01	<0.01	<0.01	<0.01
Total	100.3	99.85	100.44	99.85	100.38	99.97	100.45	101.31
Apfu								
Si	1.97	1.97	1.97	1.96	1.97	1.96	1.97	1.96
Sc	1.79	1.8	1.78	1.81	1.81	1.84	1.84	1.85
Y	0.07	0.06	0.08	0.07	0.07	0.03	0.03	0.04
Fe3+	0.04	0.03	0.03	0.04	0.03	0.04	0.04	0.02
Fe2+	0.00	0.00	0.00	0.00	0.00	0.00	0.00	0.00
Mn	0.00	0.00	0.00	0.00	0.00	0.00	0.00	0.00
Zr	0.03	0.03	0.03	0.03	0.03	0.03	0.03	0.03
Mg	0.00	0.00	0.00	0.00	0.00	0.00	0.00	0.00
Ca	0.00	0.00	0.00	0.01	0.00	0.01	0.00	0.01
Ti	0.00	0.00	0.00	0.00	0.00	0.00	0.00	0.00
Sr	0.00	0.00	0.00	0.00	0.00	0.00	0.00	0.00
La	0.00	0.00	0.00	0.00	0.00	0.00	0.00	0.00
Ce	0.00	0.00	0.00	0.00	0.00	0.00	0.00	0.00
Pr	0.00	0.00	0.00	0.00	0.00	0.00	0.00	0.00
Nd	0.00	0.00	0.00	0.00	0.00	0.00	0.00	0.00
Sm	0.00	0.00	0.00	0.00	0.00	0.00	0.00	0.00
Eu	0.00	0.00	0.00	0.00	0.00	0.00	0.00	0.00
Gd	0.00	0.00	0.00	0.00	0.00	0.00	0.00	0.00

Tb	0.00	0.00	0.00	0.00	0.00	0.00	0.00	0.00
Dy	0.00	0.00	0.00	0.00	0.00	0.00	0.00	0.00
Ho	0.00	0.00	0.00	0.00	0.00	0.00	0.00	0.00
Er	0.00	0.00	0.00	0.00	0.00	0.00	0.00	0.00
Tm	0.00	0.00	0.00	0.00	0.00	0.00	0.00	0.00
Yb	0.03	0.03	0.03	0.03	0.03	0.03	0.03	0.03
Lu	0.01	0.00	0.00	0.00	0.00	0.00	0.00	0.00
Hf	0.00	0.00	0.00	0.00	0.00	0.00	0.00	0.00
Ta	0.00	0.00	0.00	0.00	0.00	0.00	0.00	0.00
Pb	0.00	0.00	0.00	0.00	0.00	0.00	0.00	0.00
Th	0.00	0.00	0.00	0.00	0.00	0.00	0.00	0.00
U	0.00	0.00	0.00	0.00	0.00	0.00	0.00	0.00
Total	3.94	3.92	3.92	3.95	3.94	3.94	3.94	3.94
%								
Thortveitite	94.27	94.83	93.78	94.5	94.57	96.53	96.57	96.09
Kieviite-(Y)	3.71	3.43	4.42	3.81	3.82	1.8	1.66	2.3
Kieviite-(Yb)	2	1.72	1.78	1.67	1.59	1.66	1.76	1.59

	22238Tjomstøl				
	Pale1	Pale 2		Medium 1	
	23/1.	9/1.	16/1.	8/1.	11/1.
SiO2	43.76	43.57	43.83	44	44.31
Sc2O3	41.92	42.7	42.54	44.49	44.35
Y2O3	2.3	2.15	2.33	2.1	2.18
Fe2O3	1.03	1.5	1.02	1.33	0.96
FeO	1.13	0.65	1.05	0.47	0.76
MnO	1.07	0.95	0.95	0.62	0.59
ZrO2	3.71	3.55	3.48	2.7	2.65
REE2O3	2.71	2.8	2.33	2.66	2.64
MgO	0.15	0.09	0.1	0.08	0.07
CaO	0.11	0.21	0.15	0.20	0.21
TiO2	0.1	0.07	0.07	0.07	0.08
SrO	<0.01	<0.01	<0.01	<0.01	<0.01
HfO2	1.36	0.64	0.88	0.50	0.38
Ta2O5	<0.01	<0.01	<0.01	<0.01	<0.01
PbO	<0.01	<0.01	<0.01	<0.01	<0.01
ThO2	<0.01	<0.01	<0.01	<0.01	<0.01
UO2	0.06	0.04	0.05	0.04	0.03
Total	99.51	99	98.86	99.34	99.28
apfu					
Si	1.99	1.98	1.99	1.98	2.00
Sc	1.66	1.69	1.69	1.75	1.74
Y	0.05	0.05	0.05	0.05	0.05

Fe3+	0.03	0.05	0.03	0.04	0.03
Fe2+	0.04	0.02	0.04	0.01	0.02
Mn	0.04	0.03	0.03	0.02	0.02
Zr	0.08	0.07	0.07	0.05	0.05
Mg	0.01	0.00	0.00	0.00	0.00
Ca	0.00	0.01	0.00	0.01	0.01
Ti	0.00	0.00	0.00	0.00	0.00
Sr	0.00	0.00	0.00	0.00	0.00
La	0.00	0.00	0.00	0.00	0.00
Ce	0.00	0.00	0.00	0.00	0.00
Pr	0.00	0.00	0.00	0.00	0.00
Nd	0.00	0.00	0.00	0.00	0.00
Sm	0.00	0.00	0.00	0.00	0.00
Eu	0.00	0.00	0.00	0.00	0.00
Gd	0.00	0.00	0.00	0.00	0.00
Tb	0.00	0.00	0.00	0.00	0.00
Dy	0.00	0.00	0.00	0.00	0.00
Ho	0.00	0.00	0.00	0.00	0.00
Er	0.00	0.00	0.00	0.00	0.00
Tm	0.00	0.00	0.00	0.00	0.00
Yb	0.02	0.02	0.01	0.02	0.02
Lu	0.00	0.00	0.00	0.00	0.00
Hf	0.01	0.00	0.01	0.00	0.00
Ta	0.00	0.00	0.00	0.00	0.00
Pb	0.00	0.00	0.00	0.00	0.00
Th	0.00	0.00	0.00	0.00	0.00
U	0.00	0.00	0.00	0.00	0.00
Total	3.93	3.92	3.92	3.93	3.94
Thortveitite	95.56	95.73	95.71	96.01	95.91
Kieviite-(Y)	3.2	2.95	3.2	2.77	2.87
Kieviite-(Yb)	1.23	1.31	1.07	1.2	1.2

	22238Tjomstøl						
	Medium 2					Dark	
	15/1.	22/1.	12/1.	14/1.	21/1.	7/1.	10/1.
SiO2	44.23	44.4	44.17	44.34	44.59	44.44	44.09
Sc2O3	44.74	44.76	44.68	45.3	45.2	45.69	45.72
Y2O3	2.00	2.08	2.16	1.88	2.11	2.10	2.17
Fe2O3	1.10	0.84	1.27	1.13	0.76	1.12	1.76
FeO	0.62	0.85	0.47	0.55	0.84	0.45	0.04
MnO	0.60	0.56	0.54	0.52	0.46	0.39	0.41
ZrO2	2.68	2.6	2.69	2.58	2.46	2.32	2.21

REE2O3	2.5	2.75	2.63	2.38	2.96	2.64	2.47
MgO	0.10	0.09	0.08	0.10	0.11	0.08	0.06
CaO	0.19	0.10	0.28	0.19	0.09	0.2	0.24
TiO2	0.08	0.07	0.08	0.07	0.08	0.07	0.07
SrO	<0.01	<0.01	<0.01	<0.01	<0.01	<0.01	<0.01
HfO2	0.78	0.70	0.55	0.77	0.86	0.56	0.32
Ta2O5	<0.01	<0.01	<0.01	<0.01	<0.01	<0.01	<0.01
PbO	<0.01	<0.01	<0.01	<0.01	<0.01	<0.01	<0.01
ThO2	<0.01	<0.01	<0.01	<0.01	<0.01	<0.01	<0.01
UO2	0.05	0.04	0.04	0.05	0.04	0.04	0.03
Total	99.74	99.94	99.71	99.94	100.65	100.19	99.66
Apfu							
Si	1.99	1.99	1.98	1.98	1.99	1.98	1.97
Sc	1.75	1.75	1.75	1.76	1.76	1.77	1.78
Y	0.04	0.04	0.05	0.04	0.05	0.05	0.05
Fe3+	0.03	0.02	0.04	0.03	0.02	0.03	0.05
Fe2+	0.02	0.03	0.01	0.02	0.03	0.01	0.00
Mn	0.02	0.02	0.02	0.02	0.01	0.01	0.01
Zr	0.05	0.05	0.05	0.05	0.05	0.05	0.04
Mg	0.00	0.00	0.00	0.00	0.00	0.00	0.00
Ca	0.00	0.00	0.01	0.00	0.00	0.00	0.01
Ti	0.00	0.00	0.00	0.00	0.00	0.00	0.00
Sr	0.00	0.00	0.00	0.00	0.00	0.00	0.00
La	0.00	0.00	0.00	0.00	0.00	0.00	0.00
Ce	0.00	0.00	0.00	0.00	0.00	0.00	0.00
Pr	0.00	0.00	0.00	0.00	0.00	0.00	0.00
Nd	0.00	0.00	0.00	0.00	0.00	0.00	0.00
Sm	0.00	0.00	0.00	0.00	0.00	0.00	0.00
Eu	0.00	0.00	0.00	0.00	0.00	0.00	0.00
Gd	0.00	0.00	0.00	0.00	0.00	0.00	0.00
Tb	0.00	0.00	0.00	0.00	0.00	0.00	0.00
Dy	0.00	0.00	0.00	0.00	0.00	0.00	0.00
Ho	0.00	0.00	0.00	0.00	0.00	0.00	0.00
Er	0.00	0.00	0.00	0.00	0.00	0.00	0.00
Tm	0.00	0.00	0.00	0.00	0.00	0.00	0.00
Yb	0.02	0.02	0.02	0.01	0.02	0.02	0.02
Lu	0.00	0.00	0.00	0.00	0.00	0.00	0.00
Hf	0.01	0.00	0.00	0.00	0.01	0.00	0.00
Ta	0.00	0.00	0.00	0.00	0.00	0.00	0.00
Pb	0.00	0.00	0.00	0.00	0.00	0.00	0.00
Th	0.00	0.00	0.00	0.00	0.00	0.00	0.00
U	0.00	0.00	0.00	0.00	0.00	0.00	0.00
Total	3.93	3.92	3.93	3.91	3.94	3.92	3.93
End-members %							

Thortveitite	96.25	96.05	95.97	96.49	95.97	96.12	96.1
Kieviite-(Y)	2.63	2.73	2.83	2.45	2.74	2.7	2.79
Kieviite-(Yb)	1.11	1.21	1.18	1.05	1.27	1.16	1.1

	22330Torvelona								
	Pale 1	Pale 2	Pale 3	Medium 1	Medium 2		Dark		Solid
	30/1.	3/1.	25/1.	29/1.	26/1.	1/1.	24/1.	6/1.	4/1.
SiO2	41.54	42.72	42.61	42.95	43.33	42.93	43.87	43.33	43.78
Sc2O3	35.27	38.41	38.95	40.86	41.68	42.29	43.51	43.96	45.43
Y2O3	6.87	6.19	6.35	4.62	4.04	5.67	4.00	3.48	3.16
Fe2O3	2.02	0.75	1.03	1.09	1.00	0.79	1.23	1.31	1.14
FeO	0.12	0.61	0.37	0.17	0.29	-	0.27	-	-
MnO	1.59	1.17	1.00	0.84	0.83	0.35	0.52	0.56	0.4
ZrO2	3.58	2.77	2.56	2.24	2.08	1.48	1.75	1.89	1.7
REE2O3	9.05	5.24	6.12	6.49	6.24	5.78	5.00	5.4	5.39
MgO	0.09	0.05	0.04	0.02	0.05	0.06	0.03	0.06	0.08
CaO	-	0.16	0.11	0.19	0.19	0.16	0.09	0.14	0.17
TiO2	0.08	0.06	0.06	0.04	0.43	0.07	0.05	0.08	0.07
SrO	<0.01	<0.01	<0.01	<0.01	<0.01	<0.01	<0.01	<0.01	<0.01
HfO2	0.61	0.48	0.49	0.44	0.58	0.56	0.34	0.64	0.51
Ta2O5	0.01	<0.01	<0.01	<0.01	0.04	0.01	<0.01	0.01	0.01
PbO	0.02	<0.01	<0.01	<0.01	0.04	<0.01	<0.01	<0.01	<0.01
ThO2	0.04	<0.01	<0.01	<0.01	<0.01	<0.01	<0.01	<0.01	<0.01
UO2	0.01	<0.01	<0.01	<0.01	<0.01	<0.01	<0.01	<0.01	<0.01
Total	100.97	98.7	99.76	100.01	100.88	100.22	100.72	100.94	101.91
Apfu									
Si	1.98	2.01	1.99	1.99	1.98	1.98	1.99	1.96	1.96
Sc	1.46	1.57	1.58	1.65	1.66	1.69	1.72	1.73	1.77
Y	0.17	0.15	0.15	0.11	0.09	0.13	0.09	0.08	0.07
Fe3+	0.07	0.02	0.03	0.03	0.03	0.02	0.03	0.04	0.03
Fe2+	0.00	0.02	0.01	0.00	0.01	0.00	0.01	0.00	0.00
Mn	0.06	0.04	0.03	0.03	0.03	0.01	0.02	0.02	0.01
Zr	0.08	0.06	0.05	0.05	0.04	0.03	0.03	0.04	0.03
Mg	0.00	0.00	0.00	0.00	0.00	0.00	0.00	0.00	0.00
Ca	0.00	0.00	0.00	0.00	0.00	0.00	0.00	0.00	0.00
Ti	0.00	0.00	0.00	0.00	0.01	0.00	0.00	0.00	0.00
Sr	0.00	0.00	0.00	0.00	0.00	0.00	0.00	0.00	0.00
La	0.00	0.00	0.00	0.00	0.00	0.00	0.00	0.00	0.00
Ce	0.00	0.00	0.00	0.00	0.00	0.00	0.00	0.00	0.00
Pr	0.00	0.00	0.00	0.00	0.00	0.00	0.00	0.00	0.00
Nd	0.00	0.00	0.00	0.00	0.00	0.00	0.00	0.00	0.00
Sm	0.00	0.00	0.00	0.00	0.00	0.00	0.00	0.00	0.00
Eu	0.00	0.00	0.00	0.00	0.00	0.00	0.00	0.00	0.00

Gd	0.00	0.00	0.00	0.00	0.00	0.00	0.00	0.00	0.00
Tb	0.00	0.00	0.00	0.00	0.00	0.00	0.00	0.00	0.00
Dy	0.01	0.00	0.00	0.00	0.00	0.00	0.00	0.00	0.00
Ho	0.00	0.00	0.00	0.00	0.00	0.00	0.00	0.00	0.00
Er	0.01	0.00	0.00	0.00	0.00	0.00	0.00	0.00	0.00
Tm	0.00	0.00	0.00	0.00	0.00	0.00	0.00	0.00	0.00
Yb	0.06	0.04	0.05	0.06	0.05	0.05	0.04	0.04	0.04
Lu	0.01	0.01	0.01	0.01	0.01	0.01	0.01	0.01	0.01
Hf	0.00	0.00	0.00	0.00	0.00	0.00	0.00	0.00	0.00
Ta	0.00	0.00	0.00	0.00	0.00	0.00	0.00	0.00	0.00
Pb	0.00	0.00	0.00	0.00	0.00	0.00	0.00	0.00	0.00
Th	0.00	0.00	0.00	0.00	0.00	0.00	0.00	0.00	0.00
U	0.00	0.00	0.00	0.00	0.00	0.00	0.00	0.00	0.00
Total	3.91	3.92	3.9	3.93	3.91	3.92	3.94	3.92	3.92
End-members									
Thortveitite	86.06	88.53	88.12	90.39	91.43	89.92	92.36	92.96	93.47
Kieviite-(Y)	10.24	8.72	8.78	6.25	5.42	7.36	5.18	4.49	3.98
Kieviite-(Yb)	3.68	2.74	3.09	3.35	3.14	2.71	2.44	2.54	2.53

		22302Knapen						
		Pale		Medium			Dark	
		38/1.	34/1.	33/1.	37/1.	32/1.	31/1.	36/1.
SiO2		42.08	42.13	42.52	42.22	42.5	42.56	42.77
Sc2O3		37.09	37.07	39.11	39.25	39.42	39.91	40.2
Y2O3		7.00	6.20	6.05	5.94	5.69	5.46	5.34
Fe2O3		1.03	1.43	1.25	1.20	1.17	1.23	1.50
FeO		0.63	0.48	0.36	0.28	0.52	0.32	0.25
MnO		0.89	1.12	0.72	0.63	0.65	0.58	0.64
ZrO2		2.77	3.29	2.61	2.49	2.51	2.35	2.48
REE2O3		5.78	5.86	5.83	5.94	5.59	5.42	5.39
MgO		0.06	0.07	0.05	0.05	0.05	0.04	0.05
CaO		0.30	0.37	0.31	0.31	0.24	0.35	0.31
TiO2		0.14	0.12	0.10	0.10	0.12	0.12	0.11
SrO		<0.01	<0.01	<0.01	<0.01	<0.01	<0.01	<0.01
HfO2		0.82	0.92	0.64	0.64	0.54	0.50	0.46
Ta2O5		0.02	0.01	<0.01	<0.01	<0.01	<0.01	<0.01
PbO		<0.01	<0.01	<0.01	<0.01	<0.01	<0.01	<0.01
ThO2		<0.01	<0.01	<0.01	<0.01	<0.01	<0.01	<0.01
UO2		0.01	0.01	0.01	0.01	<0.01	0.01	<0.01
Total		98.7	99.14	99.64	99.13	99.08	98.91	99.58
apfu								
Si		2	1.99	1.99	1.98	1.99	1.99	1.98
Sc		1.53	1.52	1.59	1.60	1.61	1.62	1.62

Y	0.17	0.15	0.15	0.14	0.14	0.13	0.13
Fe3+	0.03	0.05	0.04	0.04	0.04	0.04	0.05
Fe2+	0.02	0.01	0.01	0.01	0.02	0.01	0.00
Mn	0.03	0.04	0.02	0.02	0.02	0.02	0.02
Zr	0.06	0.07	0.05	0.05	0.05	0.05	0.05
Mg	0.00	0.00	0.00	0.00	0.00	0.00	0.00
Ca	0.01	0.01	0.01	0.01	0.01	0.01	0.01
Ti	0.00	0.00	0.00	0.00	0.00	0.00	0.00
Sr	0.00	0.00	0.00	0.00	0.00	0.00	0.00
La	0.00	0.00	0.00	0.00	0.00	0.00	0.00
Ce	0.00	0.00	0.00	0.00	0.00	0.00	0.00
Pr	0.00	0.00	0.00	0.00	0.00	0.00	0.00
Nd	0.00	0.00	0.00	0.00	0.00	0.00	0.00
Sm	0.00	0.00	0.00	0.00	0.00	0.00	0.00
Eu	0.00	0.00	0.00	0.00	0.00	0.00	0.00
Gd	0.00	0.00	0.00	0.00	0.00	0.00	0.00
Tb	0.00	0.00	0.00	0.00	0.00	0.00	0.00
Dy	0.00	0.00	0.00	0.00	0.00	0.00	0.00
Ho	0.00	0.00	0.00	0.00	0.00	0.00	0.00
Er	0.00	0.00	0.00	0.00	0.00	0.00	0.00
Tm	0.00	0.00	0.00	0.00	0.00	0.00	0.00
Yb	0.04	0.04	0.04	0.05	0.04	0.04	0.04
Lu	0.01	0.01	0.01	0.01	0.01	0.01	0.01
Hf	0.01	0.01	0.00	0.00	0.00	0.00	0.00
Ta	0.00	0.00	0.00	0.00	0.00	0.00	0.00
Pb	0.00	0.00	0.00	0.00	0.00	0.00	0.00
Th	0.00	0.00	0.00	0.00	0.00	0.00	0.00
U	0.00	0.00	0.00	0.00	0.00	0.00	0.00
Total	3.91	3.9	3.91	3.91	3.93	3.92	3.91
End-members							
Thortveitite	87.18	88.11	88.85	88.95	89.4	89.89	90.05
Kieviite-(Y)	10.05	9.01	8.39	8.22	7.88	7.52	7.31
Kieviite-(Yb)	2.75	2.86	2.74	2.81	2.71	2.57	2.62

	22370Eptevann					22273Håvarstad			
	Pale			Medium	Dark	Pale	Medium	Dark	
	34/1	32/1.	35/1.	33/1.	31/1.	37/1.	38/1.	40/1.	39/1.
SiO2	44.51	44.49	44.47	44.81	45.97	44.41	44.74	45.32	45.31
Sc2O3	46.21	45.92	46.23	48.04	50.76	45.07	48.17	48.74	48.89
Y2O3	0.82	0.84	0.77	0.51	0.66	1.8	1.67	1.24	0.88
Fe2O3	1.35	1.38	1.49	1.28	0.56	1.56	0.97	0.91	0.85
FeO	0.53	0.56	0.53	0.29	0.12	0.19	0.16	-	0.33
MnO	0.6	0.66	0.64	0.41	0.09	0.56	0.14	0.23	0.24
ZrO2	2.8	2.93	2.83	2.33	1.47	2.72	1.68	1.78	1.96

REE2O3	1.47	1.27	1.30	1.07	1.41	2.31	2.42	2.21	2.1
MgO	0.12	0.14	0.13	0.09	0.01	0.32	0.06	0.05	0.05
CaO	0.14	0.15	0.07	0.14	0.21	0.13	0.09	0.14	0.10
TiO2	0.08	0.07	0.09	0.06	0.01	0.06	0.02	0.02	0.01
SrO	<0.01	<0.01	<0.01	<0.01	<0.01	<0.01	<0.01	<0.01	<0.01
HfO2	0.49	0.49	0.48	0.36	0.12	0.56	0.35	0.56	0.46
Ta2O5	<0.01	<0.01	<0.01	<0.01	<0.01	0.01	<0.01	<0.01	<0.01
PbO	<0.01	<0.01	<0.01	<0.01	<0.01	0.03	<0.01	<0.01	<0.01
ThO2	<0.01	<0.01	<0.01	<0.01	<0.01	<0.01	<0.01	<0.01	<0.01
UO2	0.06	0.05	0.05	0.03	<0.01	0.03	<0.01	<0.01	<0.01
Total	99.26	99.04	99.17	99.5	101.45	99.83	100.53	101.28	101.24
Apfu									
Si	1.98	1.98	1.98	1.98	1.98	1.98	1.97	1.98	1.98
Sc	1.79	1.78	1.79	1.85	1.91	1.75	1.85	1.85	1.86
Y	0.01	0.02	0.01	0.01	0.01	0.04	0.03	0.02	0.02
Fe3+	0.04	0.04	0.05	0.04	0.01	0.05	0.03	0.03	0.02
Fe2+	0.02	0.02	0.02	0.01	0.00	0.00	0.00	0.00	0.01
Mn	0.02	0.02	0.02	0.01	0.00	0.02	0.00	0.00	0.00
Zr	0.06	0.06	0.06	0.05	0.03	0.05	0.03	0.03	0.04
Mg	0.00	0.00	0.00	0.00	0.00	0.02	0.00	0.00	0.00
Ca	0.00	0.00	0.00	0.00	0.00	0.00	0.00	0.00	0.00
Ti	0.00	0.00	0.00	0.00	0.00	0.00	0.00	0.00	0.00
Sr	0.00	0.00	0.00	0.00	0.00	0.00	0.00	0.00	0.00
La	0.00	0.00	0.00	0.00	0.00	0.00	0.00	0.00	0.00
Ce	0.00	0.00	0.00	0.00	0.00	0.00	0.00	0.00	0.00
Pr	0.00	0.00	0.00	0.00	0.00	0.00	0.00	0.00	0.00
Nd	0.00	0.00	0.00	0.00	0.00	0.00	0.00	0.00	0.00
Sm	0.00	0.00	0.00	0.00	0.00	0.00	0.00	0.00	0.00
Eu	0.00	0.00	0.00	0.00	0.00	0.00	0.00	0.00	0.00
Gd	0.00	0.00	0.00	0.00	0.00	0.00	0.00	0.00	0.00
Tb	0.00	0.00	0.00	0.00	0.00	0.00	0.00	0.00	0.00
Dy	0.00	0.00	0.00	0.00	0.00	0.00	0.00	0.00	0.00
Ho	0.00	0.00	0.00	0.00	0.00	0.00	0.00	0.00	0.00
Er	0.00	0.00	0.00	0.00	0.00	0.00	0.00	0.00	0.00
Tm	0.00	0.00	0.00	0.00	0.00	0.00	0.00	0.00	0.00
Yb	0.01	0.01	0.01	0.00	0.01	0.01	0.02	0.01	0.01
Lu	0.00	0.00	0.00	0.00	0.00	0.00	0.00	0.00	0.00
Hf	0.00	0.00	0.00	0.00	0.00	0.00	0.00	0.00	0.00
Ta	0.00	0.00	0.00	0.00	0.00	0.00	0.00	0.00	0.00
Pb	0.00	0.00	0.00	0.00	0.00	0.00	0.00	0.00	0.00
Th	0.00	0.00	0.00	0.00	0.00	0.00	0.00	0.00	0.00
U	0.00	0.00	0.00	0.00	0.00	0.00	0.00	0.00	0.00
Total	3.93	3.93	3.94	3.95	3.95	3.92	3.93	3.92	3.94
End-members %									
Thortveitite	98.23	98.29	98.39	98.86	98.56	96.54	96.85	97.47	97.93

	1.07	1.10	1.00	0.64	0.78	2.36	2.05	1.51	1.08
Kieviite-(Y)	1.07	1.10	1.00	0.64	0.78	2.36	2.05	1.51	1.08
Kieviite-(Yb)	0.68	0.6	0.6	0.49	0.64	1.09	1.08	1.01	0.98

	22304Eretveit				
	Pale	Medium			Dark
	3/1.	2/1.	4/1.	5/1.	1/1.
SiO_2	40.26	40.51	41.27	40.99	41.09
Sc_2O_3	31.4	32.58	33.45	33.19	35.51
Y_2O_3	9.52	9.43	9.12	9.17	8.29
Fe_2O_3	0.99	1.74	1.32	1.98	1.92
FeO	0.92	0.33	0.54	-	-
MnO	1.38	1.18	1.14	1.15	0.76
ZrO_2	4.62	4.02	3.92	3.99	3.1
REE_2O_3	7.24	7.57	6.36	6.93	6.89
MgO	0.17	0.17	0.15	0.2	0.17
CaO	0.26	0.35	0.47	0.62	0.59
TiO_2	0.18	0.19	0.19	0.16	0.18
SrO	<0.01	<0.01	<0.01	<0.01	<0.01
HfO_2	0.80	0.77	0.56	0.80	0.73
Ta_2O_5	0.02	0.02	0.01	0.01	0.02
PbO	<0.01	<0.01	<0.01	<0.01	<0.01
ThO_2	0.03	0.03	0.02	0.01	0.03
UO_2	0.03	0.03	0.03	0.03	0.03
Total	97.9	99.00	98.63	99.31	99.37
apfu					
Si	1.99	1.97	1.99	1.98	1.96
Sc	1.35	1.38	1.41	1.39	1.48
Y	0.25	0.24	0.23	0.23	0.21
Fe3+	0.03	0.06	0.04	0.07	0.06
Fe2+	0.03	0.01	0.02	0.00	0.00
Mn	0.05	0.04	0.04	0.04	0.03
Zr	0.11	0.09	0.09	0.09	0.07
Mg	0.01	0.01	0.01	0.01	0.01
Ca	0.01	0.01	0.02	0.03	0.03
Ti	0.00	0.00	0.00	0.00	0.00
Sr	0.00	0.00	0.00	0.00	0.00
La	0.00	0.00	0.00	0.00	0.00
Ce	0.00	0.00	0.00	0.00	0.00
Pr	0.00	0.00	0.00	0.00	0.00
Nd	0.00	0.00	0.00	0.00	0.00
Sm	0.00	0.00	0.00	0.00	0.00
Eu	0.00	0.00	0.00	0.00	0.00
Gd	0.00	0.00	0.00	0.00	0.00

Tb	0.00	0.00	0.00	0.00	0.00
Dy	0.01	0.01	0.00	0.01	0.01
Ho	0.00	0.00	0.00	0.00	0.00
Er	0.01	0.01	0.00	0.01	0.01
Tm	0.00	0.00	0.00	0.00	0.00
Yb	0.05	0.05	0.05	0.05	0.05
Lu	0.01	0.01	0.01	0.01	0.01
Hf	0.01	0.01	0.00	0.01	0.01
Ta	0.00	0.00	0.00	0.00	0.00
Pb	0.00	0.00	0.00	0.00	0.00
Th	0.00	0.00	0.00	0.00	0.00
U	0.00	0.00	0.00	0.00	0.00
Total	3.92	3.9	3.91	3.93	3.94
End-members %					
Thortveitite	81.59	82.03	83.16	82.75	84.91
Kieviite-(Y)	15.1	14.5	13.84	13.96	12.1
Kieviite-(Yb)	3.29	3.45	2.98	3.27	2.97

Trace elements ppm

	22292_2Tuftane							22292_1Tuftane				22286Tuftane	
	Pale 1	Pale 2			Medium1	Medium2	Dark						
	29/1.	24 / 1 .	30/1.	25 / 1 .	26/1.	27/1.	28/1.	22/1.	23/1.	21/1.	20/1.	17/1.	20/1.
Mg25	194	420	195	440	431	438	508	462	453	410	403	749	789
Ca43	831	9432	2456	3299	1941	4059	2604	1544	1843	1887	1501	2288	2226
Ti49	232	510	264	754	642	671	384	427	451	471	529	1024	1118
Sr88	34	28	29	24	25	26	28	29	29	30	26	26	26
La139	46	18	6	13	11	15	19	19	19	18	13	26	27
Ce140	379	340	107	244	222	266	337	326	324	312	262	370	395
Pr141	111	143	48	121	108	118	145	142	142	137	122	160	167
Nd143	788	1165	421	995	946	920	1155	1160	1149	1131	1037	1402	1436
Sm147	743	1166	558	1134	1070	991	1176	1245	1214	1227	1169	1657	1674
Eu151	6	5	5	4	4	4	5	4	4	4	5	4	4
Gd157	1234	1803	1096	1791	1768	1602	1870	2058	1988	2047	1919	2878	2872
Tb159	472	626	443	616	608	571	650	713	685	716	662	919	908
Dy163	5416	6512	5157	6326	6248	5958	6651	7318	7101	7379	6797	8869	8780
Ho165	1749	1937	1660	1843	1825	1799	1985	2155	2100	2162	1988	2500	2439
Er166	11770	11102	10868	10672	10931	10701	11928	12943	12663	13117	11834	14172	13860
Tm169	4989	4322	4631	4036	4111	4201	4550	4920	4774	4902	4425	4920	4799
Yb173	84772	66864	78013	65085	65068	66488	73047	75912	74801	76714	70089	71388	70047
Lu175	19370	15444	17598	13990	14245	14712	16173	16780	16514	16973	15400	15416	14966
Hf179	3248	5111	3335	4546	4303	5602	5983	5480	5416	4721	4420	6001	5691
Ta181	3	10	2	12	11	13	10	7	7	7	10	25	32
Pb208	115	16	9	19	14	15	14	14	13	16	17	13	12
Th232	271	107	52	126	114	87	109	105	106	114	118	96	107
U238	56	67	47	70	70	67	68	66	66	71	71	47	55

	22239Ljosland													
	Pale 1			Pale 2			Medium 1					Medium2	Dark	
	10/1.	16/1.	6/1.	11/1.	9/1.	17/1.	13/1.	14/1.	8/1.	18/1.	12/.1	19/1.	15/1.	7/1.
Mg25	318	265	222	139	270	264	302	98	128	143	116	108	92	140
Ca43	1377	952	1107	1164	1242	874	933	1260	984	2005	1284	2386	814	2538
Ti49	332	325	280	269	306	318	307	201	256	176	198	197	226	168
Sr88	10	10	9	9	9	10	9	8	8	7	7	7	8	8
La139	2	2	1	1	1	2	2	<1	1	1	<1	<1	3	2
Ce140	33	27	17	23	25	26	21	11	15	10	11	11	10	9
Pr141	13	11	7	10	10	11	8	5	8	5	6	5	5	5
Nd143	116	101	70	100	93	100	75	55	79	46	64	56	48	52
Sm147	124	118	90	150	107	116	96	95	133	69	109	93	78	85
Eu151	1	1	<1	<1	<1	1	<1	<1	<1	<1	<1	<1	<1	<1
Gd157	234	239	204	304	219	236	222	227	299	174	248	218	192	206
Tb159	87	90	80	104	83	89	88	85	105	73	88	81	79	79
Dy163	1048	1104	995	1143	1022	1093	1098	990	1144	917	979	925	960	908
Ho165	390	404	373	390	382	399	407	341	383	324	331	319	338	311
Er166	2824	2961	2658	2678	2741	2924	2876	2354	2552	2240	2207	2188	2373	2113
Tm169	1313	1368	1208	1180	1260	1361	1241	1047	1103	1035	984	1013	1082	982
Yb173	26497	27411	24097	23786	25297	27105	24325	20986	21799	20525	19656	20432	21778	20204
Lu175	7366	7716	6806	6888	7086	7676	6617	5956	6237	5552	5725	5960	6188	5814
Hf179	1847	1862	1628	1876	1737	1849	1651	1568	1701	1344	1522	1569	1590	1286
Ta181	17	14	7	14	12	14	9	5	5	7	4	7	14	4
Pb208	28	32	17	8	23	32	22	8	20	24	6	7	34	45
Th232	46	48	26	28	36	48	27	18	23	20	19	19	20	11
U238	133	133	102	43	117	131	121	45	32	65	27	33	54	29

	Pale1	Pale 2		Medium 1		Medium 2					Dark	
	23/1.	9/1.	16/1.	8/1.	11/1.	15/1.	22/1.	12/1.	14/1.	21/1.	7/1.	10/1.
Mg25	953	546	620	506	448	603	572	518	510	408	611	664
Ca43	854	1558	1119	1496	1525	1379	755	2026	1491	1719	1420	653
Ti49	631	456	478	443	500	480	471	506	441	420	455	520
Sr88	5	5	4	5	5	4	5	5	5	5	4	6
La139	2	1	1	1	<1	1	1	1	1	<1	1	1
Ce140	38	26	26	23	12	25	25	20	24	9	22	32
Pr141	18	13	13	11	8	12	13	11	12	6	11	16
Nd143	187	149	134	131	96	138	146	125	134	77	126	175
Sm147	537	452	406	403	355	433	460	406	419	304	410	522
Eu151	1	<1	1	<1	<1	1	<1	<1	<1	<1	<1	<1
Gd157	921	796	706	726	691	759	822	744	744	619	712	910
Tb159	301	269	239	246	243	256	276	255	250	222	242	300
Dy163	2193	2027	1792	1874	1870	1886	2042	1908	1900	1710	1791	2254
Ho165	417	395	346	369	368	357	392	369	364	333	338	436
Er166	1907	1901	1634	1795	1790	1704	1879	1774	1762	1621	1601	2083
Tm169	764	783	671	750	749	692	774	743	751	706	665	843
Yb173	13561	14747	12009	14050	14030	13020	14187	13810	13921	13243	12401	15109
Lu175	2935	3052	2502	2967	2938	2698	3132	2903	2903	2827	2578	3318
Hf179	11577	5449	7466	4304	3298	6614	6010	4746	4801	2790	6570	7302
Ta181	77	31	42	28	28	37	31	28	25	23	35	41
Pb208	78	62	66	89	50	71	61	56	59	45	73	62
Th232	59	52	44	46	35	55	54	45	48	29	52	59
U238	553	403	446	405	335	482	434	373	397	300	499	436

Title row: 22238Tjomstøl

	22330Torvelona								
	Pale 1	Pale 2	Pale 3	Medium 1	Medium 2		Dark		Solid
	30/1.	3/1.	25/1.	29/1.	26/1.	1/1.	24/1.	6/1.	4/1.
Mg25	554	333	296	154	314	412	223	413	482
Ca43	17689	1208	810	1396	1363	1208	683	1039	1268
Ti49	529	381	360	251	2591	432	331	520	426
Sr88	25	11	13	15	24	12	12	11	12
La139	71	5	2	<1	29	4	1	3	3
Ce140	566	57	36	5	138	59	14	61	45
Pr141	206	24	19	2	25	30	7	29	21
Nd143	1772	229	195	27	164	295	78	287	205
Sm147	3430	539	505	137	282	704	236	661	473
Eu151	12	1	1	<1	2	1	<1	1	1
Gd157	5040	825	872	394	509	1102	458	981	730
Tb159	1275	250	286	189	202	333	166	298	237
Dy163	8732	2053	2472	2039	2028	2649	1545	2381	1998
Ho165	1692	476	609	570	555	602	409	536	477
Er166	7167	2737	3501	3664	3496	3348	2572	3037	2854
Tm169	2403	1367	1672	1836	1714	1550	1304	1420	1397
Yb173	37895	29847	34330	38019	35952	32017	28958	30146	30963
Lu175	8932	7597	9194	10149	9693	8057	8194	7534	7943
Hf179	5229	4150	4230	3810	4942	4793	2948	5506	4378
Ta181	91	75	45	18	381	88	32	118	87
Pb208	190	25	26	12	460	20	41	11	16
Th232	364	43	35	6	53	56	13	55	38
U238	99	43	32	8	36	57	15	49	44

	22304Eretveit					22302Knapen						
	Pale	Medium			Dark	Pale		Medium			Dark	
	3/1.	2/1.	4/1.	5/1.	1/1.	38/1.	34/1.	33/1.	37/1.	32/1.	31/1.	36/1.
Mg25	1080	1058	960	1255	1057	412	426	335	334	324	298	323

Ca43	1864	2560	3419	4479	4222	2203	2648	2263	1732	-	2543	2246
Ti49	1137	1181	1169	1000	1105	892	740	655	771	945	769	675
Sr88	13	13	12	12	12	12	12	12	11	11	11	11
La139	16	13	9	10	13	5	5	3	2	3	3	2
Ce140	212	185	127	140	182	87	97	75	47	70	62	40
Pr141	101	88	62	65	87	49	53	40	27	39	34	22
Nd143	1084	964	661	694	920	560	594	473	337	462	403	270
Sm147	2016	1906	1324	1390	1724	1325	1328	1116	851	1070	966	701
Eu151	3	2	2	4	3	1	<1	<1	<1	<1	<1	<1
Gd157	3366	3235	2333	2432	2949	2060	1998	1791	1483	1692	1607	1276
Tb159	926	928	693	728	832	564	550	503	437	481	457	393
Dy163	7087	7052	5462	5914	6488	3954	3847	3701	3339	3496	3296	3017
Ho165	1501	1481	1182	1277	1359	754	732	738	675	681	655	625
Er166	6595	6776	5523	5998	6199	3662	3645	3705	3502	3470	3369	3298
Tm169	2268	2322	1983	2118	2098	1583	1587	1618	1528	1474	1447	1483
Yb173	31796	34421	30174	32989	31276	29469	30287	31219	30046	28867	28721	29447
Lu175	6461	6916	6163	6978	6201	6614	6649	7095	6759	6523	6503	6685
Hf179	6845	6578	4757	6820	6220	7002	7816	5497	4646	4539	4264	3973
Ta181	225	202	144	150	210	168	122	68	65	76	65	50
Pb208	70	63	53	51	68	24	14	15	13	19	16	12
Th232	274	270	181	166	276	37	37	38	27	45	41	22
U238	352	309	269	272	323	113	88	95	86	117	101	78

	22370Eptevann					22273Håvarstad			
	Pale			Medium	Dark	Pale	Medium	Dark	
	34/1	32/1.	35/1.	33/1.	31/1.	37/1.	38/1.	40/1.	39/1.
Mg25	765	850	808	571	89	1945	369	344	337

Ca43	1062	1115	556	1058	1517	972	667	1065	741
Ti49	482	433	562	378	89	381	147	175	87
Sr88	3	2	3	2	3	6	5	5	5
La139	<1	<1	<1	<1	<1	6	<1	<1	-
Ce140	3	2	2	1	1	14	4	3	1
Pr141	1	1	1	1	<1	5	2	2	1
Nd143	20	17	20	12	4	52	35	28	17
Sm147	101	88	99	65	23	189	133	113	75
Eu151	1	1	1	1	3	1	4	1	2
Gd157	263	231	253	175	84	404	331	263	189
Tb159	121	107	114	84	41	157	130	109	86
Dy163	1007	890	933	717	454	1310	1215	1006	851
Ho165	189	165	172	135	121	278	296	237	207
Er166	928	795	847	668	765	1515	1639	1371	1246
Tm169	418	351	358	302	383	664	709	631	597
Yb173	8144	7050	7157	5988	8387	12784	13576	12701	12322
Lu175	1759	1509	1511	1298	2111	2922	3227	2981	2908
Hf179	4194	4236	4096	3109	1083	4831	3025	4784	3926
Ta181	56	49	55	30	3	88	13	15	4
Pb208	77	71	84	49	5	307	24	13	4
Th232	68	64	55	37	1	22	4	8	1
U238	546	516	495	349	22	300	69	75	30

Appendix 3: Garnets

Table 9: Wt.% oxide, apfu and percent end-member component for each of the analyzis-spots in the collected garnets. Vanadium and chromium are located in the trace-element section

	KB-1 Heliodorgruva					
Sample	KB-1-1	KB-1-2	KB-1-3	KB-1-4	KB-1-5	KB-1
SiO_2 wt%	36.50	36.54	36.84	36.14	36.10	35.9
Al_2O_3	19.93	20.00	20.11	19.97	20.05	19.9
FeO	17.17	16.25	17.56	14.86	15.11	14.7
Fe_2O_3	0.92	1.70	0.72	1.39	1.36	1.8
MnO	24.89	25.73	24.88	25.95	25.74	25.9
TiO_2	0.04	0.06	0.06	0.22	0.25	0.2
MgO	0.52	0.48	0.58	0.77	0.77	0.7
CaO	0.31	0.31	0.26	0.42	0.41	0.4
Na_2O	-	0.04	-	0.08	0.07	0.0
K_2O	-	-	-	-	-	-
Sc_2O_3	0.32	0.34	0.35	0.02	0.02	0.0
ZnO	0.01	0.01	0.01	0.03	0.03	0.0
Y_2O_3	0.78	0.79	0.81	0.01	0.05	0.0
REE_2O_3	0.33	0.32	0.34	0.01	0.02	0.0
TOTAL	101.70	102.57	102.52	99.88	99.98	99.9
Si apfu	2.98	2.96	2.98	2.98	2.97	2.9
Al	0.02	0.04	0.02	0.02	0.03	0.0
Σ T	3.00	3.00	3.00	3.00	3.00	3.0
V	0.00	0.00	0.00	0.00	0.00	0.0
Ti	0.00	0.00	0.00	0.01	0.02	0.0
Cr	0.00	0.00	0.00	0.00	0.00	0.0
Al	1.90	1.87	1.90	1.92	1.92	1.9
Fe3+	0.06	0.10	0.04	0.07	0.06	0.0
Fe2+	0.04	0.03	0.05	0.00	0.00	0.0
Σ B	2.00	2.00	2.00	2.00	2.00	2.0
Y	0.03	0.03	0.03	0.00	0.00	0.0
REE	0.01	0.01	0.01	0.00	0.00	0.0
Fe2+	1.13	1.07	1.14	1.02	1.04	1.0
Fe3+	0.00	0.00	0.00	0.02	0.02	0.0
Sc	0.02	0.02	0.02	0.00	0.00	0.0
Mn	1.72	1.77	1.71	1.81	1.80	1.8
Mg	0.06	0.06	0.07	0.09	0.09	0.0

Ca	0.03	0.03	0.02	0.04	0.04	0.04
Na	0.00	0.01	0.00	0.01	0.01	0.01
K	0.00	0.00	0.00	0.00	0.00	0.00
Σ A	3.00	3.00	3.01	3.00	3.00	3.00
Mn/Fe2+Mn	0.59	0.62	0.59	0.64	0.63	0.64
Yttrogarnet %	0.62	1.13	0.53	0.02	0.07	0.06
Sc garnet	0.68	0.71	0.36	0.06	0.07	0.07
Spessartine	57.39	58.9	56.9	60.37	59.86	60.49
Pyrope	2.09	1.94	2.34	3.14	3.16	3.15
Almandine	34.92	31.71	35.41	32.4	32.85	31.33
Grossular	0	0	0	0	0	0
Andradite	0	0	0	0.49	0.35	0.51
Skiagite	2.83	5.03	2.2	1.74	1.84	2.48

Table 9 continued.

	25432 Heia, Ljosland					
Sample	25432-1	25432-2	25432-3	25432-4	25432-5	25432
SiO_2 wt%	36.41	36.18	36.25	36.44	35.92	36.3
Al_2O_3	20.17	19.98	20.06	20.32	20.11	20.1
FeO	16.16	15.67	15.98	18.53	17.76	18.2
Fe_2O_3	1.65	2.33	1.34	1.37	2.71	1.50
MnO	25.15	25.42	25.36	22.79	22.91	22.9
TiO_2	0.17	0.22	0.17	0.04	0.06	0.08
MgO	0.74	0.72	0.69	0.77	0.80	0.81
CaO	0.54	0.51	0.43	0.36	0.36	0.34
Na_2O	0.01	0.02	0.01	0.04	0.03	0.03
K_2O	-	-	-	-	-	-
Sc_2O_3	0.07	0.09	0.06	0.03	0.03	0.04
ZnO	0.02	0.01	0.02	0.01	0.02	0.02
Y_2O_3	0.27	0.36	0.29	0.33	0.33	0.39
REE_2O_3	0.09	0.13	0.10	0.21	0.20	0.21
TOTAL	101.46	101.65	100.76	101.27	101.23	101.0
Si apfu	2.96	2.95	2.97	2.97	2.94	2.97
Al	0.04	0.05	0.03	0.03	0.06	0.03
Σ T	3.00	3.00	3.00	3.00	3.00	3.00
V	0.00	0.00	0.00	0.00	0.00	0.00
Ti	0.01	0.01	0.01	0.00	0.00	0.00
Cr	0.00	0.00	0.00	0.00	0.00	0.00

Al	1.90	1.86	1.91	1.92	1.87	1.9
Fe^{3+}	0.09	0.12	0.08	0.07	0.12	0.0
Fe^{2+}	0.00	0.00	0.00	0.00	0.00	0.0
Σ B	2.00	2.00	2.00	2.00	2.00	2.0
Y	0.01	0.02	0.01	0.01	0.01	0.0
REE	0.00	0.00	0.00	0.01	0.00	0.0
Fe^{2+}	1.10	1.07	1.10	1.26	1.21	1.2
Fe^{3+}	0.01	0.02	0.00	0.01	0.04	0.0
Sc	0.01	0.01	0.00	0.00	0.00	0.0
Mn	1.73	1.75	1.76	1.57	1.59	1.5
Mg	0.09	0.09	0.08	0.09	0.10	0.1
Ca	0.05	0.04	0.04	0.03	0.03	0.0
Na	0.00	0.00	0.00	0.01	0.01	0.0
K	0.00	0.00	0.00	0.00	0.00	0.0
Σ A	3.00	3.00	3.00	3.00	3.00	3.0
Mn/Fe2+Mn	0.61	0.62	0.62	0.55	0.57	0.5
Yttrogarnet %	0.39	0.52	0.42	0.48	0.47	0.5
Sc garnet	0.26	0.31	0.23	0.12	0.12	0.1
Spessartine	57.79	58.45	58.69	52.49	52.9	52.9
Pyrope	3.01	2.91	2.8	3.11	3.26	3.
Almandine	33.73	31.34	33.55	40.24	37.18	38.
Grossular	0	0	0	0	0	0
Andradite	0.76	0.5	0.51	0.77	0.76	0.6
Skiagite	2.94	4.24	2.98	1.91	3.3	2.7

Table 9 continued

	KTU-7 Tuftane, Frikstad				MS-9 Solås			
Sample	KTU-7-1	KTU-7-2	KTU-7-3	KTU-7-4	MS-9-1	MS-9-2	MS-9-3	MS-9-4
SiO_2 wt%	35.99	36.45	36	36.13	35.32	35.15	35.22	34.93
Al_2O_3	20.05	20.51	20.14	20.23	20.33	20.49	20.23	20.45
FeO	17.98	19.14	16.33	16.73	0.95	0.69	0.62	0.31
Fe_2O_3	1.73	0.91	1.8	1.34	3.29	3.66	3.72	4.01
MnO	22.53	21.69	23.87	23.85	39.78	40.07	40.09	40.19
TiO_2	0.11	0.02	0.09	0.1	0.04	0.04	0.05	0.06
MgO	0.9	0.93	0.91	0.87	-	-	-	-
CaO	0.52	0.55	0.51	0.52	0.68	0.59	0.64	0.6
Na_2O	0.02	0.04	0.08	0.05	0.03	-	0.02	-
K_2O	-	-	-	-	-	-	-	-
Sc_2O_3	0.08	0.09	0.12	0.09	0	-	-	-

REE$_2$O$_3$	0.7	0.72	0.29	0.5	0.05	0.05	0.05	0.05
ZnO	0.01	0.01	0.01	0.01	0.06	0.06	0.06	0.06
Y$_2$O$_3$	0.72	0.74	0.32	0.49	0.06	0.06	0.07	0.07
TOTAL	101.35	101.8	100.47	100.9	100.56	100.85	100.76	100.73
Si apfu	2.95	2.96	2.96	2.96	2.91	2.89	2.90	2.88
Al	0.05	0.04	0.04	0.04	0.09	0.11	0.10	0.12
Σ T	3.00	3.00	3.00	3.00	3.00	3.00	3.00	3.00
V	0.00	0.00	0.00	0.00	0.00	0.00	0.00	0.00
Ti	0.01	0.00	0.01	0.01	0.00	0.00	0.00	0.00
Cr	0.00	0.00	0.00	0.00	0.00	0.00	0.00	0.00
Al	1.88	1.93	1.90	1.91	1.89	1.88	1.86	1.87
Fe3+	0.11	0.05	0.09	0.08	0.11	0.12	0.13	0.13
Fe2+	0.00	0.02	0.00	0.00	0.00	0.00	0.00	0.00
Σ B	2.00	2.00	2.00	2.00	2.00	2.00	2.00	2.00
Y	0.03	0.03	0.01	0.02	0.00	0.00	0.00	0.00
REE	0.02	0.02	0.01	0.01	0.00	0.00	0.00	0.00
Fe2+	1.23	1.28	1.12	1.15	0.07	0.05	0.04	0.02
Fe3+	0.00	0.01	0.02	0.00	0.09	0.10	0.10	0.12
Sc	0.01	0.01	0.01	0.01	0.00	0.00	0.00	0.00
Mn	1.56	1.49	1.66	1.65	2.78	2.79	2.80	2.81
Mg	0.11	0.11	0.11	0.11	0.00	0.00	0.00	0.00
Ca	0.05	0.05	0.04	0.05	0.06	0.05	0.06	0.05
Na	0.00	0.01	0.01	0.01	0.00	0.00	0.00	0.00
K	0.00	0.00	0.00	0.00	0.00	0.00	0.00	0.00
Σ A	3.00	3.00	3.00	3.00	3.00	3.00	3.00	3.00
Mn/Fe2+Mn	0.56	0.53	0.60	0.59	0.98	0.98	0.98	0.99
Yttrogarnet %	1.05	1.04	0.46	0.72	0.09	0.09	0.1	0.1
Sc garnet	0.3	0.31	0.45	0.31	0	0	0	0
Spessartine	52.17	49.88	55.36	55.24	92.55	93.05	93.18	93.18
Pyrope	3.68	3.76	3.73	3.54	0	0	0	0
Almandine	37.64	42.22	35.84	36.47	1.66	0.74	0	0
Grossular	0	0	0	0	0	0	0	0
Andradite	0.86	1.25	0.76	0.9	1.86	1.6	1.75	1.58
Skiagite	3.49	1.22	1.55	1.79	0.53	0.85	1.42	0.71

Table 9 cont.

	25427 Steli, Tveit					
Sample	25427-1	25427-2	25427-3	25427-4	25427-5	25427-6
SiO$_2$ wt%	36.41	36.03	35.92	36.29	36.12	35.9

Al$_2$O$_3$	20.31	20.16	20.36	20.1	20.18	20.26
FeO	25.45	25.14	24.83	26.27	26.04	25.8
Fe$_2$O$_3$	0.7	1.15	1.47	1.07	1.15	1.48
MnO	16.34	16.3	16.48	15.27	15.36	15.34
TiO$_2$	0.05	0.03	0.02	0.07	0.06	0.04
MgO	0.49	0.49	0.49	0.56	0.56	0.51
CaO	0.51	0.48	0.47	0.47	0.43	0.44
Na$_2$O	0.02	-	-	0.01	0.02	0.03
K$_2$O	-	-	-	0.03	-	0.01
Sc$_2$O$_3$	0.05	0.05	0.05	0.03	0.03	0.03
ZnO	0.01	0.01	0.01	0.01	0.01	0.01
Y$_2$O$_3$	0.15	0.15	0.16	0.06	0.1	0.12
REE$_2$O$_3$	0.05	0.05	0.05	0.03	0.04	0.05
TOTAL	100.52	100.05	100.31	100.27	100.1	100.03
Si apfu	2.99	2.98	2.96	2.99	2.98	2.96
Al	0.01	0.02	0.04	0.01	0.02	0.04
Σ T	3.00	3.00	3.00	3.00	3.00	3.00
V	0.00	0.00	0.00	0.00	0.00	0.00
Ti	0.00	0.00	0.00	0.00	0.00	0.00
Cr	0.00	0.00	0.00	0.00	0.00	0.00
Al	1.95	1.94	1.94	1.94	1.94	1.94
Fe3+	0.04	0.06	0.06	0.06	0.06	0.06
Fe2+	0.00	0.00	0.00	0.00	0.00	0.00
Σ B	2.00	2.00	2.00	2.00	2.00	2.00
Y	0.01	0.01	0.01	0.00	0.00	0.01
REE	0.00	0.00	0.00	0.00	0.00	0.00
Fe2+	1.75	1.74	1.71	1.81	1.79	1.78
Fe3+	0.00	0.01	0.03	0.01	0.01	0.03
Sc	0.00	0.00	0.00	0.00	0.00	0.00
Mn	1.14	1.14	1.15	1.06	1.07	1.07
Mg	0.06	0.06	0.06	0.07	0.07	0.06
Ca	0.04	0.04	0.04	0.04	0.04	0.04
Na	0.00	0.00	0.00	0.00	0.00	0.01
K	0.00	0.00	0.00	0.00	0.00	0.00
Σ A	3.00	3.00	3.00	3.00	3.00	3.00
Mn/(Fe2+Mn)	0.39	0.40	0.40	0.37	0.37	0.38
Yttrogarnet %	0.21	0.23	0.24	0.08	0.14	0.17
Sc garnet	0.18	0.18	0.19	0.11	0.1	0.1
Spessartine	37.88	37.99	38.32	35.5	35.76	35.77
Pyrope	2.01	2.03	2	2.28	2.31	2.09

Almandine	57.55	56.59	56.17	59.1	58.76	58.78
Grossular	0	0	0	0	0	0
Andradite	1.16	1.15	1.14	1.05	0.97	1.07
Skiagite	0.68	1.2	0.77	1.21	1.09	0.6

Table 9 cont.

	25370 Kåbuland						
Sample	25370-1	25370-2	25370-3	25370-4	25370-5	25370-6	25370-7
SiO_2 wt%	35.88	36.07	35.6	36.09	35.97	36.05	36.35
Al_2O_3	20.36	20.04	20.22	20.51	20.53	20.25	19.69
FeO	18.51	18.36	17.86	20.72	20.65	20.95	19.4
Fe_2O_3	1.3	1.4	2.05	1.4	1.05	1.2	1.19
MnO	21.58	21.95	21.84	19.35	19.26	19	21.53
TiO_2	0.1	0.07	0.11	0.02	0.06	0.05	0.21
MgO	0.92	0.92	0.92	1.19	1.14	1.19	0.95
CaO	0.46	0.49	0.45	0.51	0.52	0.49	0.55
Na_2O	0.09	0.07	0.11	0.02	0.05	0.05	0.01
K_2O	-	-	-	-	-	-	0.01
Sc_2O_3	0.06	0.07	0.06	0.15	0.14	0.16	0.07
ZnO	0.01	0.01	0.01	0.01	0.01	0.01	0.01
Y_2O_3	0.88	1.05	0.99	0.53	0.32	0.65	1.04
REE_2O_3	0.44	0.48	0.47	0.33	0.19	0.39	0.48
TOTAL	100.59	100.99	100.69	100.83	99.88	100.44	101.5
Si apfu	2.95	2.96	2.93	2.95	2.96	2.96	2.97
Al	0.05	0.04	0.07	0.05	0.04	0.04	0.03
Σ T	3.00	3.00	3.00	3.00	3.00	3.00	3.00
V	0.00	0.00	0.00	0.00	0.00	0.00	0.00
Ti	0.01	0.00	0.01	0.00	0.00	0.00	0.01
Cr	0.00	0.00	0.00	0.00	0.00	0.00	0.00
Al	1.92	1.90	1.89	1.92	1.95	1.92	1.87
Fe3+	0.07	0.09	0.10	0.07	0.05	0.08	0.07
Fe2+	0.00	0.01	0.00	0.00	0.00	0.00	0.05
Σ B	2.00	2.00	2.00	2.00	2.00	2.00	2.00
Y	0.04	0.05	0.04	0.02	0.01	0.03	0.05
REE	0.01	0.01	0.01	0.01	0.00	0.01	0.01
Fe2+	1.27	1.25	1.23	1.42	1.42	1.44	1.28
Fe3+	0.01	0.00	0.02	0.01	0.02	0.00	0.00
Sc	0.00	0.00	0.00	0.01	0.01	0.01	0.00
Mn	1.50	1.53	1.52	1.34	1.34	1.32	1.49
Mg	0.11	0.11	0.11	0.15	0.14	0.15	0.12

Ca	0.04	0.04	0.04	0.04	0.05	0.04	0.05
Na	0.01	0.01	0.02	0.00	0.01	0.01	0.00
K	0.00	0.00	0.00	0.00	0.00	0.00	0.00
Σ A	3.00	3.00	3.00	3.00	3.00	3.00	3.00
Mn/Fe2+Mn	0.54	0.55	0.55	0.49	0.49	0.48	0.53
Yttrogarnet %	1.29	1.26	1.45	0.77	0.46	0.94	0.8
Sc garnet	0.23	0.24	0.22	0.54	0.48	0.59	0.24
Spessartine	50.12	50.9	50.78	44.67	44.75	44.07	49.76
Pyrope	3.74	3.75	3.76	4.85	4.66	4.86	3.88
Almandine	41.13	39.18	38.74	46.11	47.37	46.32	39.36
Grossular	0	0	0	0	0	0	0
Andradite	0.8	0.96	0.76	0.86	0.59	0.68	0.06
Skiagite	1.32	2.79	2.27	1.11	0	1.67	3.6

	25409 Landås					
Sample	25409-1	25409-2	25409-3	25409-4	25409-5	25409-6
SiO_2 wt%	35.85	35.89	35.67	34.95	35.34	35.14
Al_2O_3	20.38	20.27	20.39	20.35	20.34	20.32
FeO	15.97	16.46	16.59	14.38	15.41	14.72
Fe_2O_3	1.68	1.11	1.56	2.02	0.85	1.7
MnO	25	24.55	23.67	25.11	24.51	24.88
TiO_2	0.05	0.03	0.02	0.07	0.07	0.09
MgO	0.3	0.31	0.35	0.35	0.38	0.41
CaO	0.64	0.64	0.6	0.58	0.56	0.54
Na_2O	0.06	0.06	0.15	0.15	0.15	0.16
K_2O	-	-	-	-	-	-
Sc_2O_3	0.01	0.02	0.02	0.02	0.02	0.02
ZnO	0.02	0.02	0.02	0.02	0.02	0.02
Y_2O_3	0.62	0.78	0.91	1.94	2.01	2.12
REE_2O_3	0.3	0.51	0.43	1.15	1.19	1.2
TOTAL	100.9	100.65	100.37	101.08	100.84	101.32
Si apfu	2.95	2.96	2.95	2.89	2.93	2.90
Al	0.05	0.04	0.05	0.11	0.07	0.10
Σ T	3.00	3.00	3.00	3.00	3.00	3.00
V	0.00	0.00	0.00	0.00	0.00	0.00
Ti	0.00	0.00	0.00	0.00	0.00	0.01
Cr	0.00	0.00	0.00	0.00	0.00	0.00
Al	1.92	1.93	1.93	1.88	1.91	1.88
Fe3+	0.08	0.07	0.07	0.12	0.05	0.10

Fe2+	0.00	0.00	0.00	0.00	0.03	0.01
Σ B	2.00	2.00	2.00	2.00	2.00	2.00
Y	0.03	0.03	0.04	0.09	0.09	0.09
REE	0.01	0.01	0.01	0.03	0.03	0.03
Fe2+	1.10	1.14	1.15	1.00	1.04	1.00
Fe3+	0.03	0.00	0.03	0.01	0.00	0.01
Sc	0.00	0.00	0.00	0.00	0.00	0.00
Mn	1.74	1.71	1.66	1.76	1.72	1.74
Mg	0.04	0.04	0.04	0.04	0.05	0.05
Ca	0.06	0.06	0.05	0.05	0.05	0.05
Na	0.01	0.01	0.02	0.02	0.02	0.03
K	0.00	0.00	0.00	0.00	0.00	0.00
Σ A	3.00	3.00	3.00	3.00	3.00	3.00
Mn/(Fe2+Mn)	0.61	0.60	0.59	0.64	0.62	0.63
Yttrogarnet %	0.91	1.14	1.33	2.86	2.03	2.86
Sc garnet	0.05	0.06	0.06	0.06	0.06	0.07
Spessartine	58.03	57.23	55.25	58.9	57.56	58.24
Pyrope	1.22	1.28	1.45	1.44	1.57	1.7
Almandine	35.98	37.18	38.24	31.67	35.44	32.22
Grossular	0	0	0	0	0	0
Andradite	1.68	1.71	1.16	1.43	1.11	1.45
Skiagite	0.62	0.71	0	1.64	0	1.8

	MS2-9 Solås				25422 Frikstad			
Sample	MS2-9-1	MS2-9-2	MS2-9-3	MS2-9-4	25422-1	25422-2	25422-3	25422-4
SiO_2 wt%	35.48	35.18	34.87	35.36	36.15	35.61	35.45	35.5
Al_2O_3	20.11	20.1	19.77	19.98	20.27	20.28	20.25	19.94
FeO	12.95	11.95	11.74	12.88	18.62	18.29	17.74	17.91
Fe_2O_3	1.67	2.6	2.63	1.38	1.81	2.16	2.2	2.16
MnO	28.08	28.44	28.34	27.86	22.05	21.74	21.8	21.85
TiO_2	0.11	0.1	0.11	0.12	0.05	0.04	0.06	0.06
MgO	0.28	0.29	0.31	0.3	0.8	0.78	0.86	0.83
CaO	0.25	0.24	0.29	0.29	0.53	0.55	0.65	0.57
Na_2O	0.06	0.12	0.09	0.08	0.05	0.05	0.06	0.06
K_2O	-	-	-	-	0	-	-	-
Sc_2O_3	0.01	0.01	0.02	0.02	0.07	0.06	0.14	0.15
ZnO	0.04	0.03	0.04	0.03	0.02	0.02	0.01	0.01
Y_2O_3	1.64	1.63	1.91	1.86	0.52	0.55	0.52	0.69
REE_2O_3	0.38	0.39	0.47	0.45	0.44	0.45	0.57	0.79
TOTAL	101.08	101.09	100.59	100.61	101.38	100.58	100.32	100.52

Si apfu	2.93	2.90	2.90	2.93	2.95	2.93	2.92	2.93
Al	0.07	0.10	0.10	0.07	0.05	0.07	0.08	0.07
Σ T	3.00	3.00	3.00	3.00	3.00	3.00	3.00	3.00
V	0.00	0.00	0.00	0.00	0.00	0.00	0.00	0.00
Ti	0.01	0.01	0.01	0.01	0.00	0.00	0.00	0.00
Cr	0.00	0.00	0.00	0.00	0.00	0.00	0.00	0.00
Al	1.88	1.86	1.84	1.89	1.90	1.90	1.89	1.87
Fe3+	0.10	0.13	0.16	0.09	0.10	0.10	0.10	0.12
Fe2+	0.01	0.00	0.00	0.02	0.00	0.00	0.00	0.00
Σ B	2.00	2.00	2.00	2.00	2.00	2.00	2.00	2.00
Y	0.07	0.07	0.08	0.08	0.02	0.02	0.02	0.03
REE	0.01	0.01	0.01	0.01	0.01	0.01	0.01	0.02
Fe2+	0.89	0.83	0.82	0.88	1.27	1.26	1.22	1.24
Fe3+	0.00	0.03	0.01	0.00	0.02	0.04	0.03	0.01
Sc	0.00	0.00	0.00	0.00	0.00	0.00	0.01	0.01
Mn	1.96	1.99	2.00	1.96	1.52	1.52	1.52	1.53
Mg	0.03	0.04	0.04	0.04	0.10	0.10	0.11	0.10
Ca	0.02	0.02	0.03	0.03	0.05	0.05	0.06	0.05
Na	0.01	0.02	0.01	0.01	0.01	0.01	0.01	0.01
K	0.00	0.00	0.00	0.00	0.00	0.00	0.00	0.00
Σ A	3.00	3.00	3.00	3.00	3.00	3.00	3.00	3.00
Mn/(Fe2+Mn)	0.69	0.71	0.71	0.69	0.55	0.55	0.55	0.55
Yttrogarnet %	2.31	2.4	2.82	2.12	0.76	0.8	0.76	1.02
Sc garnet	0.05	0.05	0.08	0.08	0.25	0.22	0.52	0.54
Spessartine	65.5	66.35	66.65	65.34	50.89	50.59	50.86	51.09
Pyrope	1.16	1.2	1.28	1.25	3.25	3.19	3.55	3.43
Almandine	25.49	23.35	21.55	25.91	40.46	40.66	39.88	38.72
Grossular	0	0	0	0	0	0	0	0
Andradite	0.58	0.36	0.45	0.03	1.13	1.29	1.18	0.94
Skiagite	4.35	4.17	5.73	3.49	1.97	1.36	0.98	2.62

	MSB-5 Slobrekka					
Sample	MSB-5-1	MSB-5-2	MSB-5-3	MSB-5-4	MSB-5-5	MSB-5-6
SiO_2 wt%	35.03	34.84	34.91	34.91	34.84	34.82
Al_2O_3	20.47	20.54	20.62	20.59	20.63	20.58
FeO	17.46	16.89	17.31	17.61	17.57	17.86
Fe_2O_3	1.17	1.59	1.11	0.77	1.28	0.58
MnO	21.46	21.69	21.36	21.15	21.32	20.86
TiO_2	0.04	0.04	0.06	0.05	0.06	0.08
MgO	0.78	0.81	0.77	0.73	0.77	0.78

CaO	0.64	0.63	0.61	0.63	0.65	0.6
Na$_2$O	0.11	0.13	0.15	0.14	0.08	0.12
K$_2$O	-	-	-	-	-	-
Sc$_2$O$_3$	0.13	0.13	0.13	0.13	0.13	0.14
ZnO	0.01	0.01	0.01	0.01	0.01	0.01
Y$_2$O$_3$	1.91	1.81	1.9	1.97	1.96	1.92
REE$_2$O$_3$	1.67	1.6	1.67	1.58	1.57	1.6
TOTAL	100.9	100.7	100.61	100.27	100.87	99.95
Si apfu	2.90	2.89	2.90	2.91	2.89	2.91
Al	0.10	0.11	0.10	0.09	0.11	0.09
Σ T	3.00	3.00	3.00	3.00	3.00	3.00
V	0.00	0.00	0.00	0.00	0.00	0.00
Ti	0.00	0.00	0.00	0.00	0.00	0.01
Cr	0.00	0.00	0.00	0.00	0.00	0.00
Al	1.90	1.90	1.92	1.93	1.90	1.93
Fe3+	0.07	0.10	0.07	0.05	0.08	0.03
Fe2+	0.03	0.00	0.01	0.02	0.01	0.03
Σ B	2.00	2.00	2.00	2.00	2.00	2.00
Y	0.08	0.08	0.08	0.09	0.09	0.09
REE	0.04	0.04	0.04	0.04	0.04	0.04
Fe2+	1.18	1.17	1.19	1.21	1.21	1.22
Fe3+	0.00	0.00	0.00	0.00	0.00	0.01
Sc	0.01	0.01	0.01	0.01	0.01	0.01
Mn	1.51	1.52	1.50	1.49	1.50	1.47
Mg	0.10	0.10	0.10	0.09	0.10	0.10
Ca	0.06	0.06	0.05	0.06	0.06	0.05
Na	0.02	0.02	0.02	0.02	0.01	0.02
K	0.00	0.00	0.00	0.00	0.00	0.00
Σ A	3.00	3.00	3.00	3.01	3.01	3.01
Mn/Fe2+Mn	0.55	0.56	0.55	0.55	0.55	0.54
Yttrogarnet %	2.75	2.67	2.81	2.65	2.9	2.64
Sc garnet	0.47	0.49	0.46	0.47	0.46	0.49
Spessartine	50.47	51.04	50.31	49.95	50.13	49.4
Pyrope	3.25	3.34	3.21	3.02	3.19	3.25
Almandine	39.87	39.02	40.26	41.07	40.07	41.78
Grossular	0	0	0.42	0.8	0	0.71
Andradite	1.37	1.27	0.76	0.57	1.26	0.51
Skiagite	0.66	0.23	0	0	0.72	0

	KH-3 Hovåsen, Eptevann			
Sample	KH-3-1	KH-3-2	KH-3-3	KH-3-4
SiO_2 wt%	35.56	35.63	35.27	35.27
Al_2O_3	19.56	19.61	19.65	19.61
FeO	10.02	9.84	9.78	9.77
Fe_2O_3	2.85	2.81	2.97	3.12
MnO	31.45	31.8	31.39	31.26
TiO_2	0.15	0.1	0.15	0.12
MgO	0.18	0.14	0.22	0.2
CaO	0.24	0.25	0.23	0.23
Na_2O	0.03	0.02	0.01	0.04
K_2O	-	-	-	-
Sc_2O_3	0	0	0	0
ZnO	0.02	0.03	0.03	0.03
Y_2O_3	0.05	0.04	0.06	0.05
REE_2O_3	0.05	0.04	0.06	0.06
TOTAL	100.17	100.32	99.81	99.77
Si apfu	2.95	2.95	2.93	2.93
Al	0.05	0.05	0.07	0.07
Σ T	3.00	3.00	3.00	3.00
V	0.00	0.00	0.00	0.00
Ti	0.01	0.01	0.01	0.01
Cr	0.00	0.00	0.00	0.00
Al	1.86	1.86	1.86	1.86
Fe3+	0.13	0.13	0.13	0.14
Fe2+	0.00	0.00	0.00	0.00
Σ B	2.00	2.00	2.00	2.00
Y	0.00	0.00	0.00	0.00
REE	0.00	0.00	0.00	0.00
Fe2+	0.69	0.68	0.68	0.68
Fe3+	0.05	0.04	0.06	0.06
Sc	0.00	0.00	0.00	0.00
Mn	2.21	2.23	2.21	2.20
Mg	0.02	0.02	0.03	0.03
Ca	0.02	0.02	0.02	0.02
Na	0.00	0.00	0.00	0.01
K	0.00	0.00	0.00	0.00
Σ A	3.00	3.00	3.00	3.00
Mn/(Fe2+Mn)	0.76	0.77	0.76	0.76
Yttrogarnet %	0.08	0.06	0.08	0.08

Sc garnet	0.01	0	0.01	0
Spessartine	73.62	74.32	73.72	73.45
Pyrope	0.73	0.58	0.9	0.84
Almandine	18.54	18.22	18.33	18.59
Grossular	0	0	0	0
Andradite	0.24	0.4	0.2	0.29
Skiagite	4.62	4.48	4.35	4.08

	25444 Håvarstad					
Sample	25444-1	25444-2	25444-3	25444-4	25444-5	25444-6
SiO_2 wt%	34.91	34.78	35.96	35.76	36.07	35.78
Al_2O_3	19.67	19.24	20.12	20.05	20.29	20.34
FeO	18.57	17.09	20	20.42	20.58	20.34
Fe_2O_3	2.74	3.76	1.18	1.17	1.21	1.46
MnO	21.01	20.97	20.88	20.47	20.38	20.27
TiO_2	0.09	0.22	0.16	0.1	0.08	0.09
MgO	0.59	0.5	0.66	0.63	0.63	0.64
CaO	0.49	0.62	0.48	0.32	0.33	0.3
Na_2O	0.07	0.25	0.05	0.04	0.1	0.07
K_2O	-	0.2	-	-	-	0.05
Sc_2O_3	0.15	0.16	0.17	0.23	0.23	0.3
REE_2O_3	0.16	0.21	0.23	0.22	0.17	0.22
ZnO	0.01	0.01	0.01	0.01	0.01	0.01
Y_2O_3	0.48	0.58	0.63	0.62	0.54	0.6
TOTAL	98.97	98.61	100.55	100.04	100.63	100.48
Si apfu	2.92	2.92	2.96	2.96	2.96	2.94
Al	0.08	0.08	0.04	0.04	0.04	0.06
Σ T	3.00	3.00	3.00	3.00	3.00	3.00
V	0.00	0.00	0.00	0.00	0.00	0.00
Ti	0.01	0.01	0.01	0.01	0.01	0.01
Cr	0.00	0.00	0.00	0.00	0.00	0.00
Al	1.86	1.83	1.91	1.91	1.92	1.92
Fe3+	0.13	0.16	0.07	0.07	0.07	0.08
Fe2+	0.00	0.00	0.01	0.01	0.00	0.00
Σ B	2.00	2.00	2.00	2.00	2.00	2.00
Y	0.02	0.03	0.03	0.03	0.02	0.03
REE	0.00	0.01	0.01	0.01	0.00	0.01
Fe2+	1.30	1.20	1.36	1.40	1.41	1.40
Fe3+	0.04	0.08	0.00	0.00	0.01	0.01
Sc	0.01	0.01	0.01	0.02	0.02	0.02
Mn	1.49	1.49	1.46	1.43	1.42	1.41

Mg	0.07	0.06	0.08	0.08	0.08	0.08
Ca	0.04	0.06	0.04	0.03	0.03	0.03
Na	0.01	0.04	0.01	0.01	0.02	0.01
K	0.00	0.02	0.00	0.00	0.00	0.00
Σ A	3.00	3.00	3.00	3.00	3.00	3.00
Mn/Fe2+Mn	0.53	0.55	0.51	0.50	0.50	0.50
Yttrogarnet %	0.71	0.87	0.92	0.92	0.78	0.88
Sc garnet	0.56	0.58	0.62	0.65	0.72	0.63
Spessartine	49.7	49.93	48.53	47.81	47.23	47.12
Pyrope	2.45	2.11	2.7	2.61	2.56	2.63
Almandine	40.47	39.35	43.44	44.45	45.79	45.48
Grossular	0	0	0	0	0	0
Andradite	0.57	0.57	0.23	0	0	0
Skiagite	2.9	0.83	2.44	2.66	1.33	1.24

	25447 Røykkvartsbruddet, Birkeland			
Sample	25447-1	25447-2	25447-3	25447-4
SiO_2 wt%	34.69	34.79	34.74	34.65
Al_2O_3	20.28	20.15	20.29	20.41
FeO	0.78	0.91	1.47	0.51
Fe_2O_3	3.65	3.35	2.94	4.18
MnO	39.08	39.04	38.58	39.47
TiO_2	0.08	0.06	0.06	0.07
MgO	-	-	-	-0.03
CaO	0.79	0.79	0.77	0.73
Na_2O	0.03	0.04	0.01	0.01
K_2O	-	-	-	-
Sc_2O_3	0	0	0	0
ZnO	0.03	0.03	0.03	0.03
Y_2O_3	0.11	0.11	0.09	0.1
REE_2O_3	0.08	0.09	0.07	0.07
TOTAL	99.6	99.35	99.05	100.21
Si apfu	2.89	2.90	2.90	2.87
Al	0.11	0.10	0.10	0.13
Σ T	3.00	3.00	3.00	3.00
V	0.00	0.00	0.00	0.00
Ti	0.00	0.00	0.00	0.00
Cr	0.00	0.00	0.00	0.00
Al	1.88	1.88	1.90	1.86

Fe3+	0.12	0.11	0.09	0.13
Fe2+	0.00	0.00	0.00	0.00
Σ B	2.00	2.00	2.00	2.00
Y	0.00	0.00	0.00	0.00
REE	0.00	0.00	0.00	0.00
Fe2+	0.05	0.06	0.10	0.04
Fe3+	0.11	0.10	0.09	0.12
Sc	0.00	0.00	0.00	0.00
Mn	2.75	2.76	2.73	2.77
Mg	0.00	0.00	0.00	0.00
Ca	0.07	0.07	0.07	0.06
Na	0.01	0.01	0.00	0.00
K	0.00	0.00	0.00	0.00
Σ A	3.00	3.00	3.00	3.00
Mn/Fe2+Mn	0.98	0.98	0.96	0.99
Yttrogarnet %	0.16	0.16	0.14	0.14
Sc garnet	0.01	0.01	0.01	0.01
Spessartine	91.83	91.93	91.05	92.28
Pyrope	0	0	0	0
Almandine	1.81	2.12	3.43	0.67
Grossular	0	0	0.55	0
Andradite	2.05	2.16	1.58	1.91
Skiagite	0	0.01	0	0.5

	28372 Mølland					
Sample	28372-1	28372-2	28372-3	28372-4	28372-5	28372-6
SiO_2 wt%	36.24	35.75	35.98	35.84	36.08	35.76
Al_2O_3	20.06	20	20.12	19.82	19.92	19.69
FeO	20.34	19.68	20.07	17.77	18.23	17.68
Fe_2O_3	1.41	2.28	1.76	1.9	1.31	1.8
MnO	20.15	20.31	20.19	22.65	22.57	22.72
TiO_2	0.09	0.08	0.1	0.1	0.15	0.13
MgO	0.92	0.97	0.97	0.75	0.78	0.79
CaO	0.71	0.62	0.63	0.5	0.52	0.48
Na_2O	0.03	0.01	0.01	0.06	0.03	0.04
K_2O	-	-	-	-	-	-
Sc_2O_3	0.04	0.01	0.02	0.03	0.03	0.03
ZnO	0.01	0.01	0.01	0.01	0.01	0.01
Y_2O_3	0.02	0.03	0.08	0.23	0.23	0.21
REE_2O_3	0.01	0.01	0.03	0.08	0.08	0.08

TOTAL	100.02	99.78	99.98	99.74	99.94	99.42
Si apfu	2.98	2.95	2.96	2.97	2.98	2.97
Al	0.02	0.05	0.04	0.03	0.02	0.03
Σ T	3.00	3.00	3.00	3.00	3.00	3.00
V	0.00	0.00	0.00	0.00	0.00	0.00
Ti	0.01	0.00	0.01	0.01	0.01	0.01
Cr	0.00	0.00	0.00	0.00	0.00	0.00
Al	1.92	1.90	1.91	1.90	1.91	1.90
Fe3+	0.07	0.10	0.08	0.09	0.08	0.10
Fe2+	0.00	0.00	0.00	0.00	0.00	0.00
Σ B	2.00	2.00	2.00	2.00	2.00	2.00
Y	0.00	0.00	0.00	0.01	0.01	0.01
REE	0.00	0.00	0.00	0.00	0.00	0.00
Fe2+	1.40	1.36	1.38	1.23	1.26	1.23
Fe3+	0.02	0.04	0.03	0.02	0.01	0.02
Sc	0.00	0.00	0.00	0.00	0.00	0.00
Mn	1.40	1.42	1.41	1.59	1.58	1.60
Mg	0.11	0.12	0.12	0.09	0.10	0.10
Ca	0.06	0.06	0.06	0.04	0.05	0.04
Na	0.00	0.00	0.00	0.01	0.01	0.01
K	0.00	0.00	0.00	0.00	0.00	0.00
Σ A	3.00	3.00	3.00	3.00	3.00	3.00
Mn/Fe2+Mn	0.50	0.51	0.51	0.56	0.56	0.57
Yttrogarnet %	0.02	0.04	0.11	0.34	0.34	0.3
Sc garnet	0.13	0.04	0.06	0.11	0.1	0.12
Spessartine	46.77	47.32	46.93	52.93	52.6	53.25
Pyrope	3.77	3.96	3.97	3.07	3.18	3.24
Almandine	45.55	43.51	44.68	38.64	39.63	38.02
Grossular	0	0	0	0	0	0
Andradite	1.66	1.55	1.5	1.06	0.94	0.89
Skiagite	1.05	1.78	1.38	2.36	2.3	2.9

	25375 Ivedal					
Sample	25375-1	25375-2	25375-3	25375-4	25375-5	25375-6
SiO_2 wt%	35.61	35.47	35.27	35.07	35.08	35.35
Al_2O_3	20.42	20.59	20.58	20.12	20.32	20.21
FeO	17.47	17.2	17.21	14.89	15.3	15.95
Fe_2O_3	1.3	1.67	1.6	2.36	1.88	0.84
MnO	22.01	22.35	22.12	23.45	23.19	22.96

TiO_2	0.03	0.05	0.03	0.07	0.1	0.07
MgO	0.65	0.64	0.59	0.72	0.71	0.71
CaO	0.86	0.88	0.89	1.04	1.03	1.02
Na_2O	0.13	0.08	0.09	0.14	0.15	0.12
K_2O	-	-	-	-	-	-
Sc_2O_3	0.14	0.14	0.15	0.1	0.11	0.12
ZnO	0.02	0.02	0.02	0.01	0.01	0.01
Y_2O_3	1.23	1.21	1.2	1.63	1.63	1.57
REE_2O_3	0.93	0.93	0.93	1.49	1.51	1.44
TOTAL	100.79	101.24	100.67	101.13	101.02	100.38
Si apfu	2.93	2.91	2.91	2.90	2.90	2.93
Al	0.07	0.09	0.09	0.10	0.10	0.07
Σ T	3.00	3.00	3.00	3.00	3.00	3.00
V	0.00	0.00	0.00	0.00	0.00	0.00
Ti	0.00	0.00	0.00	0.00	0.01	0.00
Cr	0.00	0.00	0.00	0.00	0.00	0.00
Al	1.92	1.90	1.91	1.86	1.88	1.91
Fe3+	0.08	0.09	0.08	0.14	0.12	0.05
Fe2+	0.00	0.00	0.00	0.00	0.00	0.03
Σ B	2.00	2.00	2.00	2.00	2.00	2.00
Y	0.05	0.05	0.05	0.07	0.07	0.07
REE	0.02	0.02	0.02	0.04	0.04	0.04
Fe2+	1.20	1.18	1.19	1.03	1.06	1.08
Fe3+	0.00	0.01	0.01	0.01	0.00	0.00
Sc	0.01	0.01	0.01	0.01	0.01	0.01
Mn	1.54	1.55	1.55	1.64	1.62	1.61
Mg	0.08	0.08	0.07	0.09	0.09	0.09
Ca	0.08	0.08	0.08	0.09	0.09	0.09
Na	0.02	0.01	0.01	0.02	0.02	0.02
K	0.00	0.00	0.00	0.00	0.00	0.00
Σ A	3.00	3.00	3.00	3.00	3.00	3.01
Mn/Fe2+Mn	0.56	0.57	0.57	0.61	0.61	0.59
Yttrogarnet %	1.8	1.76	1.76	2.4	2.4	1.78
Sc garnet	0.51	0.52	0.54	0.38	0.41	0.42
Spessartine	51.33	51.96	51.7	54.97	54.36	54.04
Pyrope	2.65	2.61	2.41	2.99	2.92	2.94
Almandine	40.22	39.47	39.71	33.65	35.34	37
Grossular	0.5	0.12	0.75	0	0	0.87
Andradite	1.43	1.78	1.22	2.5	2.34	1.52
Skiagite	0	0	0	0.82	0.06	0

	25412 Røykkvartsbruddet, Birkeland					
Sample	25412-1	25412-2	25412-3	25412-4	25412-5	25412-6
SiO_2 wt%	36.15	36.08	36.56	36.35	36.2	35.81
Al_2O_3	20.47	20.5	20.3	20.56	20.44	20.67
FeO	7.18	5.8	7.91	7.23	7.54	6.38
Fe_2O_3	1.58	3.12	0.86	1.59	1.1	2.47
MnO	34.32	34.21	34.46	34.94	34.29	34.92
TiO_2	0.01	0.01	0.04	0.02	0.01	0.03
MgO	0.02	0.01	0	0.01	-	0.01
CaO	0.51	0.46	0.49	0.49	0.49	0.51
Na_2O	0.12	0.15	0.06	0.04	0.08	0.08
K_2O	-	0.44	-	-	-	-
Sc_2O_3	0	0	0	0	0	0
ZnO	0.06	0.06	0.06	0.06	0.06	0.06
Y_2O_3	0.37	0.41	0.35	0.46	0.41	0.42
REE_2O_3	0.06	0.07	0.06	0.08	0.07	0.07
TOTAL	100.86	101.33	101.15	101.82	100.69	101.43
Si apfu	2.96	2.94	2.99	2.96	2.97	2.92
Al	0.04	0.06	0.01	0.04	0.03	0.08
Σ T	3.00	3.00	3.00	3.00	3.00	3.00
V	0.00	0.00	0.00	0.00	0.00	0.00
Ti	0.00	0.00	0.00	0.00	0.00	0.00
Cr	0.00	0.00	0.00	0.00	0.00	0.00
Al	1.94	1.91	1.95	1.93	1.95	1.91
Fe3+	0.06	0.08	0.05	0.07	0.05	0.08
Fe2+	0.00	0.00	0.00	0.00	0.00	0.00
Σ B	2.00	2.00	2.00	2.00	2.00	2.00
Y	0.02	0.02	0.02	0.02	0.02	0.02
REE	0.00	0.00	0.00	0.00	0.00	0.00
Fe2+	0.49	0.40	0.54	0.49	0.52	0.44
Fe3+	0.04	0.11	0.00	0.03	0.02	0.07
Sc	0.00	0.00	0.00	0.00	0.00	0.00
Mn	2.38	2.36	2.39	2.41	2.39	2.42
Mg	0.00	0.00	0.00	0.00	0.00	0.00
Ca	0.05	0.04	0.04	0.04	0.04	0.04
Na	0.02	0.02	0.01	0.01	0.01	0.01
K	0.00	0.05	0.00	0.00	0.00	0.00
Σ A	3.00	3.00	3.00	3.00	3.00	3.00
Mn/Fe2+Mn	0.83	0.86	0.82	0.83	0.82	0.85

Yttrogarnet %	0.54	0.59	0.29	0.66	0.6	0.6
Sc garnet	0	0	0	0	0	0
Spessartine	79.47	79.3	79.6	80.29	79.54	80.56
Pyrope	0.07	0.02	0.01	0.02	0	0.03
Almandine	16.41	13.28	17.51	15.57	17.28	14.54
Grossular	0.67	1.3	0	0	0.28	0.08
Andradite	0.81	0	1.38	1.36	1.12	1.33
Skiagite	0	0	0.55	0.83	0	0

	25374 Frøyså					
Sample	25374-1	25374-2	25374-3	25374-4	25374-5	25374-6
SiO_2 wt%	35.38	35.41	35.48	35.64	35.79	35.26
Al_2O_3	20.58	20.61	20.81	20.66	20.63	20.15
FeO	1.58	2.13	1.41	2.04	2.17	1.35
Fe_2O_3	3.03	2.48	3.22	2.51	2.54	3.34
MnO	39.06	38.48	39.25	38.85	39.11	38.89
TiO_2	0.04	0.05	0.06	0.03	0.04	0.04
MgO	-	-	-	-	-	-
CaO	0.84	0.89	0.8	0.75	0.7	0.78
Na_2O	0.02	0.03	0.06	0.06	0.03	0.06
K_2O	-	-	-	-	-	0.05
Sc_2O_3	0	0	0	0	0	0
ZnO	0.03	0.03	0.03	0.03	0.03	0.03
Y_2O_3	0.16	0.17	0.17	0.14	0.15	0.14
REE_2O_3	0.11	0.12	0.12	0.08	0.1	0.08
TOTAL	100.82	100.37	101.37	100.79	101.3	100.15
Si apfu	2.91	2.92	2.90	2.92	2.92	2.92
Al	0.09	0.08	0.10	0.08	0.08	0.08
Σ T	3.00	3.00	3.00	3.00	3.00	3.00
V	0.00	0.00	0.00	0.00	0.00	0.00
Ti	0.00	0.00	0.00	0.00	0.00	0.00
Cr	0.00	0.00	0.00	0.00	0.00	0.00
Al	1.90	1.92	1.90	1.92	1.91	1.88
Fe3+	0.10	0.08	0.09	0.08	0.09	0.12
Fe2+	0.00	0.00	0.00	0.00	0.00	0.00
Σ B	2.00	2.00	2.00	2.00	2.00	2.00
Y	0.01	0.01	0.01	0.01	0.01	0.01
REE	0.00	0.00	0.00	0.00	0.00	0.00
Fe2+	0.11	0.15	0.10	0.14	0.15	0.09

Fe3+	0.09	0.08	0.10	0.08	0.07	0.09
Sc	0.00	0.00	0.00	0.00	0.00	0.00
Mn	2.72	2.69	2.72	2.70	2.71	2.72
Mg	0.00	0.00	0.00	0.00	0.00	0.00
Ca	0.07	0.08	0.07	0.07	0.06	0.07
Na	0.00	0.00	0.01	0.01	0.00	0.01
K	0.00	0.00	0.00	0.00	0.00	0.00
Σ A	3.00	3.00	3.00	3.00	3.00	3.00
Mn/Fe2+Mn	0.96	0.95	0.97	0.95	0.95	0.97
Yttrogarnet %	0.24	0.25	0.25	0.21	0.22	0.2
Sc garnet	0	0	0	0	0	0
Spessartine	90.59	89.53	90.5	90.01	90.25	90.88
Pyrope	0	0	0	0	0.02	0
Almandine	3.61	4.9	3.21	4.67	4.94	3.11
Grossular	0.54	1.36	1.15	1.22	0.21	0.06
Andradite	1.79	1.09	1	0.89	1.7	2.13
Skiagite	0	0	0	0	0	0

	MB-3 Brattekleiv				22330 Torvelona			
Sample	MB-3-1	MB-3-2	MB-3-3	MB-3-4	22330-1	22330-2	22330-3	22330-4
SiO_2 wt%	35.68	35.62	35.75	35.66	35.72	35.52	35.24	35.38
Al_2O_3	20.36	20.22	20.3	20.37	19.35	19.42	19.2	19.29
FeO	20.74	20.42	21.25	21.72	11.66	11.56	11.11	11.17
Fe_2O_3	1.17	1.65	1.17	1.23	1.96	2.25	2.97	2.86
MnO	19.79	20.01	19.49	18.97	28.27	28.37	28.37	28.62
TiO_2	0.14	0.12	0.08	0.09	0.19	0.2	0.21	0.23
MgO	0.51	0.52	0.52	0.53	0.71	0.7	0.72	0.69
CaO	0.62	0.65	0.47	0.51	0.69	0.6	0.67	0.67
Na_2O	0.07	0.06	0.07	0.05	0.09	0.08	0.08	0.06
K_2O	-	-	-	-	-	-	-	-
Sc_2O_3	0.16	0.18	0.11	0.11	0.32	0.31	0.3	0.29
ZnO	0.01	0.01	0.01	0.01	0.01	0.02	0.01	0.01
Y_2O_3	0.65	0.64	0.54	0.57	0.78	0.76	0.73	0.73
REE_2O_3	0.5	0.48	0.46	0.5	0.47	0.45	0.43	0.45
TOTAL	100.38	100.56	100.21	100.32	100.24	100.24	100.03	100.45
Si apfu	2.94	2.94	2.95	2.95	2.96	2.94	2.93	2.93
Al	0.06	0.06	0.05	0.05	0.04	0.06	0.07	0.07
Σ T	3.00	3.00	3.00	3.00	3.00	3.00	3.00	3.00
V	0.00	0.00	0.00	0.00	0.00	0.00	0.00	0.00

Ti	0.01	0.01	0.01	0.01	0.01	0.01	0.01	0.01
Cr	0.00	0.00	0.00	0.00	0.00	0.00	0.00	0.00
Al	1.92	1.90	1.93	1.93	1.84	1.84	1.81	1.81
Fe3+	0.07	0.09	0.06	0.07	0.12	0.14	0.18	0.17
Fe2+	0.00	0.00	0.00	0.00	0.02	0.01	0.00	0.00
Σ B	2.00	2.00	2.00	2.00	2.00	2.00	2.00	2.00
Y	0.03	0.03	0.02	0.03	0.03	0.03	0.03	0.03
REE	0.01	0.01	0.01	0.01	0.01	0.01	0.01	0.01
Fe2+	1.43	1.41	1.47	1.50	0.79	0.79	0.77	0.77
Fe3+	0.01	0.01	0.01	0.01	0.00	0.00	0.01	0.00
Sc	0.01	0.01	0.01	0.01	0.02	0.02	0.02	0.02
Mn	1.38	1.40	1.36	1.33	1.98	1.99	2.00	2.01
Mg	0.06	0.06	0.06	0.07	0.09	0.09	0.09	0.09
Ca	0.05	0.06	0.04	0.04	0.06	0.05	0.06	0.06
Na	0.01	0.01	0.01	0.01	0.02	0.01	0.01	0.01
K	0.00	0.00	0.00	0.00	0.00	0.00	0.00	0.00
Σ A	3.00	3.00	3.00	3.00	3.01	3.00	3.00	3.00
Mn/Fe2+Mn	0.49	0.50	0.48	0.47	0.71	0.71	0.72	0.72
Yttrogarnet %	0.95	0.94	0.79	0.84	0.08	0.14	0.17	1.29
Sc garnet	0.57	0.63	0.39	0.38	0.11	0.1	0.1	0.23
Spessartine	46.17	46.64	45.52	44.29	35.5	35.76	35.77	50.12
Pyrope	2.1	2.14	2.16	2.19	2.28	2.31	2.09	3.74
Almandine	47.37	45.71	48.41	49.45	59.1	58.76	58.78	41.13
Grossular	0	0	0	0	0	0	0	0
Andradite	0.83	0.89	0.76	0.82	1.05	0.97	1.07	0.8
Skiagite	0.41	1.29	0.6	0.63	1.21	1.09	0.6	1.32

	25421 Frikstad				KH-1 Hovåsen, Eptevann			
Sample	25421-1	25421-2	25421-3	25421-4	KH-1-1	KH-1-2	KH-1-3	KH-1-4
SiO_2 wt%	35.25	35.13	35.11	35.39	36.14	35.92	36.32	36.11
Al_2O_3	20.45	20.73	20.61	20.4	19.98	19.93	20.02	20.03
FeO	1.12	0.41	0.53	1.07	13.06	12.94	13.02	12.8
Fe_2O_3	3.1	3.53	3.66	2.86	1.76	1.56	1.63	1.61
MnO	39.31	40	39.87	39.7	28.54	28.42	28.77	28.78
TiO_2	0.06	0.05	0.05	0.04	0.18	0.21	0.11	0.1
MgO	0.01	-	0.01	0	0.52	0.52	0.5	0.47
CaO	0.75	0.79	0.74	0.73	0.27	0.31	0.26	0.28
Na_2O	0.05	0.02	0.02	0.01	0.03	0.02	0.03	0.03
K_2O	0	-	-	-	-	-	-	-
Sc_2O_3	0	-	-	-	0.04	0.05	0.06	0.06

ZnO	0.06	0.06	0.06	0.06	0.02	0.02	0.02	0.02
Y_2O_3	0.14	0.13	0.13	0.12	0.77	0.81	0.9	0.92
REE_2O_3	0.07	0.07	0.07	0.07	0.19	0.19	0.22	0.22
TOTAL	100.37	100.87	100.86	100.47	101.49	100.9	101.85	101.42
Si apfu	2.91	2.88	2.88	2.92	2.96	2.95	2.96	2.96
Al	0.09	0.12	0.12	0.08	0.04	0.05	0.04	0.04
Σ T	3.00	3.00	3.00	3.00	3.00	3.00	3.00	3.00
V	0.00	0.00	0.00	0.00	0.00	0.00	0.00	0.00
Ti	0.00	0.00	0.00	0.00	0.01	0.01	0.01	0.01
Cr	0.00	0.00	0.00	0.00	0.00	0.00	0.00	0.00
Al	1.90	1.89	1.88	1.90	1.88	1.88	1.88	1.89
Fe3+	0.10	0.11	0.12	0.10	0.11	0.10	0.10	0.10
Fe2+	0.00	0.00	0.00	0.00	0.00	0.00	0.01	0.01
Σ B	2.00	2.00	2.00	2.00	2.00	2.00	2.00	2.00
Y	0.01	0.01	0.01	0.01	0.03	0.04	0.04	0.04
REE	0.00	0.00	0.00	0.00	0.00	0.01	0.01	0.01
Fe2+	0.08	0.03	0.04	0.07	0.89	0.89	0.88	0.87
Fe3+	0.09	0.11	0.11	0.08	0.00	-0.01	0.00	0.00
Sc	0.00	0.00	0.00	0.00	0.00	0.00	0.00	0.00
Mn	2.75	2.78	2.77	2.77	1.98	1.98	1.99	1.99
Mg	0.00	0.00	0.00	0.00	0.06	0.06	0.06	0.06
Ca	0.07	0.07	0.07	0.06	0.02	0.03	0.02	0.02
Na	0.01	0.00	0.00	0.00	0.00	0.00	0.00	0.00
K	0.00	0.00	0.00	0.00	0.00	0.00	0.00	0.00
Σ A	3.00	3.00	3.00	3.00	3.00	3.00	3.00	3.00
Mn/Fe2+Mn	0.97	0.99	0.99	0.97	0.69	0.69	0.69	0.69

Yttrogarnet %	0.2	0.18	0.19	0.18	0.62	1.13	0.53	0.02
Sc garnet	0	0	0	0	0.68	0.71	0.36	0.06
Spessartine	91.58	92.74	92.52	92.41	57.39	58.9	56.9	60.37
Pyrope	0.06	0	0.03	0.02	2.09	1.94	2.34	3.14
Almandine	2.58	0.93	1.22	2.42	34.92	31.71	35.41	32.4
Grossular	0	0.76	0.16	0	0	0	0	0
Andradite	1.6	1.39	1.87	2.02	0	0	0	0.49
Skiagite	0	0	0	0.05	2.83	5.03	2.2	1.74

	KT-1 Thortveitittgruva				
Sample	KT-1-1	KT-1-2	KT-1-3	KT-1-4	KT-1-5
SiO_2 wt%	36.58	36.42	36.21	36.03	36.41
Al_2O_3	19.92	19.82	20.06	19.88	20.21
FeO	14.95	14.47	14.7	13.69	13.8
Fe_2O_3	1.94	2.06	1.42	1.72	1.88
MnO	25.23	25.35	25.05	26.17	26.54
TiO_2	0.15	0.19	0.18	0.19	0.17
MgO	1.1	1.13	1.13	1.01	1.03
CaO	0.95	1.11	0.74	0.72	0.73
Na_2O	0.05	0.04	0.1	0.08	0.05
K_2O	-	-	0	-	0
Sc_2O_3	0.36	0.35	0.35	0.29	0.18
ZnO	0.01	0.01	0.01	0.01	0.01
Y_2O_3	0.92	1.02	0.97	0.76	0.24
REE_2O_3	0.6	0.64	0.62	0.48	0.07
TOTAL	102.75	102.61	101.56	101.03	101.34
Si apfu	2.95	2.94	2.95	2.95	2.96
Al	0.05	0.06	0.05	0.05	0.04
Σ T	3.00	3.00	3.00	3.00	3.00
V	0.00	0.00	0.00	0.00	0.00
Ti	0.01	0.01	0.01	0.01	0.01
Cr	0.00	0.00	0.00	0.00	0.00
Al	1.84	1.83	1.87	1.87	1.89
Fe3+	0.12	0.13	0.09	0.11	0.10
Fe2+	0.03	0.03	0.03	0.01	0.00
Σ B	2.00	2.00	2.00	2.00	2.00
Y	0.04	0.04	0.04	0.03	0.01
REE	0.01	0.02	0.02	0.01	0.00
Fe2+	0.98	0.95	0.97	0.93	0.94

Fe3+	0.00	0.00	0.00	0.00	0.02
Sc	0.03	0.02	0.03	0.02	0.01
Mn	1.72	1.73	1.73	1.81	1.83
Mg	0.13	0.14	0.14	0.12	0.13
Ca	0.08	0.10	0.06	0.06	0.06
Na	0.01	0.01	0.02	0.01	0.01
K	0.00	0.00	0.00	0.00	0.00
Σ A	3.00	3.00	3.00	3.00	3.00
Mn/Fe2+Mn	0.63	0.64	0.63	0.66	0.66
Yttrogarnet %	0.07	0.06	0.39	0.52	0.42
Sc garnet	0.07	0.07	0.26	0.31	0.23
Spessartine	59.86	60.49	57.79	58.45	58.69
Pyrope	3.16	3.15	3.01	2.91	2.8
Almandine	32.85	31.33	33.73	31.34	33.55
Grossular	0	0	0	0	0
Andradite	0.35	0.51	0.76	0.5	0.51
Skiagite	1.84	2.48	2.94	4.24	2.98

	MS-6 Solås				KG2-5 Granatgruva, Knipan			
Sample	MS-6-1	MS-6-2	MS-6-3	MS-6-4	KG2-5-1	KG2-5-2	KG2-5-3	KG2-5-4
SiO_2 wt%	35.96	35.77	35.68	35.38	35.54	35.46	35.42	35.35
Al_2O_3	20.23	19.9	19.98	19.81	19.77	19.48	19.92	19.97
FeO	16.69	16.55	16.16	14.97	15.68	15.49	14.4	14.48
Fe_2O_3	1.18	1.32	1.62	3.01	2.06	2.1	2.15	2.11
MnO	24.04	24.08	24.7	24.07	24.68	24.32	25.6	25.44
TiO_2	0.04	0.08	0.07	0.09	0.17	0.25	0.22	0.25
MgO	0.62	0.61	0.52	0.65	0.68	0.59	0.71	0.66
CaO	0.34	0.31	0.32	0.34	0.41	0.45	0.43	0.45
Na_2O	0.1	0.09	0.05	0.22	0.05	0.19	0.09	0.11
K_2O	-	-	-	0.14	-	-	-	-
Sc_2O_3	0.02	0.03	0.02	0.03	0.12	0.12	0.25	0.23
ZnO	0.03	0.03	0.03	0.03	0.02	0.02	0.02	0.02
Y_2O_3	0.67	0.57	0.81	0.84	0.82	0.77	1.12	1.07
REE_2O_3	0.25	0.16	0.42	0.48	0.28	0.3	0.6	0.5
TOTAL	100.17	99.5	100.38	100.06	100.3	99.56	100.93	100.64
Si apfu	2.97	2.97	2.95	2.93	2.94	2.95	2.92	2.92
Al	0.03	0.03	0.05	0.07	0.06	0.05	0.08	0.08
Σ T	3.00	3.00	3.00	3.00	3.00	3.00	3.00	3.00
V	0.00	0.00	0.00	0.00	0.00	0.00	0.00	0.00

Ti	0.00	0.01	0.00	0.01	0.01	0.02	0.01	0.02
Cr	0.00	0.00	0.00	0.00	0.00	0.00	0.00	0.00
Al	1.93	1.92	1.90	1.87	1.87	1.86	1.85	1.86
Fe3+	0.06	0.07	0.10	0.13	0.12	0.12	0.13	0.12
Fe2+	0.00	0.00	0.00	0.00	0.00	0.00	0.00	0.00
Σ B	2.00	2.00	2.00	2.00	2.00	2.00	2.00	2.00
Y	0.03	0.03	0.04	0.04	0.04	0.03	0.05	0.05
REE	0.01	0.00	0.01	0.01	0.01	0.01	0.02	0.01
Fe2+	1.15	1.15	1.12	1.04	1.09	1.08	0.99	1.00
Fe3+	0.01	0.01	0.00	0.06	0.01	0.01	0.00	0.01
Sc	0.00	0.00	0.00	0.00	0.01	0.01	0.02	0.02
Mn	1.68	1.69	1.73	1.69	1.73	1.72	1.79	1.78
Mg	0.08	0.08	0.06	0.08	0.08	0.07	0.09	0.08
Ca	0.03	0.03	0.03	0.03	0.04	0.04	0.04	0.04
Na	0.02	0.02	0.01	0.04	0.01	0.03	0.01	0.02
K	0.00	0.00	0.00	0.02	0.00	0.00	0.00	0.00
Σ A	3.00	3.00	3.00	3.00	3.00	3.00	3.00	3.00
Mn/Fe2+Mn	0.59	0.60	0.61	0.62	0.61	0.61	0.64	0.64
Yttrogarnet %	0.48	0.47	0.56	1.05	1.04	0.46	0.72	0.09
Sc garnet	0.12	0.12	0.13	0.3	0.31	0.45	0.31	0
Spessartine	52.49	52.9	52.93	52.17	49.88	55.36	55.24	92.55
Pyrope	3.11	3.26	3.3	3.68	3.76	3.73	3.54	0
Almandine	40.24	37.18	38.87	37.64	42.22	35.84	36.47	1.66
Grossular	0	0	0	0	0	0	0	0
Andradite	0.77	0.76	0.62	0.86	1.25	0.76	0.9	1.86
Skiagite	1.91	3.3	2.72	3.49	1.22	1.55	1.79	0.53

	KG-4 Granatgruva, Knipan					
Sample	KG-4-1	KG-4-2	KG-4-3	KG-4-4	KG-4-5	KG-4-6
SiO_2 wt%	36.29	36.12	36.66	35.32	36.27	36.53
Al_2O_3	20.21	20.12	20.03	20.01	20.28	20.15
FeO	17.53	17.35	17.93	16.47	17.77	16.64
Fe_2O_3	1.93	1.62	0.84	1.57	1.47	1.32
MnO	23.42	23.44	23.24	23.24	23.17	24.28
TiO_2	0.15	0.22	0.09	0.17	0.2	0.14
MgO	0.81	0.8	0.82	0.82	0.84	0.82
CaO	0.56	0.57	0.69	0.55	0.51	0.45
Na_2O	0.02	0.03	0.02	0.05	0.04	0.1
K_2O	-	-	-	-	-	0.04
Sc_2O_3	0.16	0.26	0.22	0.07	0.22	0.24
ZnO	0.01	0.01	0.01	0.01	0.01	0.01

Y_2O_3	0.26	0.15	0.21	0.59	0.21	0.18
REE_2O_3	0.19	0.08	0.11	0.26	0.13	0.09
TOTAL	101.56	100.78	100.87	99.13	101.11	100.99
Si apfu	2.95	2.96	2.99	2.94	2.96	2.98
Al	0.05	0.04	0.01	0.06	0.04	0.02
Σ T	3.00	3.00	3.00	3.00	3.00	3.00
V	0.00	0.00	0.00	0.00	0.00	0.00
Ti	0.01	0.01	0.01	0.01	0.01	0.01
Cr	0.00	0.00	0.00	0.00	0.00	0.00
Al	1.89	1.90	1.92	1.91	1.91	1.91
Fe3+	0.10	0.09	0.05	0.08	0.08	0.08
Fe2+	0.00	0.00	0.02	0.00	0.00	0.00
Σ B	2.00	2.00	2.00	2.00	2.00	2.00
Y	0.01	0.01	0.01	0.03	0.01	0.01
REE	0.00	0.00	0.00	0.01	0.00	0.00
Fe2+	1.19	1.19	1.20	1.15	1.21	1.13
Fe3+	0.02	0.01	0.00	0.02	0.01	0.00
Sc	0.01	0.02	0.02	0.01	0.02	0.02
Mn	1.61	1.62	1.61	1.64	1.60	1.68
Mg	0.10	0.10	0.10	0.10	0.10	0.10
Ca	0.05	0.05	0.06	0.05	0.04	0.04
Na	0.00	0.00	0.00	0.01	0.01	0.02
K	0.00	0.00	0.00	0.00	0.00	0.00
Σ A	3.00	3.00	3.00	3.00	3.00	3.00
Mn/Fe2+Mn	0.58	0.58	0.57	0.59	0.57	0.60
Yttrogarnet %	0.09	0.1	0.1	0.21	0.23	0.24
Sc garnet	0	0	0	0.18	0.18	0.19
Spessartine	93.05	93.18	93.18	37.88	37.99	38.32
Pyrope	0	0	0	2.01	2.03	2
Almandine	0.74	0	0	57.55	56.59	56.17
Grossular	0	0	0	0	0	0
Andradite	1.6	1.75	1.58	1.16	1.15	1.14
Skiagite	0.85	1.42	0.71	0.68	1.2	0.77

Trace elements

Sample	KB-1 Heliodorgruva						25432 Heia, Ljosland					
	KB-1-1	KB-1-2	KB-1-3	KB-1-4	KB-1-5	KB-1-6	25432-1	25432-2	25432-3	25432-4	25432-5	25432-6
Sc45 ppm	2055	2209	2265	104	132	133	565	414	429	225	217	234
V51	10	10	11	4	5	4	14	12	12	6	6	6
Cr53	7	-	-	5	-	5	-	-	-	-	-	-
Zn66	80	93	80	263	243	245	115	128	122	116	135	139
Y89	6110	6191	6342	96	389	318	2859	2288	1955	2636	2559	3042
La139	-	-	-	-	-	-	-	-	-	-	-	-
Ce140	0.1	0.1	0.1	-	0.2	-	0.1	0.1	0.1	-	-	-
Pr141	0.1	0.1	0.1	0.03	0.03	-	0.1	0.2	0.2	-	-	-
Nd143	4	4	4	1	1	1	5	7	7	-	0.8	0.4
Sm147	29	29	28	23	25	24	44	58	60	6	9	9
Eu151	-	-	-	-	-	-	-	-	-	-	-	-
Gd157	118	119	112	69	90	84	144	169	165	51	62	64
Tb159	44	44	43	9	17	14	40	39	38	20	22	23
Dy163	383	379	386	13	44	37	266	220	209	190	198	216
Ho165	78	78	81	1	3	3	42	31	27	48	46	50
Er166	335	329	344	1	7	6	137	90	71	235	218	236
Tm169	107	103	110	0.1	1	1	33	20	15	77	68	75
Yb173	1506	1454	1557	1	11	9	345	209	139	1022	887	973
Lu175	305	288	311	0.1	1	1	54	30	19	234	202	214

		MS-9 Solås			KTU-7 Tuftane, Frikstad			
Sample	MS-9-1	MS-9-2	MS-9-3	MS-9-4	KTU-7-1	KTU-7-2	KTU-7-3	KTU-7-4
Sc45 ppm	3	-	1	-	553	562	814	569
V51	0.2	-	-	-	7	7	14	5
Cr53	-	-	-	-	-	7	12	-
Zn66	478	476	501	468	77	87	72	72
Y89	499	500	531	560	5700	5866	2484	3876
La139	-	-	-	-	-	0.1	-	-
Ce140	0.04	0.05	0.1	0.1	-	0.1	-	-
Pr141	0.1	0.05	0.1	0.05	-	0.1	-	-
Nd143	2	2	2	2	1	1	0.2	1
Sm147	32	32	33	33	10	11	3	6
Eu151	-	-	-	-	0.1	0.04	-	-
Gd157	113	113	118	116	67	70	23	46
Tb159	49	49	51	52	31	32	12	21
Dy163	219	216	226	231	369	385	159	270
Ho165	9	9	10	10	118	124	54	90
Er166	9	9	9	10	696	723	323	540
Tm169	1	1	1	1	246	254	108	182
Yb173	11	11	11	10	3670	3781	1516	2601
Lu175	2	2	2	1	909	938	370	666

Sample	25427 Steli, Tveit						25370 Kåbuland						
	25427-1	25427-2	25427-3	25427-4	25427-5	25427-6	25370-1	25370-2	25370-3	25370-4	25370-5	25370-6	25370-7
Sc45 ppm	182	176	230	333	336	340	433	402	404	886	1079	1092	469
V51	4	4	5	5	5	5	1	1	1	6	9	10	1
Cr53	-	-	9	-	-	-	-	-	-	-	-	-	-
Zn66	111	113	112	98	97	100	70	74	71	64	64	64	74
Y89	763	932	504	1218	1295	1049	8268	7783	7671	2498	5111	4088	8720
La139	-	-	-	-	-	-	-	-	-	-	-	-	-
Ce140	-	-	0.05	0.1	-	0.1	0.1	0.2	-	-	-	-	0.04
Pr141	0.1	0.1	-	0.1	0.1	0.1	0.1	0.1	0.1	-	-	0.1	0.1
Nd143	3	3	2	3	4	3	2	2	2	0.3	1	1	3
Sm147	28	29	31	31	30	31	28	22	26	3	8	6	30
Eu151	-	-	-	-	-	-	0.1	-	-	-	-	-	0.1
Gd157	83	90	91	97	102	96	183	159	170	28	64	50	200
Tb159	20	22	19	29	31	27	71	64	66	14	31	24	78
Dy163	111	129	86	168	177	150	722	663	672	185	390	314	787
Ho165	14	17	9	19	20	16	189	183	177	61	125	105	205
Er166	32	43	20	42	43	33	788	786	745	307	619	540	843
Tm169	5	7	3	7	7	5	178	180	171	78	161	144	188
Yb173	35	54	26	51	52	37	1687	1703	1643	838	1726	1589	1763
Lu175	4	6	3	5	5	3	305	316	294	157	315	313	316

	25409 Landås						MS2-9 Solås			
Sample	25409-1	25409-2	25409-3	25409-4	25409-5	25409-6	MS2-9-1	MS2-9-2	MS2-9-3	MS2-9-4
Sc45 ppm	88	100	107	108	112	118	86	93	141	149
V51	5	6	4	0.3	-	-	2	2	2	2
Cr53	-	-	-	-	-	-	-	-	6	-
Zn66	187	176	179	154	156	160	294	281	284	279
Y89	4912	6151	7158	15300	15817	16685	12966	12924	15027	14619
La139	-	-	-	-	-	-	-	-	-	-
Ce140	-	-	-	-	0.04	-	0.1	0.1	0.1	0.1
Pr141	-	-	-	-	0.1	0.04	0.1	0.1	0.2	0.1
Nd143	1	0.4	1	1	1	1	5	5	7	5
Sm147	6	6	7	13	12	14	47	46	58	46
Eu151	-	-	0.1	-	-	-	0.03	-	-	-
Gd157	55	55	65	120	124	128	283	276	332	292
Tb159	28	29	35	68	71	73	117	116	136	125
Dy163	352	420	489	1010	1060	1078	1064	1059	1247	1186
Ho165	115	158	169	358	375	381	201	203	240	233
Er166	537	853	805	1870	1951	1968	590	601	727	708
Tm169	129	226	189	502	518	527	108	111	136	131
Yb173	1241	2327	1731	5239	5444	5449	846	884	1097	1047
Lu175	196	417	248	867	879	874	100	104	130	123

	25422 Frikstad	25444 Håvardstad

Sample	25422-1	25422-2	25422-3	25422-4	25444-1	25444-2	25444-3	25444-4	25444-5	25444-6
Sc45 ppm	295	474	734	944	1005	1033	1133	1479	1479	1952
V51	1	2	7	12	80	48	67	44	44	47
Cr53	-	-	10	-	-	-	-	-	-	-
Zn66	144	142	95	91	83	76	83	77	81	77
Y89	5866	3661	4060	4092	3772	4583	4979	4917	4219	4740
La139	-	-	-	-	-	-	-	-	-	0.2
Ce140	-	-	0.03	-	0.1	-	0.1	-	-	-
Pr141	-	-	-	0.04	0.1	0.1	0.1	-	-	-
Nd143	1	0.4	0.4	1	3	3	2	2	2	2
Sm147	8	5	5	5	33	30	29	21	20	22
Eu151	-	-	-	-	-	-	-	-	-	-
Gd157	79	45	46	46	176	168	165	127	117	124
Tb159	38	22	23	24	61	62	65	53	48	52
Dy163	496	302	329	327	441	497	539	470	403	438
Ho165	165	108	124	126	66	86	96	93	72	77
Er166	832	574	718	739	192	281	309	325	232	264
Tm169	225	158	211	226	40	60	68	71	51	68
Yb173	2450	1801	2580	2813	361	560	636	679	498	747
Lu175	455	366	586	671	48	81	91	98	69	112

	MSB-5 Slobrekka							KH-3 Hovåsen, Eftevann			
Sample	MSB-5-1	MSB-5-2	MSB-5-3	MSB-5-4	MSB-5-5	MSB-5-6		KH-3-1	KH-3-2	KH-3-3	KH-3-4

Element										
Sc45 ppm	845	874	831	833	830	883		12	14	10	9
V51	5	5	5	4	4	4		2	2	2	2
Cr53	10	-	20	-	-	-		7	-	9	-
Zn66	84	80	82	85	83	86		238	192	216	231
Y89	15053	14227	14935	15490	15464	15134		375	403	430	448
La139	-	-	-	-	-	-		-	0.1	-	-
Ce140	-	-	-	-	-	-		0.3	0.5	0.2	0.2
Pr141	-	-	-	0.1	-	-		0.4	0.4	0.2	0.2
Nd143	1	1	1	1	1	1		10	9	7	7
Sm147	11	10	10	9	10	10		103	94	91	96
Eu151	-	-	-	-	-	-		-	-	-	-
Gd157	115	109	113	113	116	113		231	217	254	267
Tb159	67	63	67	65	68	65		35	34	40	42
Dy163	1089	1015	1098	1069	1061	1045		68	72	80	83
Ho165	457	431	466	447	445	434		2	3	2	2
Er166	2685	2534	2722	2599	2573	2556		2	5	2	2
Tm169	715	686	717	683	678	685		0.2	1	0.2	0.2
Yb173	7897	7647	7840	7369	7395	7572		2	14	2	2
Lu175	1629	1565	1584	1469	1457	1519		0.3	3	0.2	0.2

	25447 Røykkvartsbruddet, Birkeland				28372 Mølland					
Sample	25447-1	25447-2	25447-3	25447-4	28372-1	28372-2	28372-3	28372-4	28372-5	28372-6
Sc45 ppm	15	11	11	13	239	68	112	191	190	208

V51	0.6	0.8	0.8	0.7	4	4	5	7	7	7
Cr53	13	-	-	-	-	-	-	-	-	-
Zn66	262	267	259	260	114	105	103	97	97	97
Y89	819	837	725	731	121	198	596	1821	1803	1628
La139	0.1	-	-	-	-	-	-	-	-	-
Ce140	0.1	0.1	0.05	0.1	-	-	0.1	-	-	0.04
Pr141	0.1	0.1	0.1	0.1	-	-	0.1	0.1	0.1	0.1
Nd143	2	2	2	2	1	1	2	3	2	3
Sm147	12	12	12	11	7	18	24	26	25	26
Eu151	-	-	-	0.1	-	-	-	0.1	0.1	-
Gd157	38	38	33	34	12	38	75	94	93	92
Tb159	28	28	25	26	2	6	16	26	26	25
Dy163	303	310	273	283	12	24	72	169	166	155
Ho165	47	48	42	42	2	3	8	27	26	24
Er166	124	127	109	109	6	8	22	89	86	79
Tm169	20	21	17	17	2	2	5	22	21	19
Yb173	128	132	107	106	33	26	54	243	237	214
Lu175	13	13	10	11	8	6	10	42	41	37

	25375 Ivedal						25412 Røykkvartsbruddet, Birkeland					
Sample	25375-1	25375-2	25375-3	25375-4	25375-5	25375-6	25412-1	25412-2	25412-3	25412-4	25412-5	25412-6
Sc45 ppm	916	944	984	740	756	755	2	2	2	3	2	2
V51	9	9	9	12	12	13	-	-	-	-	-	-

Cr53	-	-	-	-	-	-	-	-	-	-	-	-
Zn66	140	136	136	117	116	117	476	485	486	450	489	472
Y89	9653	9493	9460	12854	12350	13699	2947	3216	2767	3584	3252	3281
La139	-	-	-	-	-	-	0.1	-	-	-	-	-
Ce140	-	-	-	-	-	-	-	0.02	-	0.1	0.03	-
Pr141	-	-	-	-	-	-	0.03	-	-	0.05	-	-
Nd143	0.4	0.3	0.4	0.5	1	1	1	1	1	1	1	1
Sm147	4	4	5	7	7	8	19	20	19	18	16	17
Eu151	-	-	-	-	-	-	-	-	-	-	-	-
Gd157	55	57	57	92	87	99	137	150	139	139	117	121
Tb159	36	36	37	57	54	60	53	58	53	56	48	49
Dy163	604	607	616	929	886	967	276	301	267	332	303	299
Ho165	254	257	260	394	378	414	19	21	17	30	28	27
Er166	1496	1495	1496	2340	2233	2464	26	27	22	48	46	47
Tm169	409	407	407	654	622	681	3	4	3	6	6	6
Yb173	4455	4451	4414	7247	6895	7592	27	25	20	39	36	44
Lu175	856	849	842	1503	1438	1579	4	3	3	4	4	6

	25374 Frøyså						MB-3 Brattekleiv			
Sample	25374-1	25374-2	25374-3	25374-4	25374-5	25374-6	MB-3-1	MB-3-2	MB-3-3	MB-3-4
Sc45 ppm	2	2	2	4	2	4	1107	876	926	700
V51	-	-	-	-	-	0.2	10	10	10	13
Cr53	-	-	-	-	-	-	-	-	-	-

Zn66	258	250	252	262	263	260	74	71	80	78
Y89	1294	1373	1348	1114	1194	1089	5362	4784	4612	4225
La139	-	-	-	-	-	-	-	-	-	-
Ce140	0.04	0.1	0.05	0.03	0.1	0.04	0.03	0.04	-	0.1
Pr141	0.1	0.1	0.1	0.1	0.05	0.1	0.04	0.04	0.03	0.03
Nd143	1	2	2	1	1	1	2	1	1	0.8
Sm147	11	12	11	9	10	8	11	10	9	7
Eu151	0.04	0.04	0.05	0.04	0.03	0.04	0.1	-	-	-
Gd157	36	39	38	32	34	30	61	55	53	46
Tb159	28	30	30	25	27	24	30	27	26	23
Dy163	353	376	368	301	331	286	356	317	315	288
Ho165	63	68	68	48	56	47	108	95	92	89
Er166	193	209	208	129	162	128	585	524	486	498
Tm169	36	40	40	21	29	22	197	179	161	171
Yb173	245	271	271	131	187	137	2676	2455	2153	2385
Lu175	21	24	24	11	16	12	560	518	440	523

	22330 Torvelona				25421 Frikstad				KH-1 Hovåsen, Eftevann			
Sample	22330-1	22330-2	22330-3	22330-4	25421-1	25421-2	25421-3	25421-4	KH-1-1	KH-1-2	KH-1-3	KH-1-4
Sc45 ppm	2090	2020	1949	1922	2	-	3	-	279	323	385	405
V51	8	8	8	8	-	-	-	-	2	2	3	3
Cr53	7	-	-	-	7	-	7	-	-	-	13	-
Zn66	86	137	79	79	444	428	446	456	155	121	124	128

Y89	6104	5999	5747	5719	1000	1002	1038	1016	6029	6355	7053	7233
La139	-	0.5	-	-	-	-	-	-	-	-	0.1	0.2
Ce140	0.03	2	0.05	0.03	0.03	0.04	0.05	0.1	0.1	0.2	0.4	0.6
Pr141	0.1	0.4	0.1	0.1	0.1	0.1	0.1	0.1	0.2	0.2	0.3	0.3
Nd143	2	4	2	2	2	2	2	2	4	5	5	5
Sm147	18	20	17	17	33	29	34	35	40	43	46	43
Eu151	0.04	0.1	0.1	-	-	0.02	-	-	-	-	-	-
Gd157	66	69	62	63	127	112	132	131	184	200	212	208
Tb159	25	25	24	24	56	50	58	57	68	73	77	79
Dy163	243	240	229	231	291	267	300	294	499	527	583	593
Ho165	61	60	58	59	17	17	17	17	73	76	86	87
Er166	340	325	312	326	19	21	20	19	202	209	245	249
Tm169	142	135	128	136	2	3	2	2	44	45	54	54
Yb173	2600	2479	2317	2490	15	22	17	15	445	448	546	552
Lu175	668	630	582	642	2	3	2	2	57	56	70	70

	KT-1 Thortveittgruva					MS-6 Solås				KG2-5 Granatgruva, Knipan			
Sample	KT-1-1	KT-1-2	KT-1-3	KT-1-4	KT-1-5	MS-6-1	MS-6-2	MS-6-3	MS-6-4	KG2-5-1	KG2-5-2	KG2-5-3	KG2-5-4
Sc45 ppm	2353	2279	2316	1920	1159	123	166	141	165	755	797	1629	1497
V51	58	57	57	41	9	3	4	4	5	7	7	3	5
Cr53	-	-	-	-	-	-	-	7	-	11	-	6	-
Zn66	46	46	46	50	48	243	221	242	242	188	195	154	129
Y89	7232	8059	7646	5973	1927	5247	4484	6374	6622	6461	6051	8815	8452

La139	-	-	-	-	-	0.2	-	-	-	0.1	-	0.1	-
Ce140	-	0.05	0.02	0.1	0.1	0.2	0.1	-	-	0.1	0.1	0.2	0.2
Pr141	0.1	0.1	0.1	0.04	0.04	0.1	0.04	0.02	-	0.1	0.1	0.2	0.3
Nd143	2	3	2	1	2	1	1	1	1	4	4	6	7
Sm147	20	23	21	17	23	12	12	9	9	32	29	34	38
Eu151	0.04	0.1	0.1	0.1	0.1	0.1	0.03	0.1	0.1	0.03	0.05	0.05	0.04
Gd157	94	107	101	96	82	107	103	85	80	133	112	139	153
Tb159	39	44	42	38	23	45	40	40	38	47	40	51	54
Dy163	402	455	428	355	151	456	346	462	465	398	348	496	497
Ho165	103	118	110	85	22	110	67	137	149	79	73	122	114
Er166	548	620	584	432	73	418	227	657	739	314	311	593	520
Tm169	203	221	212	156	18	89	49	167	194	90	98	201	170
Yb173	3142	3309	3226	2456	211	801	465	1755	2098	1141	1346	2943	2359
Lu175	732	742	737	576	34	127	79	353	438	220	277	662	510

	KG-4 Granatgruva, Knipan					
Sample	KG-4-1	KG-4-2	KG-4-3	KG-4-4	KG-4-5	KG-4-6
Sc45 ppm	461	1058	1716	1445	1069	1342
V51	10	5	5	5	7	2
Cr53	-	-	7	-	2	-
Zn66	88	50	109	96	82	80
Y89	4628	2062	1151	1616	2591	2303
La139	-	-	-	0.1	-	-

Ce140	0.1	-	-	0.2	0.02	0.2
Pr141	0.1	-	0.1	0.1	0.1	0.2
Nd143	3	1	2	2	2	5
Sm147	33	6	14	14	18	30
Eu151	0.04	-	0.06	0.07	0.03	0.2
Gd157	143	30	35	42	69	81
Tb159	48	12	10	14	23	22
Dy163	388	133	86	119	201	163
Ho165	77	36	19	27	44	33
Er166	304	193	90	119	194	143
Tm169	84	67	28	37	59	45
Yb173	1006	994	351	475	777	595
Lu175	186	224	69	91	158	120

Micas

	2190Landås 7				22300Torvelona			
	1	2	3	4	1	2	3	4
SiO2	34.54				35.55			
Sc2O3	0.056(9)*	0.05	0.06	0.06	0.153(9)*	0.16	0.15	0.15
Fe2O3	23.34				22.78			
FeO	3.93				1.52			
MgO	5.45				6.54			
K2O	9.47				9.71			
Al2O	16.11				15.77			
Na2O	0.04				0.14			
CaO	-				-			
TiO2	2.77				3.07			
MnO	1.00				1.77			
Total	96.65				95.239			
Molecular proportions based on 12 oxygen								
Si apfu	2.82				2.87			
Sc	0.00				0.011			
Fe3+	1.43				1.38			
Fe2+	0.26				0.103			
Mg	0.66				0.78			
K	0.99				1.00			
Al	1.55				1.50			
Na	0.00				0.022			
Ca	0.00				0			
Ti	0.17				0.18			
Mn	0.06				0.121			
Total	7.94				7.967			

	Thor.for Eptevann				26762Heia			
	1	2	3	4	1	2	3	4
SiO2	35.41				35.16			
Sc2O3	0.135(4)*	0.132367	0.138042	0.136968	0.1162(9)*	0.0762	0.0755	0.0756
Fe2O3	22.15				23.36			
FeO	-				-			
MgO	8.64				8.89			
K2O	9.63				9.61			
Al2O	16.49				15			
Na2O	0.12				0.11			
CaO	-				-			
TiO2	3.2				3.2			
MnO	1.07				0.67			
Total	96.845				96.1162			
Molecular proportions based on 12 oxygen								
Si apfu	2.82				2.83			
Sc	0.009				0.008			
Fe3+	1.32				1.41			
Fe2+	0				0			
Mg	1.02				1.06			
K	0.97				0.98			
Al	1.54				1.42			
Na	0.019				0.018			
Ca	0				0			
Ti	0.19				0.19			
Mn	0.072				0.045			
Total	7.96				7.961			

* Sc2O3 in point 1 is the average of Sc2O3 of point 2, 3 and 4
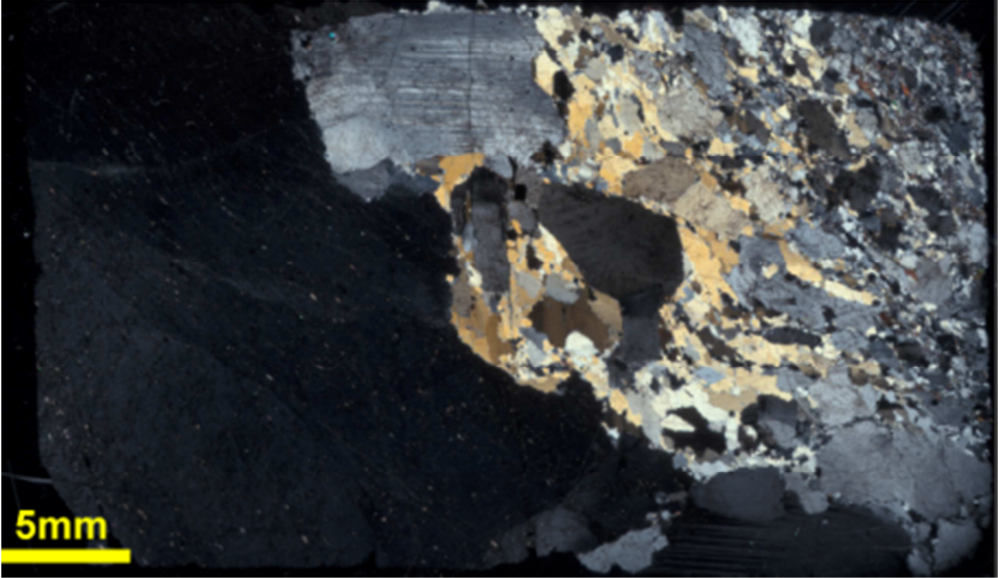
Appendix 4: Thin-sections

Figure 40: KG2-2

5mm

5mm

Figure 42: KG2-7